
Is one annotation enough?

A data-centric image classification benchmark for noisy and ambiguous label estimation

Lars Schmarje^{1*} Vasco Grossmann¹ Claudius Zelenka¹ Sabine Dippel² Rainer Kiko³
 Mariusz Oszust⁴ Matti Pastell⁶ Jenny Stracke⁵ Anna Valros⁷ Nina Volkmann⁷
 Reinhard Koch¹

¹MIP, Kiel University ²ITT, Friedrich-Loeffler-Institut ³LOV, Sorbonne Université

⁴Rzeszow University of Technology ⁵ITW, University Bonn ⁶University of Helsinki

⁷Luke, Natural Resources Institute Finland ⁸WING, University of Veterinary Medicine Hannover

Abstract

High-quality data is necessary for modern machine learning. However, the acquisition of such data is difficult due to noisy and ambiguous annotations of humans. The aggregation of such annotations to determine the label of an image leads to a lower data quality. We propose a data-centric image classification benchmark with ten real-world datasets and multiple annotations per image to allow researchers to investigate and quantify the impact of such data quality issues. With the benchmark we can study the impact of annotation costs and (semi-)supervised methods on the data quality for image classification by applying a novel methodology to a range of different algorithms and diverse datasets. Our benchmark uses a two-phase approach via a data label improvement method in the first phase and a fixed evaluation model in the second phase. Thereby, we give a measure for the relation between the input labeling effort and the performance of (semi-)supervised algorithms to enable a deeper insight into how labels should be created for effective model training. Across thousands of experiments, we show that one annotation is not enough and that the inclusion of multiple annotations allows for a better approximation of the real underlying class distribution. We identify that hard labels can not capture the ambiguity of the data and this might lead to the common issue of overconfident models. Based on the presented datasets, benchmarked methods, and analysis, we create multiple research opportunities for the future directed at the improvement of label noise estimation approaches, data annotation schemes, realistic (semi-)supervised learning, or more reliable image collection. ²

1 Introduction

High-quality data is the fuel of modern machine learning and almost all models improve with higher quality data [8, 80, 50]. Therefore, such data are a key component for developing future techniques. The acquisition of a large amount of data is considered particularly challenging due to the participation of humans in the process. Their mistakes or subjective interpretations of annotation tasks can lead to *noisy* or *ambiguous* labels, respectively [54, 16, 61, 28, 52, 9, 18, 29]. Consequently, the labels suffer from heteroscedastic aleatoric uncertainty which means that the data contains inherent noise, which is class- or even sample-dependent and negatively affects the quality [14].

In Figure 1, we present the impact of this uncertainty on the class "cat" in the CIFAR-10 dataset [32]. While all images have the same ground truth label in CIFAR-10, humans created agreeing annotations

*Corresponding Author, las@informatik.uni-kiel.de

²The source code is available at <https://github.com/Emprime/dcic>.

The datasets are available at <https://doi.org/10.5281/zenodo.7152309>.

only with varying rates from four to 100 percent [54]. This means that individual annotations can be expected to be noisy as they diverge from the majority opinion. Furthermore, a majority vote across multiple annotations can not capture the ambiguity between different images. In some extreme cases (red borders), we even see a disagreeing majority vote across all annotators from the expected ground truth class. We raise the question if all images should be treated equally if human annotations show such varying certainties. Taking a *data-centric* perspective [47, 62, 45, 25], we investigate the data in contrast to only the model for answering this question. Specifically, we propose a data-centric image classification (DCIC) benchmark that indirectly measures a method’s ability to identify noisy and ambiguous labels and correct them. DCIC consists of ten real-world datasets of different domains (see Figure 2) and multiple human annotations for each image. The benchmark focuses on a data-centric view of the image classification problem by separating the data quality improvement and the classification performance into two tasks.

The main structure of the benchmark is divided into a *Labeling* and an *Evaluation* phase (see Figure 3a) which is comparable to established Teacher-Student-Approaches [70, 36]. Using this denotation, the benchmarked method will, as a teacher, improve labels during the first phase. These are then benchmarked in the second phase by analyzing their quality as training input to a student model. Be aware that we do not allow a knowledge transfer from the second phase to the first phase.

In detail, during the Labeling phase, we use samples from the distribution of the above-mentioned annotations to get different realistic label estimates as an *initialization*. The task of the benchmarked method is to improve these estimates for better performance of an other classification model in the second phase. In that phase (Evaluation), the obtained labels are used as input for training a fixed model and its performance is measured on a testing subset of the original data. In contrast to common model-centric deep learning approaches (see Figure 3b), we can vary the initialization for the same method and better separate its performance from the data improvement. The fixed model is used for the evaluation to facilitate distinguishing between performance gains due to improved input data and better learning of the method itself.

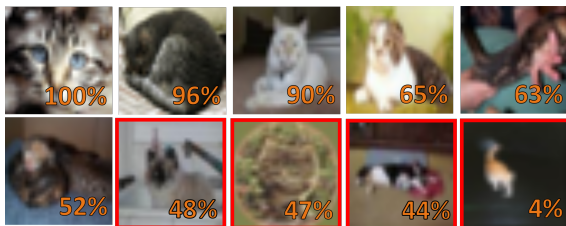


Figure 1: Are all images showing a cat? – Based on their ground truth labels from CIFAR-10 [32] they should all be cats. However, we give the agreement rate with the class cat from [54] in the lower right corner and see a wide range from four to 100%. Based on a majority vote, the last images (red border) would have not to be labeled as a cat but as dog, frog, dog, and deer, respectively. Based on these observations, we answer in our paper the question of whether all images should be treated equally as cats or if we should use multiple annotations and the resulting soft labels to capture this intrinsic noise and ambiguity.

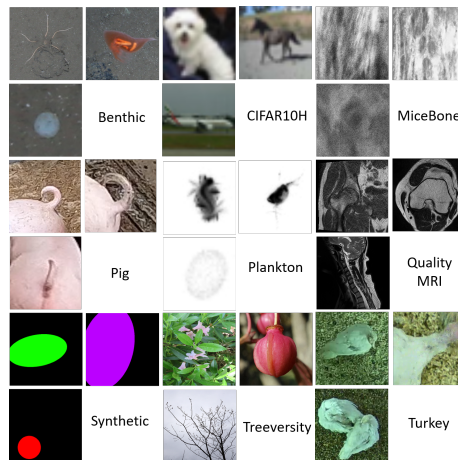


Figure 2: Three example images for all datasets. Details about the statistics of the dataset are given in Table 1.

Our benchmark is not only useful to evaluate existing methods, but will support research into algorithms for realistic datasets. Especially, it can bridge the research between semi-supervised learning and noise estimation based on realistic ambiguous noise patterns. We provide multiple algorithms as baselines and support the integration of more algorithms by common dataloaders for the two most popular deep learning frameworks: Tensorflow [1] and Pytorch [53]. We analyzed thousands of combinations of baseline methods, different initializations, and datasets. The obtained results confirm that the improvement of data quality leads to performance gains. Additionally, we investigated factors that influence the data quality and identified trends that lead to better learning of the underlying distribution.

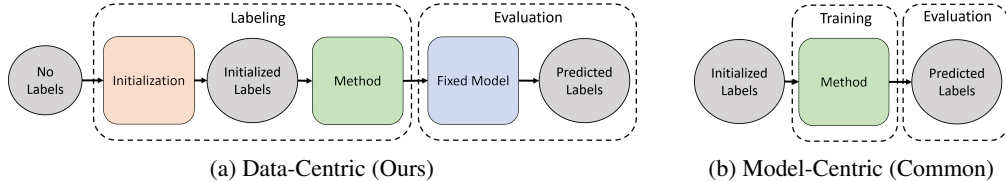


Figure 3: Comparison of our data-centric approach with the commonly used model-centric approach. The circles and arrows represent the available label information in addition to the corresponding images. The squares represent the methods which generate / change these label. There are two main differences between our and the common model-centric approach. Firstly, we also look at how the raw unlabeled data is initialized and thus how many annotations are required. Secondly, we use a fixed model to evaluate the output of the benchmarked method. These differences lead to a greater separation of data quality and method performance on the final scores on the predicted labels.

Our key contributions are: (1) We collected and created ten real-world image classification datasets with multiple annotations per image. These annotations allow a realistic simulation of noise patterns and will be helpful for future research in machine learning on real world data sets. (2) We provide a multi-domain benchmark based on these datasets for noisy and ambiguous label estimation. We implemented 20 methods as comparison. The benchmark also covers the topic of cost and bridges research between semi-supervised learning and ambiguous label estimation. (3) We show that one annotation per image is not enough because model performance improves as more labels are given for each input. We identify that the current focus on hard labels for classifications is ill-suited to learn the underlying ground truth distribution. A change in data preprocessing especially in annotation protocols could mitigate this and lead to less overconfident models.

1.1 Related Work

Human annotations of one image can differ due to complex reasons. Next to mere individual errors, cognitive sciences have shown that human judgement under uncertainty is driven by a subjective bias and the context of the annotation process [66]. As labeling relies on human perception, data quality problems, including issues with noisy and ambiguous labels, have been broadly discussed in the literature [68, 4, 54, 77, 3]. While voting strategies have proven to be robust tools to remove outlying annotation errors in a single label scenario, they also eliminate subjective disagreement, even in cases with more than just one valid interpretation [56]. The impact of this information loss has been discussed in numerous studies, indicating limitations in capturing ground truth by just one label [71, 17, 22, 6]. We empirically support these arguments across 9 datasets and 20 methods.

As label noise can severely degrade the classification performance [50], learning with flawed training data has become a substantial field of research in which numerous strategies have been proposed: while sample selection methods separate clean and noisy data by evaluating small-loss or disagreement [78, 79], correction methods aim at relabeling wrongly assigned labels by either learning class prototypes [24] or by pseudo-labeling strategies that utilize confident predictions [38]. Multiple methods have been proposed, but are often evaluated on synthetic noise [44, 40]. However, Wei et al. showed that synthetic noise is different from real noise by humans, which limits the generality of findings [77]. Gao et al. proposed synthetic annotators with individual labeling behavior instead of random noise to reduce uncertainty in predictions [20]. We go beyond this by using human annotations to reproduce realistic noise pattern and we do not only look at annotation errors but also at ambiguous annotations from subjective interpretations.

Datasets like CIFAR-10H [54] and CIFAR-10N [77] address the problem of realistic noise by providing multiple annotations per image for example of the original CIFAR-10 dataset. By doing so, both publications demonstrate an improved performance and a higher robustness, while also claiming that further research in dealing with human noise is still inevitable. The utilization of soft label distributions instead of hard one-hot label encodings enables the detailed representation of subjective disagreement and improves the generalization with ambiguous datasets [54, 5, 34]. In our benchmark, we extend this idea to eight diverse datasets apart from CIFAR-10 for a broader evaluation.

If we want to use multiple annotations per image, we need to consider the cost of such annotations to make it feasible in a project. Current research such as semi-supervised learning [12, 67, 64, 63] could

be used to analyze only a portion of the data with multiple annotations. However, approaches which combine noisy labels with semi-supervised learning have not been extended to real-world image classification tasks or do not consider the possibility that one labels is not enough to capture the ambiguity of subjectivity [42, 81, 76]. We provide with our benchmark the datasets and infrastructure to bridge the research between semi-supervised learning and noise estimation.

Prediction uncertainty can be attributed to unexplainable noise in the given training or test dataset (aleatoric uncertainty) or a wrong model inference (epistemic uncertainty) and it can be difficult to approximate and differentiate between them [58, 2, 72, 30]. Several real-world noisy datasets have been utilized as a foundation for classification benchmarks [41, 39, 54], Song et al. provide a current survey on datasets and methods [68]. Moreover, most robust methods are evaluated based on the test set accuracy [40, 68, 77, 59, 82]. However, even a small change in the structure or parameters of a method can directly impact its performance, limiting the comparability [31]. Other fields, such as Bayesian Neural Networks, address this issue by comparing results to statistical simulations, for example [27]. A recent benchmark [49] tries to overcome this issue by providing a baseline for noisy labels as a form of uncertainty estimation [14]. However, this benchmark relies on synthetic noise or noisy datasets without knowledge about the underlying ground truth distributions [41]. We use a data-centric approach to minimize the impact of implementation detail differences and measure the impact of the data indirectly during the Labeling phase by evaluating on a fixed model.

2 Benchmark

Our benchmark is divided into two major phases: *Labeling* and *Evaluation*. In alignment with the Data-Centric Idea [47], we separate the improvement of the data (Labeling) from the improvement of the models (Evaluation). The benchmark can be utilized to analyze a variety of research questions, but we focus on evaluating methods that estimate noisy or ambiguous labels.

We use the terms *noisy* and *ambiguous* throughout this work synonymously because we often do not differentiate between their cause during the annotation process. As mentioned above, these causes are errors or mistakes of human annotators which can be recovered for noisy label or noise. Subjective interpretations, imprecise task descriptions or poor image quality lead to ambiguous labels.

In general, we have an image dataset X with k known classes and use human annotations to approximate the image labels. Each image $x \in X$ has an often unknown soft ground truth label $\hat{l}_x \in [0, 1]^k$. Therefore, we use N hard human annotations $a_i \in \{0, 1\}^k$ with $i \in 1, \dots, N$ as estimates of \hat{l}_x . We assume that an average of annotations ($l_x = \sum_{i=0}^N \frac{a_i}{N}$) is an approximation of this target label \hat{l}_x as in [64]. Based on this definition, an annotation a_i or hard label sampled from the distribution l_x are in general of lower quality because they can not capture the aleatoric uncertainty of the soft label l_x . We split the data equally and randomly in five *folders* and ensure a similar class distribution between the folds as best as possible. For one run, we use three folds as training (X_T) and one fold each as validation (X_V) and test (X_E) data, respectively. We call such an assignment of folds to the training, validation and test data *slice*.

Labeling The Labeling phase consists of two steps. In the first step an initialization is used to get label estimates and in the second step, the benchmarked method Θ aims to improve these labels. As initialization, we acquire $m \in \mathbb{N}$ annotations for $n \in [0, 100]$ percent of the training and validation images.

We call the total number of required annotations *budget* $b = m \cdot n$ and report it as proportions of training and validation images ($|X_T \cup X_V|$). In general, a classification task gets easier with more annotations or a higher budget. Be aware that the same initialization results in the the same budget while the same budget can achieved by different initializations.

The used initialization schemes per method are defined later in this section. We chose fixed initialization schemes for better comparability between the methods. How these labels are improved by the method Θ is not restricted. However, annotations aside from the given initialization are not allowed to be used. Since we measure the quality by training a different fixed network in the next phase, a good label would be presumably as close as possible to l_x .

Table 1: Overview of the used datasets – # is an abbreviation for number. The class imbalance is given as the percentage of the smallest and largest class with regard to the complete dataset. The agreement is the percentage of annotations that agree with the majority vote. The scores ACC and \hat{ACC} are given for the supervised baseline across three test folds. The access describes if the (raw) data is available openly, requires permission (restricted) or was not previously available (N/A). In the last column, datasets with modifications to the original data are marked with X. A modification might be adding more annotations or crop images to a region of interest.

Name	# classes	Input size [px]	# Images	Class Imbalance [%]		Agreement [%]	# Annotations	ACC [%]	\hat{ACC} [%]	Access	Updated
				Smallest	Largest	Mean \pm STD	Mean \pm STD	Mean \pm STD	Mean \pm STD		
Benthic	10	112×112	4867	2.31	39.66	82.61 \pm 19.67	4.54 \pm 2.01	64.17 \pm 0.63	83.36 \pm 0.47	Restricted	X
CIFAR-10H	10	32×32	10000	9.88	10.16	95.44 \pm 8.91	51.10 \pm 1.54	90.75 \pm 0.39	95.72 \pm 0.12	Open	X
Mice Bone	3	224×224	7240	14.75	70.48	85.06 \pm 17.52	15.30 \pm 21.90	61.88 \pm 9.44	78.39 \pm 1.95	Restricted	X
Pig	4	96×96	10237	7.82	41.23	65.32 \pm 19.50	7.26 \pm 2.29	35.97 \pm 3.61	64.77 \pm 0.79	N/A	X
Plankton	10	96×96	12280	4.16	30.37	93.26 \pm 13.60	24.38 \pm 44.17	89.89 \pm 0.82	92.41 \pm 0.41	Restricted	X
Quality MRI	2	224×224	310	34.84	64.16	71.56 \pm 12.27	99.94 \pm 13.44	66.62 \pm 3.55	75.81 \pm 0.17	Restricted	X
Synthetic	6	224×224	15000	16.17	17.57	74.41 \pm 24.28	98.86 \pm 0.99	87.85 \pm 0.48	74.65 \pm 0.34	N/A	X
Treeversity#1	6	224×224	9489	9.98	30.67	88.60 \pm 16.13	14.78 \pm 7.06	79.50 \pm 1.53	89.20 \pm 0.31	Open	X
Treeversity#6	6	224×224	9826	8.77	31.26	66.53 \pm 19.48	35.45 \pm 11.47	56.71 \pm 4.89	68.88 \pm 0.72	Open	X
Turkey	3	192×192	8040	10.88	75.95	91.56 \pm 13.82	14.85 \pm 20.95	75.51 \pm 2.80	86.89 \pm 1.03	Restricted	X

Evaluation In the Evaluation phase, the model and its hyperparameters are fixed to measure only the impact of the provided labels ($\Theta(x)$). The training of this fixed model Φ is calculated on the provided $\Theta(x)$ with $x \in X_T$. The best network parameters during training are selected based on a minimal divergence between $\Phi(x)$ and $\Theta(x)$ with $x \in X_V$. The generalization is then tested by measuring the difference between $\Phi(x)$ and l_x for $x \in X_E$.

Metrics Kullback-Leibler divergence (KL) [35] between $\Phi(x)$ and l_x for $x \in X_E$ has been used as our main metric since it is an established method to measure the difference between two distributions [48]. We averaged in a 3-fold cross-validation per dataset for a high reproducibility. We used the three slices defined by $X_{V_i} = \{f_{i+1}\}$, $X_{E_i} = \{f_{i+2}\}$ and the rest as training ($X_{T_i} = \{f_i, f_{((i+2)\%5)+1}, f_{((i+3)\%5)+1}\}$ with % for modulo) for the folds f_1, \dots, f_5 with $i \in 1, 2, 3$ as the index of the slices. While KL directly allows to measure the desired distribution divergence, we provide additional metrics as comparisons. We evaluate the accuracy (ACC) and F1-Score ($F1$) between $\Phi(x)$ and l_x for $x \in X_E$ per class and report the mean across the classes, which is commonly called the macro value and allows evaluation even in the presence of class imbalance. We used the most likely class based on the evaluated distributions for these metrics. We analyze the calibration of the models by reporting the Expected Calibration Error (ECE) [23]. As reference, we provide all of these metrics also on the difference between the proposed label before the second training $\Theta(x)$ and the expected ground-truth l_x for $x \in X_E$. The metrics are noted as \hat{ACC} , $\hat{F1}$ and \hat{ECE} . We report the Cohen’s Kappa Score (κ) [46] as the measurement of the consistency of $\Theta(x)$ between the folds because more consistent labels result in higher model performance.

Datasets We include ten real-world classification datasets in our benchmark. Since we need multiple annotations per image for the evaluation of the quality of labels and this information is often not available in existing datasets or insufficient for our benchmark, we collected, adopted, or extended annotations of the following datasets. Their details are shortly described below, while their properties and exemplary images are shown in Table 1 and Figure 2, respectively. As presented, the datasets vary across all reported properties, giving an opportunity to comprehensively evaluate considered methods. More challenging datasets are characterized by a high-class imbalance, a low average agreement, or a low number of annotations per image. Detailed reports about the collection process and remaining dataset specifics are given in the supplementary.

1. *Benthic* depicts images from the seafloor and consists of underwater flora and fauna. We used annotations from [65, 37] but filtered for at least three annotations per object and cropped the main image to this object. We combined classes with too few images in agreement with domain experts. 2. *CIFAR-10H* is a variant of CIFAR-10 [32] introduced in [54]. Peterson et al. analyzed the underlying class distribution like us by reannotating the CIFAR-10 test set. In contrast to other variants like CIFAR-10N [77], this dataset provides more annotations per image. 3. *MiceBone* consists of Second-Harmonic-Generation images of collagen fibers in mice [60]. The raw images were preprocessed as described in [64]. Since there is a need for multiple annotations per image, we hired workers to increase their number by a factor of five. 4. *Pig* consists cropped tail images from European farms. The annotations were collected by hired workers with high domain knowledge. The goal is

Table 2: Overview of used methods grouped into supervised, semi-supervised and self-supervised. The second to fifth column describe if the method uses unlabeled data, makes noise estimation, what pretraining is the used input of the initialized dataset are hard or soft labels, respectively. The initialization schemes columns describe which schemes were evaluated for individual methods. The average runtime of the labeling phase is given in the last column.

Name	Unlabeled Data	Noise Estimation	Pretraining	Labels	Initialization Schemes				Avg. Runtime [h]
					SL	SL+	SSL	SSL+	
Baseline				Soft	X	X	X	X	0.00
Heteroscedastic (Het) [15]		X		Hard	X	X	X	X	0.50
SNGP [43]		X		Hard	X	X	X	X	0.29
ELR+ [44]		X	ImageNet	Hard	X	X	X	X	0.09
Mean-Teacher (Mean) [70]	X			Hard	X		X		1.08
Mean-Teacher (Mean+DC3) [64]	X			Hard	X		X		1.20
π -Model (π) [36]	X			Hard	X		X		1.03
π -Model (π +DC3) [64]	X			Hard	X		X		1.15
FixMatch [67]	X			Hard	X		X		4.53
FixMatch+DC3 [64]	X			Hard	X		X		4.01
Pseudo-Label (Pseudo v1) [38]	X			Hard	X		X		1.10
Pseudo-Label (Pseudo v1 +DC3) [64]	X			Hard	X		X		1.40
Pseudo-Label (Pseudo v2 hard) [38]	X		ImageNet	Hard	X	X	X	X	0.16
Pseudo-Label (Pseudo v2 soft) [38]	X		ImageNet	Soft	X	X	X	X	0.12
Pseudo-Label (Pseudo v2 not) [38]	X			Soft	X	X	X	X	0.12
DivideMix [40]	X	X	ImageNet	Hard	X	X	X	X	1.39
BYOL [21]	X		Self-Supervised	Hard	X		X		2.59
MOCOv2 [13]	X		Self-Supervised	Hard	X		X		7.94
SimCLR [11]	X		Self-Supervised	Hard	X		X		5.89
SWAV [10]	X		Self-Supervised	Hard	X		X		4.17

the classification of the injury degree of the tail. 5. *Plankton* is a collection of underwater plankton images with multiple annotations from citizen scientists [61]. We use the preprocessing described in [64]. 6. *QualityMRI* consists of human magnetic resonance images (MRI) with a varying quality and multiple subjective quality ratings gathered in tests with radiologists. It was introduced and evaluated in [51, 69]. 7. *Synthetic* dataset was generated for the purpose of this study. It consists of images that contain one blue, red, or green circle or ellipse on a black background. To create ambiguous images, we added color and axis interpolations of these classes. 8+9. *TreeVersity* is a publicly available crowdsourced dataset of plant images from the Arnold Arboretum of Harvard University³. In the crowdsourcing project, the images were tagged with a given set of labels. We used a simplified version with six classes where we combined classes with too few images. Only images with at least three tags were used. Tags are not the same as class labels, therefore, we provide two subsets of TreeVersity. In TreeVersity#1, we filtered for exactly one given tag of the six possible ones per user which is similar to a classification. In TreeVersity#6, we filtered for a maximum of six different tags which means we did not apply any restrictions. 10. *Turkey* is a dataset with images of turkeys and their injuries [74, 75]. We used the preprocessing described in [64] and extended the original annotations, increasing their number by a factor of five with hired workers.

Methods We compare a variety of recent supervised, self-supervised, and semi-supervised algorithms against our baseline. The baseline does not adjust the initialized dataset in the first phase in any way and just forwards these labels to the supervised training of the second phase. Thus it is equivalent to supervised learning in a model-centric benchmark. We selected the other methods based on their recency, access to authors code or reimplementations and if they are state-of-the-art or commonly used as comparisons in the literature. The *supervised* methods are Heteroscedastic [15], SNGP [43], and ELR+ [44]. The *semi-supervised* methods are Mean-Teacher [70], π -Model [36], FixMatch [67], DC3 [64], Pseudo-Label [38], and DivideMix [40]. The *self-supervised* methods are BYOL [21], MOCOv2 [13], SimCLR [11], and SWAV [10]. Detailed descriptions about most of them are given in [63] and their key characteristics are presented in Table 2. We use the reported hyperparameters for Imagenet [33] or Webvision [41] by the original authors to ensure a comparison out-of-the-box across different image domains. For DC3[64], we investigated the combinations with Mean-Teacher, π -Model, FixMatch, and Pseudo-Label. For Pseudo-Label, we used two different implementations (v1 and v2) and variants with or without pretraining and soft or hard labels as input. In total, this results in 20 investigated methods. For better referencing, we group them as described above but put methods that *use soft labels* into their own group.

³<https://arboretum.harvard.edu/research/data-resources/>

Initialization Schemes We investigated a fixed set of initialization schemes and note them m - n for m annotations for a subset of data with a relative size n . For easier reference, we group them as

- *Supervised Learning (SL)* 01-1.00
- *Supervised Learning+ (SL+)* 03-1.00, 05-1.00, 10-1.00
- *Semi-Supervised Learning (SSL)* 01-0.10, 01-0.20, 01-0.50
- *Semi-Supervised Learning (SSL+)* 10-0.10, 05-0.20, 02-0.50

Implementation Details The final results depend on a good set of fixed hyperparameters like learning rate for the model Φ for each dataset during the evaluation. Therefore, we determined them by applying Hyperopt [7] with 100 search trials across the same grid of parameters for all datasets. The target was the minimization of KL between $\Phi(x)$ and l_x for the baseline experiment with exactly ten annotations per image across one slice. We executed these and later experiments on an Nvidia RTX 3090 with 24GB VRAM or comparable hardware. Some combinations of models and input sizes could not fit on this hardware and therefore were ignored to keep the needed hardware to a minimum. Details about the used parameter grid are given in the supplementary. We ensure that all folds are randomly generated, while restrictions about similar images are considered. Without these restrictions, similar images, e.g., frames from the same camera might lead to an information leakage between the folds which would negatively influence the interpretability of the results.

3 Analysis

The evaluation was conducted across combinations of all datasets, methods, initialization schemes, and slices. A complete cross-combination would result in 5400 experiments from which we selected 3456 experiments to save resources since some combinations would not add more insights e.g. due to inferior performance of similar methods. A detailed overview of the initialization schemes used per method can be found in Table 2. As shown in Table 1, we have a large variability between the datasets, especially in ACC and \hat{ACC} that range from 36% to 96% for the baseline. Due to the fact that the baseline does not adjust the initialization, \hat{ACC} can be seen as the performance of humans in improving the labels for the given budget. The datasets Benthic, MiceBone, Pig, Treeversity#6, and Turkey have an over 10% lower ACC than the expected \hat{ACC} , which marks them as particularly challenging for the model. Moreover, the datasets Benthic, MiceBone, Pig, QualitMRI, and Treeversity#6 have an \hat{ACC} of lower than 85% which marks them as difficult even for humans. The \hat{ACC} of Synthetic is even lower due to the artificially created labels. Due to this variability, an average across the scores can be misleading. For this reason, we report the median in this paper and report the full results including the standard error of the mean (SEM) in the supplementary.

What metrics should we use? We analyzed the correlations between our metrics to determine which contain the same or similar information and which are complementary. All calculated Pearson correlation coefficients have a p-value < 0.01 and the four strongest correlations are ACC vs. $F1$ (0.99), KL vs. ECE (0.68) $F1$ vs. κ (0.77) and ACC vs. κ (0.77). The other correlations are around -0.5. Selected correlations are illustrated in Figure 4 and additional graphics and analysis are given in the supplementary. $F1$ balances the precision and recall but in our experiments we see almost identical values to ACC which we credit to the averaging per class. This means we only need to concentrate on ACC as a classification score. Overconfident models are a problem of modern machine learning [23] and the higher correlation between KL and ECE compared to any of the two with ACC , $F1$ or κ indicates that our focus on classification metrics like ACC and $F1$ could be the issue. Only metrics like KL and ECE consider the complete distribution and which justifies using mainly KL for the evaluation of this benchmark.

One annotation is not enough It is to be expected that more and better data should lead to increased performance which we quantify in Figure 5a. It can be seen that all metrics improve with an increased budget in the form of more annotated data or more annotations per image. However, the impact is lower for more annotations per image. For example, ACC increases from around 55% to 69% for the full supervision. Up to 10 annotations per image increase the score only to around 72%. This difference can be explained by the fact that additional annotations are most valuable to improve uncertain labels. In alignment with previous research [71, 22, 6], these results across thousands of

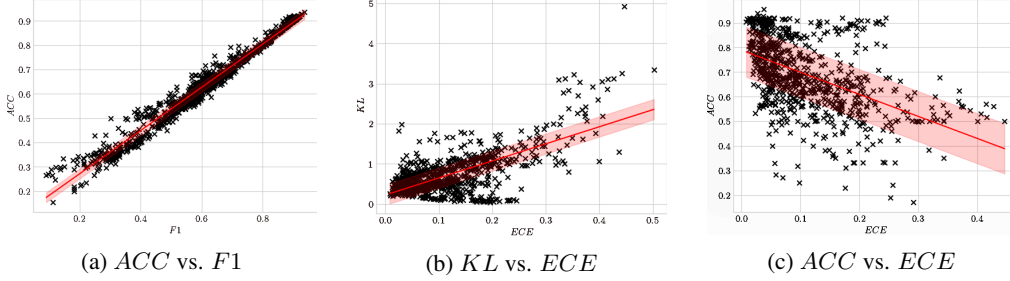


Figure 4: Correlations between selected metrics across all experiments. The red line represents the linear regression between the metrics and the light red area the mean absolute error of the regression.

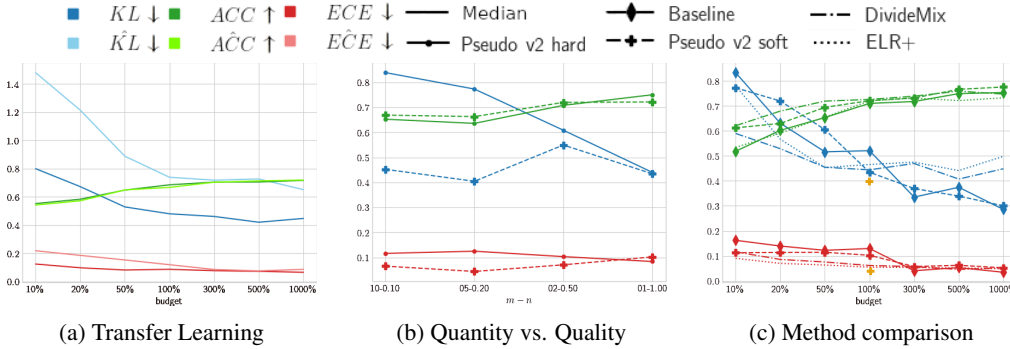


Figure 5: Analysis of all or selected methods across different budgets or initialization schemes. For details about the definitions see section 2. The orange crosses in (c) represent the best performance of Pseudo v2 soft with another initialization scheme see (b). The budget is increased by an raised portion of labeled data (n) until 1.00 and then increased further by using additionally multiple annotations per image (m).

experiments empirically justify that one annotation is not enough to capture the ground-truth of an item. Some improvements can be gained from correction annotation errors via a majority vote but the high disagreement and low \hat{ACC} of the baseline on some datasets support the hypothesis that ambiguous annotations are a main source for the improvement. This ambiguity can not be described with a single hard majority vote and thus highlights the importance of using soft labels. Additionally, we see that KL is about half as small as \hat{KL} , ECE is around 3-10% lower than \hat{ECE} and ACC is 1-2% better than \hat{ACC} . As shown previously by Hinton et al. [26, 12] the knowledge distillation via a neural network into soft labels can be beneficial for ACC . We find the impact for metrics like KL and ECE even higher which supports our design of a two-phase benchmark.

Limits of current state-of-the-art To determine the best-performing state-of-the-art method, we gathered their relative improvements over the baseline in Table 3a. The best algorithm for each type of the soft, semi-supervised, supervised, self-supervised approaches based on the average performance across the budgets of 10%, 100%, and 1000% are Pseudo v2 soft, DivideMix, ELR+, and Mocov2, respectively. We visualize the best three of them in Figure 5c and give detailed results across the datasets for the budget 100% in Table 3b. The full results can be found in the supplementary. All top three methods are pretrained on ImageNet and outperform the rest in the field they were designed for. DivideMix is the best during partial supervision (budget < 100%), ELR+ is more noise robust (budget > 100%), and Pseudo v2 soft has the lowest KL score (budget > 100%). It is important to note that ImageNet pretraining leads to improvements on many datasets (see Pseudo v2 not in the supplementary) but also to worse results on others. It needs to be investigated if other pretraining such as CLIP [55] or unsupervised pretraining on larger datasets [12, 57] could improve on these results. Overall, the current state-of-the-art methods are insufficient for a label preprocessing across all domains. For a high budget any investigated method is worse than the supervised baseline without adjustments of the initialized dataset which shows the lack of appropriate algorithms for such budgets.

Table 3: Results for the best performing methods – The best metric is marked bold while the 2nd and 3rd best are italic. Only methods with at least one top3 ranking across the budgets are presented. The full results are in the supplementary. (a) show the relative improvement over the baseline. (b) are detailed results for the budget of 100% across all datasets.

(a) Improvements						(b) Details 100% Budget											
Budget	10%		100%		1000%		Dataset	Benthic	CIFAR10H	MiceBone	Pig	Plankton	QualityMRI	Synthetic	Treeveristy#1	Treeveristy#6	Turkey
	Median	Mean \pm SEM	Median	Mean \pm SEM	Median	Mean \pm SEM											
ELR+	-0.16	-0.59 \pm 0.22	-0.13	-0.17 \pm 0.06	<i>0.15</i>	<i>0.24 \pm 0.06</i>	Baseline	1.17 \pm 0.04	0.41 \pm 0.02	0.55 \pm 0.06	0.75 \pm 0.05	0.34 \pm 0.02	1.73 \pm 0.48	0.08 \pm 0.01	0.49 \pm 0.04	1.02 \pm 0.03	0.40 \pm 0.08
SNGP	-0.26	-0.59 \pm 0.27	0.00	-0.15 \pm 0.08	0.20	<i>0.26 \pm 0.04</i>	ELR+	0.70 \pm 0.01	0.29 \pm 0.02	0.29 \pm 0.01	<i>0.62 \pm 0.09</i>	0.24 \pm 0.03	1.44 \pm 0.83	0.18 \pm 0.02	0.46 \pm 0.01	0.47 \pm 0.05	0.52 \pm 0.05
DivideMix	-0.21	-0.78 \pm 0.25	-0.03	-0.17 \pm 0.08	<i>0.19</i>	<i>0.31 \pm 0.07</i>	SNGP	1.11 \pm 0.05	0.38 \pm 0.01	0.56 \pm 0.14	0.77 \pm 0.07	0.33 \pm 0.02	0.25 \pm 0.14	0.10 \pm 0.00	0.46 \pm 0.01	1.07 \pm 0.05	0.42 \pm 0.08
Mean	-0.14	-0.59 \pm 0.22	<i>-0.12</i>	-0.22 \pm 0.08	N/A	N/A	DivideMix	0.87 \pm 0.07	0.36 \pm 0.02	<i>0.48 \pm 0.05</i>	0.95 \pm 0.04	0.34 \pm 0.01	0.46 \pm 0.26	0.33 \pm 0.00	0.47 \pm 0.01	0.62 \pm 0.05	0.43 \pm 0.08
π	-0.33	-0.63 \pm 0.19	-0.06	-0.17 \pm 0.05	N/A	N/A	Mean	0.80 \pm 0.06	0.28 \pm 0.02	<i>0.48 \pm 0.02</i>	<i>0.64 \pm 0.03</i>	0.32 \pm 0.01	<i>0.15 \pm 0.11</i>	0.09 \pm 0.01	0.61 \pm 0.01	0.52 \pm 0.03	0.75 \pm 0.07
π +DC3	-0.32	-0.62 \pm 0.20	-0.10	-0.22 \pm 0.06	N/A	N/A	π	<i>0.71 \pm 0.02</i>	0.33 \pm 0.02	<i>0.48 \pm 0.00</i>	0.83 \pm 0.18	<i>0.40 \pm 0.02</i>	0.98 \pm 0.04	0.08 \pm 0.01	0.52 \pm 0.01	<i>0.51 \pm 0.03</i>	0.55 \pm 0.01
Pseudo v2 hard	-0.30	-0.39 \pm 0.16	-0.03	-0.19 \pm 0.08	0.19	0.28 \pm 0.04	π +DC3	<i>0.72 \pm 0.06</i>	0.30 \pm 0.02	0.39 \pm 0.04	0.67 \pm 0.06	<i>0.29 \pm 0.07</i>	0.88 \pm 0.34	0.08 \pm 0.00	0.48 \pm 0.01	<i>0.49 \pm 0.06</i>	0.44 \pm 0.08
Pseudo v2 soft	-0.28	-0.40 \pm 0.19	-0.04	-0.17 \pm 0.06	0.01	0.00 \pm 0.02	Pseudo v2 hard	0.97 \pm 0.10	0.43 \pm 0.02	0.45 \pm 0.10	0.67 \pm 0.04	0.31 \pm 0.03	0.29 \pm 0.05	0.10 \pm 0.01	0.46 \pm 0.03	0.99 \pm 0.09	0.39 \pm 0.05
MOCOv2	-0.29	<i>-0.63 \pm 0.22</i>	-0.08	-0.13 \pm 0.10	N/A	N/A	Pseudo v2 soft	1.00 \pm 0.08	0.41 \pm 0.02	0.40 \pm 0.08	0.70 \pm 0.06	0.32 \pm 0.06	0.62 \pm 0.16	0.10 \pm 0.01	0.46 \pm 0.01	0.83 \pm 0.13	0.37 \pm 0.08
							MOCOv2	0.91 \pm 0.05	0.98 \pm 0.02	<i>0.37 \pm 0.04</i>	0.56 \pm 0.01	0.52 \pm 0.01	0.29 \pm 0.11	0.13 \pm 0.01	0.80 \pm 0.03	0.61 \pm 0.01	0.42 \pm 0.08

Moreover, an average better performance does not mean that the gains are equal across all datasets. For example, ELR+ has the lowest KL at a budget of 100% for five out of ten datasets but on the QualityMRI dataset, it is among the worst methods. This means while some methods might work on some datasets they might not generalize to other datasets. Overall, we see the highest KL for the datasets Benthic, Pig, Quality MRI and Treeveristy#6 which also have the lowest agreement as seen in Table 1 except for the synthetic dataset. These datasets also show the largest variance in results across the methods. We conclude that the impact of the data is larger than the impact of the current preprocessing of state-of-the-art methods. This highlights the importance for investigating the data and label generation more if they are more impactful than the method itself.

While a higher budget leads to improved metrics, it also matters how it is used. In Figure 5b, we investigated the impact on KL and ACC for a budget of 100% for Pseudo-Label using hard or soft labels. We find that the accuracy is comparable between the methods and increases with a rising percentage of labeled data (m). For hard labels, the KL improves equally. If we use soft labels for training, we see lower results for 05-0.20 and 10-0.10. We conclude that we should investigate more how we distribute our budget if increasing it is not an option.

4 Discussion

Overall, we can confirm several previous research hypotheses while identifying missing information and thus new research opportunities with our novel datasets and benchmark.

We can demonstrate that data quality positively impacts the classifications scores like ACC and $F1$ and distribution-based scores like KL and ECE . Knowledge distillation can improve the approximation of the underlying distribution further. We agree with previous research [71, 17, 22, 6] that one annotation is not enough and we need to use soft labels to handle ambiguous data. KL and ECE are highly correlated (0.7) and are improved more when using soft labels. We believe that focusing on learning the real distribution and thus minimizing KL can lead to less overconfident models. Using soft labels as input seems to be crucial for achieving this since hard labels and classification metrics like ACC lead to models which slightly ignore the real ground truth distribution.

Nevertheless, most of the investigated state-of-the-art method do not use soft labels and often interpret noise only as errors in the annotation process. These issues need to be addressed in future research and a simple method like Pseudo v2 soft illustrates how the KL score can be lowered with this approach. For the largest budget, the baseline is the best model and even special noise estimation algorithms like ELR+ [44] and SNGP [43] can not achieve better results. We see a high variance across the datasets for different methods in our benchmark. However, we need methods which work across a variety of domains out-of-the-box to allow an easy application to current research question in other domains. Another practical issue is that we need to find solutions for acquiring soft labels even with a limited budget. In many research projects, it is difficult to annotate thousands of images with domain experts and annotating them multiple times would only increase the costs further. Thus, we need to bridge the research in semi-supervised learning and ambiguous and noise estimation. Such combinations could allow the usage of soft labels on a subset of images and simultaneously determine annotation errors. Our benchmark and datasets allowed the identification of these issues and thus could also be used to research new methods to solve these issues. We are confident that our benchmark and datasets can facilitate the bridged research on the topic of semi-supervised learning and ambiguous image estimation for real world image classification problems.

Impact This work as a benchmark provides ten datasets and a detailed evaluation across 20 algorithms on this benchmark. The provided data can allow the investigation of research questions on the topics of e.g. noise estimation, data annotation scheme, or realistic semi-supervised learning. This work is intended to allow and spark future research and thus no direct social impacts are expected. However, this basic research is time and resource-consuming. For the final evaluation, we conducted experiments with about 5500 GPU hours which equals around 600kg CO_2 . For this reason, we limited the evaluation always to necessary elements when possible in order to not increase the needed GPU hours further.

Limitations The 20 investigated algorithms are only evaluated with one fixed set of hyperparameters across different datasets during the labeling phase. For optimal performance, a tuning per algorithm would have been required. We were interested in the general performance out-of-the-box and therefore neglected this issue due to resource minimization. The researched datasets are all below 15,000 images and the unsupervised learning potential on millions of images could not be investigated. We want to provide a detailed analysis in relation to the underlying distribution l_x per image which is only possible with multiple annotations per image. For larger datasets, this effort was just not feasible. Classification with hundreds or more classes are also not feasible because the annotation costs increase with the number of classes. As described above we conducted more than a thousand experiments but we had to select and combine several results in a comprehensive manner in this paper. These aggregations can not capture all details. Much more detailed analysis e.g., per dataset would be possible and thus we included all raw results in the supplementary. Due to the fixed initialization scheme, we can not investigate active learning approaches. However, this restriction is chosen to allow a better comparability and future researchers could decide against such a restriction.

Conclusion In alignment with previous research, we show that one annotation is not enough to handle ambiguous and noisy images and their underlying ground truth distribution. Multiple annotations and some kind of soft label are required to capture the difference in the images. Future research needs to investigate in more detail how annotations are being created, including annotation costs. We show that current state-of-the-art can help under certain budget or dataset constraints. However, methods with consistent results across a variety of datasets and budgets are missing. We release all datasets and the benchmark publicly to enrich future research on these topics.

Acknowledgments and Disclosure of Funding

We thank Mark Collier for his valuable feedback and discussion about the benchmark. We thank the annotators Kristina Ahlqvist, Daniel Grundig, Stine Heindorff, Jana Krambeck, Kathrin Körner, Richard Lange, Miina Tuominen-Brinkas and Emirhan Ustalar for their valuable work.

We acknowledge funding of L. Schmarje by the ARTEMIS project (Grant number 01EC1908E) funded by the Federal Ministry of Education and Research (BMBF, Germany). R. Kiko also acknowledges support via a “Make Our Planet Great Again” grant of the French National Research Agency within the “Programme d’Investissements d’Avenir”; reference “ANR-19-MPGA-0012”. V. Grossmann is employed with funds provided by Kiel Marine Science (KMS) and Future Ocean Network (FON) by Kiel University. Funds to conduct the PlanktonID project were granted to R. Kiko and R. Koch (CP1733) by the Cluster of Excellence 80 “Future Ocean” within the framework of the Excellence Initiative by the Deutsche Forschungsgemeinschaft (DFG) on behalf of the German federal and state governments. Turkey data set was collected as part of the project “RedAlert – detection of pecking injuries in turkeys using neural networks” which was supported by the “Animal Welfare Innovation Award” of the “Initiative Tierwohl”.

References

- [1] Martin Marten, Armin Abadi, Paul Barham, Jianmin Chen, Zhifeng Chen, Andy Davis, Jeffrey Dean, Matthieu Devin, Sanjay Ghemawat, Geoffrey Irving, Michael Isard, Manjunath Kudler, Josh Levensberg, Rajat Monga, Sherry Moore, Derek Murray, Benoit Steiner, Paul Tucker, Vijay Vasudevan, Pete Warden, Martin Wicke, Yuan Yu, Xiaoqiang Zheng, and Others. TensorFlow: A System for Large-Scale Machine Learning. In *12th USENIX symposium on operating systems design and implementation (OSDI 16)*, pages 265–283, 2016.

- [2] Moloud Abdar, Farhad Pourpanah, Sadiq Hussain, Dana Rezazadegan, Li Liu, Mohammad Ghavamzadeh, Paul Fieguth, Xiaochun Cao, Abbas Khosravi, U. Rajendra Acharya, Vladimir Makarenkov, and Saeid Nahavandi. A review of uncertainty quantification in deep learning: Techniques, applications and challenges. *Information Fusion*, 76:243–297, 2021. ISSN 15662535. doi: 10.1016/j.inffus.2021.05.008.
- [3] P. F.E. E E Addison, D. J. Collins, R. Trebilco, S. Howe, N. Bax, P. Hedge, G. Jones, P. Miloslavich, C. Roelfsema, M. Sams, R. D. Stuart-Smith, P. Scanes, P. Von Baumgarten, and A. McQuatters-Gollop. A new wave of marine evidence-based management: Emerging challenges and solutions to transform monitoring, evaluating, and reporting. *ICES Journal of Marine Science*, 75(3):941–952, 2018. ISSN 10959289. doi: 10.1093/icesjms/fsx216.
- [4] Görkem Algan and Ilkay Ulusoy. Image Classification with Deep Learning in the Presence of Noisy Labels: A Survey. *Knowledge-Based Systems*, 2020. ISSN 23318422. doi: 10.1016/j.knosys.2021.106771.
- [5] Hessem Bagherinezhad, Maxwell Horton, Mohammad Rastegari, and Ali Farhadi. Label refinery: Improving imagenet classification through label progression. *arXiv preprint arXiv:1805.02641*, 2018.
- [6] Valerio Basile, Michael Fell, Tommaso Fornaciari, Dirk Hovy, Silviu Paun, Barbara Plank, Massimo Poesio, and Alexandra Uma. We Need to Consider Disagreement in Evaluation. In *BPPF*, 2021.
- [7] James Bergstra, Daniel Yamins, and David Cox. Making a science of model search: Hyperparameter optimization in hundreds of dimensions for vision architectures. In *International conference on machine learning*, pages 115–123. PMLR, 2013.
- [8] Lucas Beyer, Olivier J. Hénaff, Alexander Kolesnikov, Xiaohua Zhai, and Aäron van den Oord. Are we done with ImageNet? *arXiv preprint arXiv:2006.07159*, 2020.
- [9] J Brünger, S Dippel, R Koch, and C Veit. ‘Tailception’: using neural networks for assessing tail lesions on pictures of pig carcasses. *Animal*, 13(5):1030–1036, 2019. ISSN 17517311. doi: 10.1017/S1751731118003038.
- [10] Mathilde Caron, Priya Goyal, Ishan Misra, Piotr Bojanowski, Julien Mairal, and Armand Joulin. Unsupervised Learning of Visual Features by Contrasting Cluster Assignments. *Proceedings of Advances in Neural Information Processing Systems (NeurIPS)*, 2020. ISSN 23318422.
- [11] Ting Chen, Simon Kornblith, Mohammad Norouzi, and Geoffrey Hinton. A Simple Framework for Contrastive Learning of Visual Representations. *arXiv preprint arXiv:2002.05709*, (PMLR): 1597–1607, 2020. ISSN 23318422.
- [12] Ting Chen, Simon Kornblith, Kevin Swersky, Mohammad Norouzi, and Geoffrey Hinton. Big Self-Supervised Models are Strong Semi-Supervised Learners. *Advances in Neural Information Processing Systems 33 pre-proceedings (NeurIPS 2020)*, 2020.
- [13] Xinlei Chen, Haoqi Fan, Ross Girshick, and Kaiming He. Improved Baselines with Momentum Contrastive Learning. *arXiv preprint arXiv:2003.04297*, 2020.
- [14] Mark Collier, Basil Mustafa, Efi Kokiopoulou, Rodolphe Jenatton, and Jesse Berent. A Simple Probabilistic Method for Deep Classification under Input-Dependent Label Noise. *arXiv preprint arXiv:2003.06778*, 2020.
- [15] Mark Collier, Basil Mustafa, Efi Kokiopoulou, Rodolphe Jenatton, and Jesse Berent. Correlated Input-Dependent Label Noise in Large-Scale Image Classification. *Proceedings of the IEEE/CVF Conference on Computer Vision and Pattern Recognition*, (c):1551–1560, 2021.
- [16] Phil Culverhouse, Robert Williams, Beatriz Reguera, Vincent Herry, and Sonsoles González-Gil. Do experts make mistakes? A comparison of human and machine identification of dinoflagellates. *Marine Ecology Progress Series*, 247:17–25, 2003. doi: 10.3354/meps247017.
- [17] Aida Mostafazadeh Davani, Mark Díaz, and Vinodkumar Prabhakaran. Dealing with Disagreements: Looking Beyond the Majority Vote in Subjective Annotations. 2021.

- [18] Jeffrey De Fauw, Joseph R Ledsam, Bernardino Romera-Paredes, Stanislav Nikolov, Nenad Tomasev, Sam Blackwell, Harry Askham, Xavier Glorot, Brendan O’Donoghue, Daniel Visentin, Others, Brendan O’Donoghue, Daniel Visentin, and Others. Clinically applicable deep learning for diagnosis and referral in retinal disease. *Nature medicine*, 24(9):1342–1350, 2018.
- [19] Laurens der Maaten and Geoffrey Hinton. Visualizing data using t-SNE. *Journal of machine learning research*, 9(11), 2008.
- [20] Zhengqi Gao, Fan-Keng Sun, Mingran Yang, Sucheng Ren, Zikai Xiong, Marc Engeler, Antonio Burazer, Linda Wildling, Luca Daniel, and Duane S. Boning. Learning from Multiple Annotator Noisy Labels via Sample-wise Label Fusion. 2022.
- [21] Jean-Bastien Grill, Florian Strub, Florent Altché, Corentin Tallec, Pierre H. Richemond, Elena Buchatskaya, Carl Doersch, Bernardo Avila Pires, Zhaohan Daniel Guo, Mohammad Gheshlaghi Azar, Bilal Piot, Koray Kavukcuoglu, Rémi Munos, and Michal Valko. Bootstrap your own latent: A new approach to self-supervised Learning. *Advances in Neural Information Processing Systems 33 pre-proceedings (NeurIPS 2020)*, 2020.
- [22] Vasco Grossmann, Lars Schmarje, and Reinhard Koch. Beyond Hard Labels: Investigating data label distributions. *ICML 2022 Workshop DataPerf: Benchmarking Data for Data-Centric AI*, 2022.
- [23] Chuan Guo, Geoff Pleiss, Yu Sun, and Kilian Q Weinberger. On calibration of modern neural networks. In *International Conference on Machine Learning*, pages 1321–1330. PMLR, 2017.
- [24] Jiangfan Han, Ping Luo, and Xiaogang Wang. Deep self-learning from noisy labels. In *Proceedings of the IEEE/CVF international conference on computer vision*, pages 5138–5147, 2019.
- [25] Tony Hey. The Fourth Paradigm – Data-Intensive Scientific Discovery. In *Communications in Computer and Information Science*, pages 1–1. 2012. doi: 10.1007/978-3-642-33299-9_1.
- [26] Geoffrey Hinton, Oriol Vinyals, and Jeff Dean. Distilling the Knowledge in a Neural Network. 2015.
- [27] Pavel Izmailov, Sharad Vikram, Matthew D. Hoffman, and Andrew Gordon Gordon Wilson. What Are Bayesian Neural Network Posteriors Really Like? *International Conference on Machine Learning*, pages 4629–4640, 2021.
- [28] Alain Jungo, Raphael Meier, Ekin Ermis, Marcela Blatti-Moreno, Evelyn Herrmann, Roland Wiest, and Mauricio Reyes. On the effect of inter-observer variability for a reliable estimation of uncertainty of medical image segmentation. In *Medical Image Computing and Computer Assisted Interventions, MICCAI*, pages 682–690. Springer, 2018.
- [29] D Karimi, G Nir, L Fazli, P C Black, L Goldenberg, and S E Salcudean. Deep Learning-Based Gleason Grading of Prostate Cancer From Histopathology Images—Role of Multiscale Decision Aggregation and Data Augmentation. *IEEE Journal of Biomedical and Health Informatics*, 24(5):1413–1426, 2020. doi: 10.1109/JBHI.2019.2944643.
- [30] Alex Kendall and Yarin Gal. What Uncertainties Do We Need in Bayesian Deep Learning for Computer Vision? 2017.
- [31] Alexander Kolesnikov, Xiaohua Zhai, and Lucas Beyer. Revisiting self-supervised visual representation learning. In *Proceedings of the IEEE conference on Computer Vision and Pattern Recognition*, pages 1920–1929, 2019.
- [32] Alex Krizhevsky, Geoffrey Hinton, and Others. Learning multiple layers of features from tiny images. Technical report, 2009.
- [33] Alex Krizhevsky, Ilya Sutskever, and Geoffrey E. Hinton. Imagenet classification with deep convolutional neural networks. In *Advances in neural information processing systems*, volume 60, pages 1097–1105. Association for Computing Machinery, 2012. doi: 10.1145/3065386.

- [34] Ujwal Krothapalli and A Lynn Abbott. Adaptive label smoothing. *arXiv preprint arXiv:2009.06432*, 2020.
- [35] S Kullback and R A Leibler. On Information and Sufficiency. *Ann. Math. Statist.*, 22(1):79–86, 1951. doi: 10.1214/aoms/1177729694.
- [36] Samuli Laine and Timo Aila. Temporal ensembling for semi-supervised learning. In *International Conference on Learning Representations*, 2017.
- [37] Daniel Langenkämper, Robin van Kevelaer, Autun Purser, and Tim W Nattkemper. Gear-Induced Concept Drift in Marine Images and Its Effect on Deep Learning Classification. *Frontiers in Marine Science*, 7, 2020. ISSN 2296-7745. doi: 10.3389/fmars.2020.00506.
- [38] Dong-Hyun Lee. Pseudo-label: The simple and efficient semi-supervised learning method for deep neural networks. In *Workshop on challenges in representation learning, ICML*, volume 3, page 2, 2013.
- [39] Kuang-Huei Lee, Xiaodong He, Lei Zhang, and Linjun Yang. Cleannet: Transfer learning for scalable image classifier training with label noise. In *Proceedings of the IEEE conference on computer vision and pattern recognition*, pages 5447–5456, 2018.
- [40] Junnan Li, Richard Socher, and Steven C. H. Hoi. DivideMix: Learning with Noisy Labels as Semi-supervised Learning. In *International Conference on Learning Representations*, pages 1–14, 2020.
- [41] Wen Li, Limin Wang, Wei Li, Eirikur Agustsson, and Luc Van Gool. WebVision Database: Visual Learning and Understanding from Web Data. 2017.
- [42] Zhenghua Li, Min Zhang, and Wenliang Chen. Ambiguity-aware Ensemble Training for Semi-supervised Dependency Parsing. In *Proceedings of the 52nd Annual Meeting of the Association for Computational Linguistics (Volume 1: Long Papers)*, pages 457–467. Association for Computational Linguistics, 2014. doi: 10.3115/v1/P14-1043.
- [43] Jeremiah Liu, Zi Lin, Shreyas Padhy, Dustin Tran, Tania Bedrax Weiss, and Balaji Lakshminarayanan. Simple and principled uncertainty estimation with deterministic deep learning via distance awareness. *Advances in Neural Information Processing Systems*, 33:7498–7512, 2020.
- [44] Sheng Liu, Jonathan Niles-Weed, Narges Razavian, and Carlos Fernandez-Granda. Early-Learning Regularization Prevents Memorization of Noisy Labels. *Advances in neural information processing systems*, 33:20331–20342, 2020.
- [45] Adam Marcu, Antonia; Prugel-Bennett. On Data-centric Myths. *NeurIPS 2021 Data-centric AI workshop*, 2021.
- [46] Mary L McHugh. Interrater reliability: the kappa statistic. *PubMed, Biochemia*(3):276–82, 2012.
- [47] Mohammad Motamedi, Nikolay Sakharnykh, and Tim Kaldewey. A Data-Centric Approach for Training Deep Neural Networks with Less Data. *NeurIPS 2021 Data-centric AI workshop*, 2021.
- [48] Kevin P Murphy. *Machine learning: a probabilistic perspective*. MIT press, 2012.
- [49] Zachary Nado, Neil Band, Mark Collier, Josip Djolonga, Michael W Dusenberry, Sebastian Farquhar, Angelos Filos, Marton Havasi, Rodolphe Jenatton, Ghassen Jerfel, and Others. Uncertainty Baselines: Benchmarks for uncertainty & robustness in deep learning. *arXiv preprint arXiv:2106.04015*, 2021.
- [50] Curtis G. Northcutt, Anish Athalye, and Jonas Mueller. Pervasive Label Errors in Test Sets Destabilize Machine Learning Benchmarks. *35th Conference on Neural Information Processing Systems (NeurIPS 2021) Track on Datasets and Benchmarks*, 2021.
- [51] Rafal Obuchowicz, Mariusz Oszust, and Adam Piorkowski. Interobserver variability in quality assessment of magnetic resonance images. *BMC Medical Imaging*, 20(1):109, 2020. ISSN 1471-2342. doi: 10.1186/s12880-020-00505-z.

- [52] E.A. A Ooms, H.M. M Zonderland, M.J.C. J C Eijkemans, M. Kriege, B. Mahdavian Delavary, C.W. W Burger, and A.C. C Ansink. Mammography: Interobserver variability in breast density assessment. *The Breast*, 16(6):568–576, 2007. ISSN 09609776. doi: 10.1016/j.breast.2007.04.007.
- [53] Adam Paszke, Sam Gross, Francisco Massa, Adam Lerer, James Bradbury, Gregory Chanan, Trevor Killeen, Zeming Lin, Natalia Gimelshein, Luca Antiga, Alban Desmaison, Andreas Kopf, Edward Yang, Zachary DeVito, Martin Raison, Alykhan Tejani, Sasank Chilamkurthy, Benoit Steiner, Lu Fang, Junjie Bai, and Soumith Chintala. PyTorch: An Imperative Style, High-Performance Deep Learning Library. In *Advances in Neural Information Processing Systems 32*, pages 8024–8035. Curran Associates, Inc., 2019.
- [54] Joshua Peterson, Ruairidh Battleday, Thomas Griffiths, and Olga Russakovsky. Human uncertainty makes classification more robust. *Proceedings of the IEEE International Conference on Computer Vision*, 2019-Octob:9616–9625, 2019. ISSN 15505499. doi: 10.1109/ICCV.2019.00971.
- [55] Alec Radford, Jong Wook Kim, Chris Hallacy, Aditya Ramesh, Gabriel Goh, Sandhini Agarwal, Girish Sastry, Amanda Askell, Pamela Mishkin, Jack Clark, Gretchen Krueger, and Ilya Sutskever. Learning Transferable Visual Models From Natural Language Supervision. 2021.
- [56] Sai Rajeswar, Pau Rodriguez, Soumye Singhal, David Vazquez, and Aaron Courville. Multi-label iterated learning for image classification with label ambiguity. In *Proceedings of the IEEE/CVF Conference on Computer Vision and Pattern Recognition*, pages 4783–4793, 2022.
- [57] Pierre H. Richemond, Jean-Bastien Grill, Florent Altché, Corentin Tallec, Florian Strub, Andrew Brock, Samuel Smith, Soham De, Razvan Pascanu, Bilal Piot, and Michal Valko. BYOL works even without batch statistics. *arXiv preprint arXiv:2010.10241*, 2020.
- [58] Abhishek Singh Sambyal, Narayanan C. Krishnan, and Deepti R. Bathula. Towards Reducing Aleatoric Uncertainty for Medical Imaging Tasks. 2021.
- [59] Monty Santarossa, Ayse Kilic, Claus von der Burchard, Lars Schmarje, Claudius Zelenka, Stefan Reinhold, Reinhard Koch, and Johann Roider. MedRegNet: unsupervised multimodal retinal-image registration with GANs and ranking loss. In *Medical Imaging 2022: Image Processing*, volume 12032, pages 321–333. SPIE, 2022.
- [60] Lars Schmarje, Claudius Zelenka, Ulf Geisen, Claus-C. Glüer, and Reinhard Koch. 2D and 3D Segmentation of uncertain local collagen fiber orientations in SHG microscopy. *DAGM German Conference of Pattern Regocnition*, 11824 LNCS(November):374–386, 2019. ISSN 23318422. doi: 10.1007/978-3-030-33676-9_26.
- [61] Lars Schmarje, Johannes Brünger, Monty Santarossa, Simon-Martin Schröder, Rainer Kiko, and Reinhard Koch. Fuzzy Overclustering: Semi-Supervised Classification of Fuzzy Labels with Overclustering and Inverse Cross-Entropy. *Sensors*, 21(19):6661, 2021. ISSN 1424-8220. doi: 10.3390/s21196661.
- [62] Lars Schmarje, Yuan-Hong Liao, and Reinhard Koch. A Data-Centric Image Classification Benchmark. *NeurIPS 2021 Data-centric AI workshop*, 2021.
- [63] Lars Schmarje, Monty Santarossa, Simon-Martin Schroder, Reinhard Koch, Simon-Martin Schröder, Reinhard Koch, Simon-Martin Schroder, and Reinhard Koch. A Survey on Semi-, Self-and Unsupervised Learning for Image Classification. *IEEE Access*, pages 1–1, 2021. ISSN 2169-3536. doi: 10.1109/ACCESS.2021.3084358.
- [64] Lars Schmarje, Monty Santarossa, Simon-Martin Schröder, Claudius Zelenka, Rainer Kiko, Jenny Stracke, Nina Volkmann, and Reinhard Koch. A data-centric approach for improving ambiguous labels with combined semi-supervised classification and clustering. *Proceedings of the European Conference on Computer Vision (ECCV)*, 2022.
- [65] T Schoening, A Purser, D Langenkämper, I Suck, J Taylor, D Cuvelier, L Lins, E Simon-Lledó, Y Marcon, D O B Jones, T Nattkemper, K Köser, M Zurowietz, J Greinert, and J Gomes-Pereira. Megafauna community assessment of polymetallic-nodule fields with cameras:

- platform and methodology comparison. *Biogeosciences*, 17(12):3115–3133, 2020. doi: 10.5194/bg-17-3115-2020.
- [66] Philipp Schustek and Rubén Moreno-Bote. Instance-based generalization for human judgments about uncertainty. *PLOS Computational Biology*, 14(6):e1006205, jun 2018. ISSN 1553-7358. doi: 10.1371/journal.pcbi.1006205. URL <https://dx.plos.org/10.1371/journal.pcbi.1006205>.
- [67] Kihyuk Sohn, David Berthelot, Chun-Liang Li, Zizhao Zhang, Nicholas Carlini, Ekin D. Cubuk, Alex Kurakin, Han Zhang, and Colin Raffel. FixMatch: Simplifying Semi-Supervised Learning with Consistency and Confidence. *Advances in Neural Information Processing Systems 33 pre-proceedings (NeurIPS 2020)*, 2020.
- [68] Hwanjun Song, Minseok Kim, Dongmin Park, Jae-Gil Lee, Yooju Shin, and Jae-Gil Lee. Learning From Noisy Labels With Deep Neural Networks: A Survey. *IEEE Transactions on Neural Networks and Learning Systems*, pages 1–19, 2022. ISSN 2162-237X. doi: 10.1109/TNNLS.2022.3152527.
- [69] Igor Stępień, Rafał Obuchowicz, Adam Piórkowski, and Mariusz Oszust. Fusion of Deep Convolutional Neural Networks for No-Reference Magnetic Resonance Image Quality Assessment. *Sensors*, 21(4), 2021. ISSN 1424-8220. doi: 10.3390/s21041043.
- [70] Antti Tarvainen and Harri Valpola. Mean teachers are better role models: Weight-averaged consistency targets improve semi-supervised deep learning results. In *ICLR*, 2017.
- [71] Alexandra N. Uma, Tommaso Fornaciari, Dirk Hovy, Silviu Paun, Barbara Plank, and Massimo Poesio. Learning from Disagreement: A Survey. *Journal of Artificial Intelligence Research*, 72: 1385–1470, 2021. ISSN 1076-9757. doi: 10.1613/jair.1.12752.
- [72] Matias Valdenegro-Toro and Daniel Saromo. A Deeper Look into Aleatoric and Epistemic Uncertainty Disentanglement. 2022.
- [73] Nina Volkmann, Johannes Brünger, Jenny Stracke, Claudius Zelenka, Reinhard Koch, Nicole Kemper, and Birgit Spindler. So much trouble in the herd: Detection of first signs of cannibalism in turkeys. In *Recent advances in animal welfare science VII Virtual UFAW Animal Welfare Conference*, page 82, 2020.
- [74] Nina Volkmann, Johannes Brünger, Jenny Stracke, Claudius Zelenka, Reinhard Koch, Nicole Kemper, and Birgit Spindler. Learn to train: Improving training data for a neural network to detect pecking injuries in turkeys. *Animals 2021*, 11:1–13, 2021. doi: 10.3390/ani11092655.
- [75] Nina Volkmann, Claudius Zelenka, Archana Malavalli Devaraju, Johannes Brünger, Jenny Stracke, Birgit Spindler, Nicole Kemper, and Reinhard Koch. Keypoint Detection for Injury Identification during Turkey Husbandry Using Neural Networks. *Sensors*, 22(14):5188, 2022. ISSN 1424-8220. doi: 10.3390/s22145188.
- [76] Zhuowei Wang, Jing Jiang, Bo Han, Lei Feng, Bo An, Gang Niu, and Guodong Long. SemiNLL: A Framework of Noisy-Label Learning by Semi-Supervised Learning. 2020.
- [77] Jiaheng Wei, Zhaowei Zhu, Hao Cheng, Tongliang Liu, Gang Niu, and Yang Liu. Learning with Noisy Labels Revisited: A Study Using Real-World Human Annotations. 2021.
- [78] Quanming Yao, Hansi Yang, Bo Han, Gang Niu, and James Kwok. Searching to exploit memorization effect in learning from corrupted labels. *arXiv preprint arXiv:1911.02377*, 2019.
- [79] Xingrui Yu, Bo Han, Jiangchao Yao, Gang Niu, Ivor Tsang, and Masashi Sugiyama. How does disagreement help generalization against label corruption? In *International Conference on Machine Learning*, pages 7164–7173. PMLR, 2019.
- [80] Sangdoon Yun, Seong Joon Oh, Byeongho Heo, Dongyoon Han, Junsuk Choe, and Sanghyuk Chun. Re-Labeling ImageNet: From Single to Multi-Labels, From Global to Localized Labels. In *Proceedings of the IEEE/CVF Conference on Computer Vision and Pattern Recognition (CVPR)*, pages 2340–2350, 2021.

- [81] Xin Zhang, Zixuan Liu, Kaiwen Xiao, Tian Shen, Junzhou Huang, Wei Yang, Dimitris Samaras, and Xiao Han. CoDiM: Learning with Noisy Labels via Contrastive Semi-Supervised Learning. 2021.
- [82] Zizhao Zhang, Han Zhang, Serkan O. Arik, Honglak Lee, and Tomas Pfister. Distilling Effective Supervision from Severe Label Noise. *Conference on Computer Vision and Pattern Recognition*, 2020.

Checklist

1. For all authors...
 - (a) Do the main claims made in the abstract and introduction accurately reflect the paper's contributions and scope? [Yes] All claims are either introduced in Section 2 or are concluded in Section 4
 - (b) Did you describe the limitations of your work? [Yes] See Section 4
 - (c) Did you discuss any potential negative societal impacts of your work? [Yes] See Section 4
 - (d) Have you read the ethics review guidelines and ensured that your paper conforms to them? [Yes] All raw data was acquired from open data or in agreement with ethical guidelines.
2. If you are including theoretical results...
 - (a) Did you state the full set of assumptions of all theoretical results? [N/A] No theoretical claims made
 - (b) Did you include complete proofs of all theoretical results? [N/A] No theoretical claims made
3. If you ran experiments (e.g. for benchmarks)...
 - (a) Did you include the code, data, and instructions needed to reproduce the main experimental results (either in the supplemental material or as a URL)? [Yes] See Supplementary or the main repository.
 - (b) Did you specify all the training details (e.g., data splits, hyperparameters, how they were chosen)? [Yes] See Section 2
 - (c) Did you report error bars (e.g., with respect to the random seed after running experiments multiple times)? [Yes] See Section 1, As explained in 3 most reported values are median values due to outliers, error bars would clutter the graphics and decrease their interpretability. We give all results (including SEM) in the supplementary for any interested reader.
 - (d) Did you include the total amount of compute and the type of resources used (e.g., type of GPUs, internal cluster, or cloud provider)? [Yes] See the implementation details in Section 2
4. If you are using existing assets (e.g., code, data, models) or curating/releasing new assets...
 - (a) If your work uses existing assets, did you cite the creators? [Yes] We credited all authors when we used or extended their datasets. See under datasets in Section 2
 - (b) Did you mention the license of the assets? [Yes] All license information are in the license file in the Git Repository
 - (c) Did you include any new assets either in the supplemental material or as a URL? [Yes] Multiple datasets are created or extended by us, also the source code for the benchmark is new. The source code and datasets are reachable as described in the access section in the supplementary or in the main repository.
 - (d) Did you discuss whether and how consent was obtained from people whose data you're using/curating? [Yes] We either used own datasets, public datasets or received personal permission from respective data owners.
 - (e) Did you discuss whether the data you are using/curating contains personally identifiable information or offensive content? [N/A] The datasets are images of animals, objects or plants and thus can not identify people. Our data does not contain offensive content.
5. If you used crowdsourcing or conducted research with human subjects...
 - (a) Did you include the full text of instructions given to participants and screenshots, if applicable? [N/A] We either used preliminary existing crowd sourcing materials or used only selected few workers as annotators and gave only oral instructions. We give credit and reference all previous instructions.
 - (b) Did you describe any potential participant risks, with links to Institutional Review Board (IRB) approvals, if applicable? [N/A] Not applicable, we see no potential risk for humans by annotating images.

- (c) Did you include the estimated hourly wage paid to participants and the total amount spent on participant compensation? [Yes] We included hourly wages where applicable in the supplementary.

A Supplementary

A.1 Access to datasets and benchmark

The source code is available at <https://github.com/Emprime/dcic>. The datasets are available at <https://doi.org/10.5281/zenodo.7152309>.

Please check the licenses which vary between datasets and source code. You also need to credit all sources appropriately if you want to use them.

A.2 Additional Results

A.2.1 More annotations are better

As stated in the main paper, the datasets Benthic, MiceBone, Pig, QualitMRI, and Treeveritsy#6 have an \hat{ACC} of lower than 85% which marks them as difficult even for humans. Thus, we call them *difficult* and the rest *easy* datasets in the following.

We include in Figure 7a all measured scores over the all calculated budgets. We see as in Figure 5a an improvement of the scores with increasing budget. For easier datasets, we see in Figure 7b that the improvements with additional annotations are lower or do not exist, supporting the observation that uncertain labels benefit more from additional annotations. If we check in Figure 7c which methods benefit the most from additional annotations, we see up to 0.15 lower relative KL and ECE for soft labels. We can confirm similar observations on a t-SNE [19] visualization of the Plankton dataset in Figure 6. We use the method Pseudolabel v2 soft for these experiments. For a budget of 10%, the clusters are not as distinct as with 100% while for a budget of 1000% we can see more linear transitions in alignment with the soft ground truth label. In agreement with [22], we see that more annotated data helps to structure the feature space while linear transitions clarify with the added benefit of soft labels.

A.2.2 Correlations

Extending on the mentioned correlations in the main paper, we want to highlight to important conclusion from the investigated correlations. $F1$ balances the precision and recall and is general not the same as ACC but in our experiments we see almost identical values to ACC which we

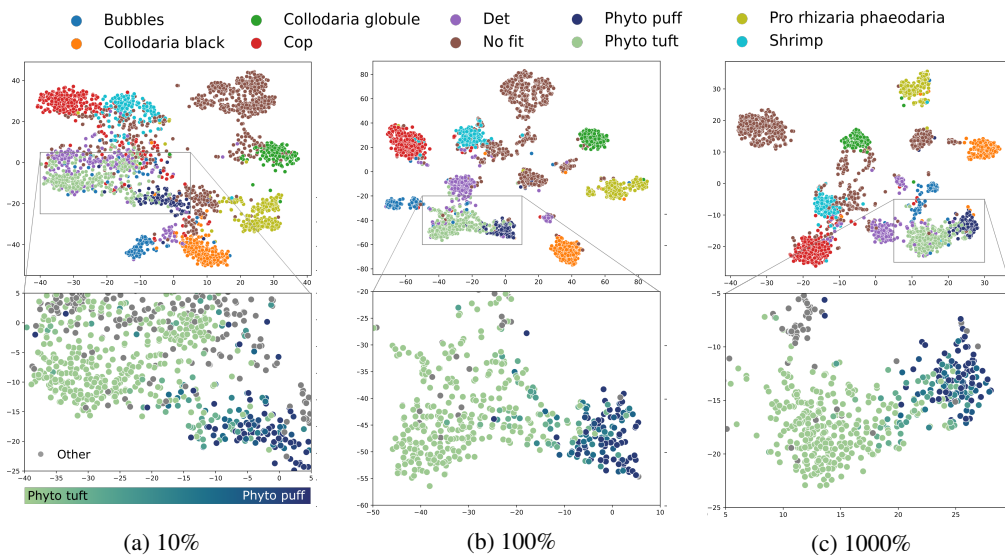


Figure 6: T-SNE evaluation on Plankton dataset on a budget of 10%, 100% and 1000% – On the top, all images are colored based on the majority class of the ground truth distribution. The lower images are zoomed in regions where we color only two classes accordingly to their actual ground truth distribution.

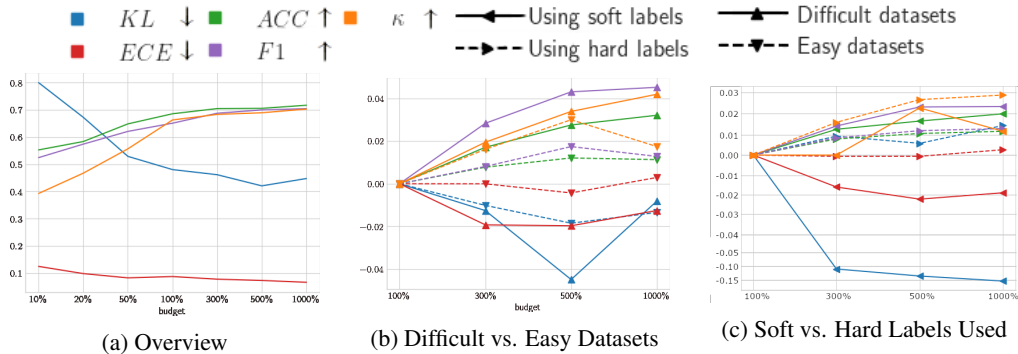


Figure 7: Impact of increased budget across all methods and datasets – The last two images show the relative changes in comparison to a budget of 100% from different subgroups of the datasets and methods respectively.

credit to the averaging per class. A high correlation also exists between ACC and κ which means that higher consistency in the input labels for different folds leads to better classification scores. This is a particularly useful result since consistency can be calculated without training a network or knowing anything about the ground truth distribution. This discovery allows the opportunity to roughly estimate the ACC of dataset without the knowledge of any labels.

A.3 Further implementation details and insights

A.4 Details about \hat{ACC}

In this section, we describe in detail why \hat{ACC} measures the human performance on the baseline method. \hat{ACC} measures the impact of the initialized labels against the ground truth for the baseline method. This is special for the baseline because it does not change the initialised labels. The ground truth is based on human annotations and the initialised labels on the ground truth and thus also human annotations.

The difference is the following: For example, if we have 20 annotations for an image x and the resulting ground truth distribution for the image would be $l_x = [0.8, 0.05, 0.15]$ for three classes.. The initialized labels are sampled from l_x . This means for one annotation per image ($m = 1$) defined by an initialization scheme, the initialized label would be $[1\ 0\ 0]$ in 80% of the cases, $[0\ 1\ 0]$ in 5% of the cases and $[0\ 0\ 1]$ in 15% of the cases. In this case, the initialized label often represents the majority vote, but in about 20% of the cases it would be a hard vote for a clear minority. For \hat{ACC} we only look at the majority vote of the ground truth and thus the expected result would be class 0 for image x even if we feed in 20% of the cases a different training label for image x in the training. This would of course negatively impact the classification performance as it would confuse the network.

An important detail is that we normally do not use the initialized label directly for the evaluation (it is not allowed to initialize labels on the test set). However, the baseline is designed to forward the sampled initialized labels in the test stage which effectively means that we sample one ($m=1$) or multiple human(s) ($m>1$) from the ground truth distribution. By doing so, the \hat{ACC} measures the performance of the sampled annotation against the complete ground truth.

In short, \hat{ACC} measure the impact of sample human annotation against the complete ground truth which we interpret as the performance of a human annotator against the combined ground truth.

A.5 About the improvement of Semi- and Self-supervised methods

In this section, we describe how Semi- and Self-supervised methods can be used to improve the labels in the first phase. When we talk about self-supervised methods, we mean the self-supervised training on a proxy task (e.g. maximizing agreement in SimCLR) and then a fine-tuning to the given classification task.

The improvement can be credited to two properties. Firstly, in many experiments the labels are initialized only on a small portion of the dataset and thus predicting a label on the rest of the unlabeled data creates / improves them in contrast to the previously unknown state. Secondly, when the network generalizes well, errors or ambiguities in the training data should be mitigated. For example, the network should predict a similar probability distribution for similar images even if the used training labels diverge. As seen in Figure 5a, these two benefits lead to a lower KL score in the second phase in comparison to the first phase \hat{KL} .

A.5.1 Self-supervised methods

We investigated the four self-supervised methods BYOL [21], MOCOv2 [13], SimCLR [11] and SWAV [10]. On large datasets like ImageNet [33] these methods have been shown to be comparable to or even surpass semi-supervised methods like FixMatch [67]. However, we assume all self-supervised methods to be inferior to most other benchmarked methods due to three main reasons. Firstly, the self-supervised methods are more difficult to tune. The models learn in the first phase without any supervision and thus depend on properly selected image augmentations [21]. For better comparability, we enforced the same set of hyperparameters including image augmentations across all datasets. This was problematic for some methods on specific datasets (e.g., BYOL on CIFAR-10H). Secondly, self-supervised methods are typically trained on large datasets. We trained only on a few thousand images and restricted the batch size for a comparable hardware usage. These two restrictions are often not considered in the literature and therefore might negatively impact the performance. Thirdly, many of the compared methods are pretrained on ImageNet. If we compare to not-pretrained methods such as Pseudo v2 not, we see that the self-supervised method is performing comparable or better.

A.5.2 Hyperparameter optimization

We used the public framework Ray Tune ⁴ for the hyperparameter optimization of the evaluation phase. As stated in the main paper we determined them by applying Hyperopt [7] with 100 search trials across the same grid of parameters for all datasets. The target was the minimization of KL between $\Phi(x)$ and l_x for the baseline experiment with exactly ten annotations per image across one fold. Below we show the used parameter grid.

```
config={
  'weights': weights,
  'batch_size': tune.choice([8,32,128]),
  'epochs': tune.choice([20]),
  'lr': tune.choice([1e-1,3e-1,1e-4,1e-5]),
  'dropout': tune.choice([0, 0.5]),
  'network': tune.choice(['wideresnet28-10', 'resnet50v2_large',
    'densenet121', 'inceptionv2', 'resnet50v2', 'wideresnet16-8' ]),
  'augmentation': tune.choice([0,1,2,3]),
  'opt': tune.choice(['sgd', 'adam', 'sgdw', 'sgdwr']),
  'input_upsampling': tune.choice([True, False]),
  'weight_decay': tune.choice([5e-4, 1e-3]),
},
```

As initialization, we used a heuristically determined set of hyperparameters from our preliminary studies. The details about these parameters can be found in the source code.

A.6 Detailed dataset descriptions

In this section, we describe in detail from where and how we collected the raw data, how we preprocessed the data and the labels, and give additional information per dataset. For all datasets, we split the data into five folds. We ensured during the splitting that the class distribution and the total size are similar between the folds. Moreover, we ensured that very similar images, e.g. consecutive slices in MiceBone are in the same fold. In multiple cases, we simplified the class labels due to very long tail distributions or missing data. In these cases, we give the mapping as 'original_label' : 'our_label'. If our label is None, we ignored the class completely.

⁴<https://docs.ray.io/en/latest/tune/index.html>

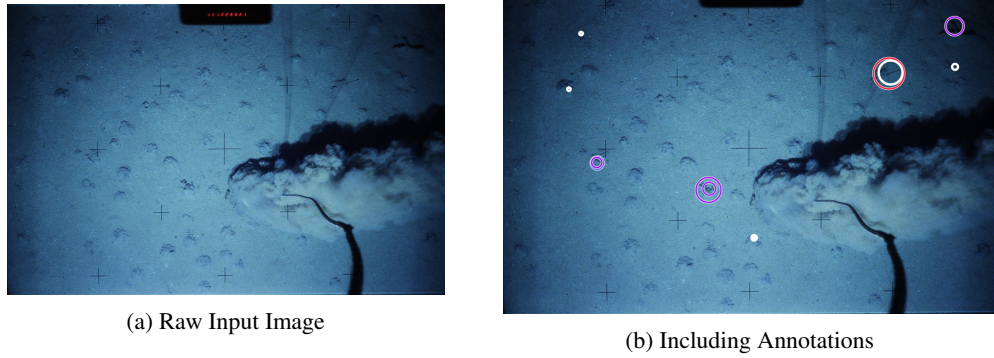


Figure 8: Raw example image without and with annotations. Every circle represents one annotation.

A.6.1 Benthic

The raw data was provided to us by the authors of [65, 37]. In their studies, multiple annotators labeled any objects they could detect on seafloor images. One example image without and with annotations is given in Figure 8.

We see that some items are only annotated once while others have multiple annotations. We sorted all annotations in descending order of their size. We merged all overlapping annotations with nearby centers. If at least three annotations were found, we used a cutout region around the largest found annotation as an image and the average across all annotations as the ground truth label. The total number of annotations and the agreement with the majority vote per image can be seen as a histogram in Figure 9. In agreement with the original authors, we simplified the original class with the following mapping:

```

"Anemone": "other_fauna",
"Coral": "coral",
"Crustacean": "crustacean",
"Epifauna": "other_fauna",
"Ipnops fish": "other_fauna",
"Jellyfish": "other_fauna",
"Litter": None,
"Mollusc": "other_fauna",
"Octopus / squid": None,
"Ophiuroid": "star",
"Other fauna": "other_fauna",
"Other fish": "other_fauna",
"Polychaete (sessile)": "worm",
"Sea Urchin": "other_fauna",
"Sea cucumber": "cucumber",
"Small encrusting": "encrusting",
"Spiral worm": "worm",
"Sponge": "sponge",
"Stalk (no head)": "other_fauna",
"Stalked crinoid": "other_fauna",
"Stalked sponge": "other_fauna",
"Starfish (not ophiuroid)": "star",
"polychaete (mobile)": "worm",
'lost+found': None,

```

A.6.2 CIFAR-10H

This dataset was originally described and created by [54]. The total number of annotations and the agreement with the majority vote per image can be seen as a histogram in Figure 10.

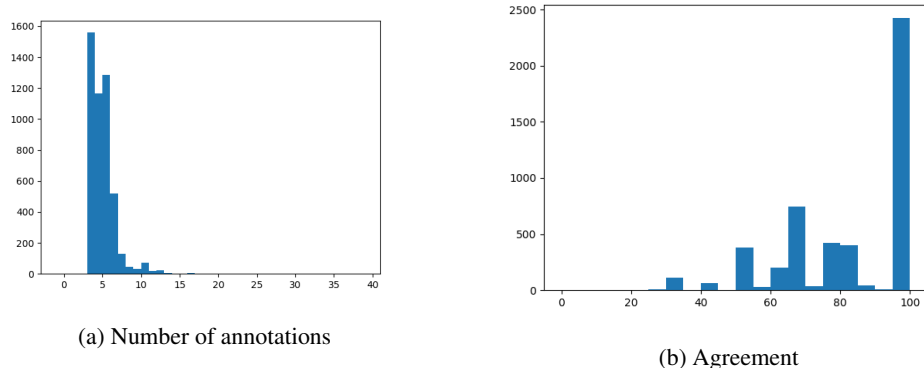


Figure 9: Histograms for the Benthic Dataset

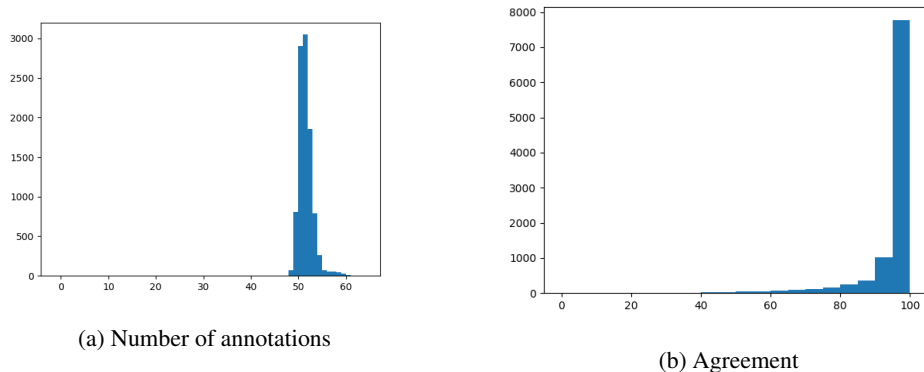


Figure 10: Histograms for the CIFAR-10H Dataset

A.6.3 MiceBone

We used the preprocessing described in [64] and reproduced their description here with the authors permission:

The Mice Bone dataset is based on the raw data which was published in [60]. The raw data are 3D scans from collagen fibers in mice bones. The three proposed classes are similar ("g") and dissimilar ("ug") collagen fiber orientations and not relevant ("nr") regions due to noise or background. We used the given segmentations to cut image regions from the original 2D image slices which mainly consist of one class.

We collected the annotations with four human workers. Three of them were hired workers which replied to a local job advertisement and were paid 11€ per hour. The last worker was a domain expert who desired no further payment than their contribution to science. All workers received reference images as guidance from the domain expert and oral explanations of the different classes. All reference images are shown in Figure 11 with the written explanations. The annotation process was structured in a partial first annotation of the data and multiple following annotations. The first partial annotation was used to get familiar with the annotation process and the classes. No results from this first part were used in this publication. We checked that all annotators achieved a similar classification performance than the domain expert with himself after this first part. All annotators annotated as much as possible during a fixed time frame of 15 hours. We either annotated the full dataset or subset of 10% multiple times. The total number of annotations and the agreement with the majority vote per image can be seen as a histogram in Figure 12.

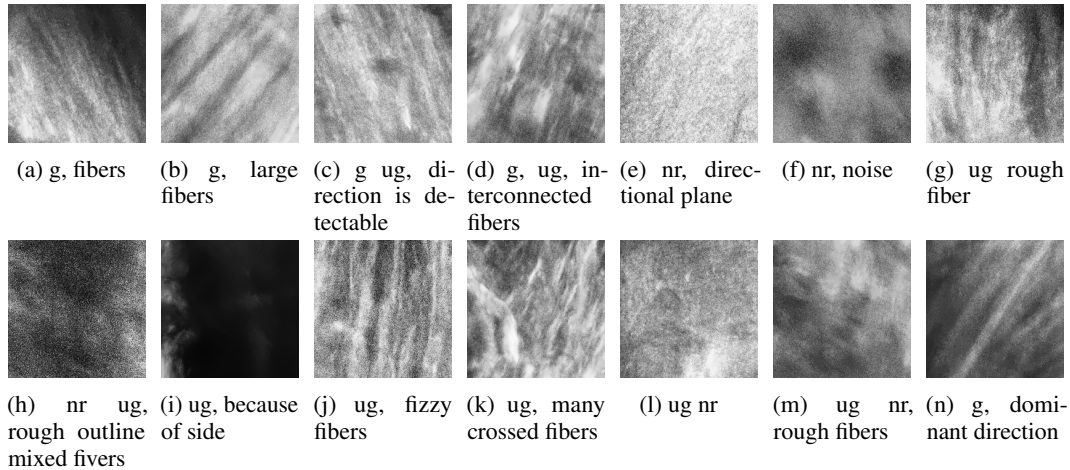


Figure 11: Reference images for the annotation of the MiceBone Dataset

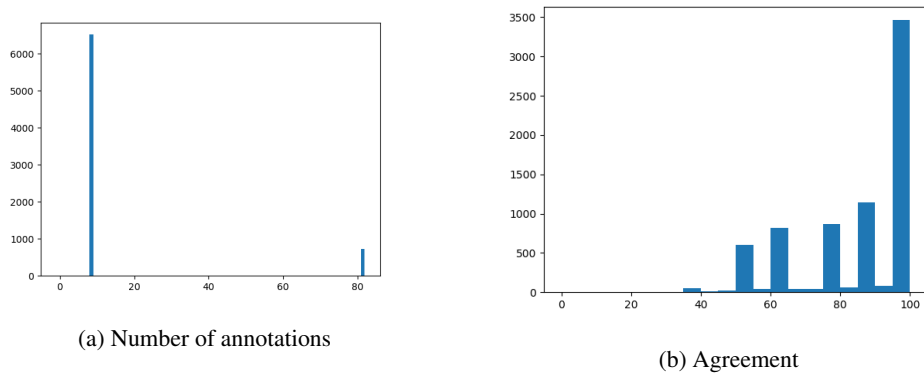


Figure 12: Histograms for the MiceBone Dataset

A.7 Pig

The raw data was collected at European farms for pigs. The animals were captured via a camera during their arrival and departure. We only received and worked with cropped regions of the tail provided to us by the University of Helsinki to protect data privacy and personal interest of the farms. We created an annotation catalog for the four classes, ‘no injury’, ‘shortened tail but healed’, ‘fresh wound at tail’ and ‘tail not visible’ as instruction. If annotators were uncertain they should decide themselves for the more probable class and in edge cases for the more severe class. We tracked the consistency between the annotators and it stayed at around 50% agreement over all annotations and annotators. The data was annotated in multiple rounds and a subset of 20% was annotated more often. The 6 annotators were domain experts with one exception, a hired worker only for this task which was trained and instructed as the others. This hired worker was paid 11€ per hour and the domain expert did the work as part of their daily job.

A.7.1 Plankton

We used the preprocessing described in [64] and reproduced their description here with the authors’ permission.

The Plankton dataset was introduced in [61]. The dataset contains 10 plankton classes and has multiple labels per image due to the help of citizen scientists. In contrast to [61], we include ambiguous images in the training and validation set and do not enforce a class balance.

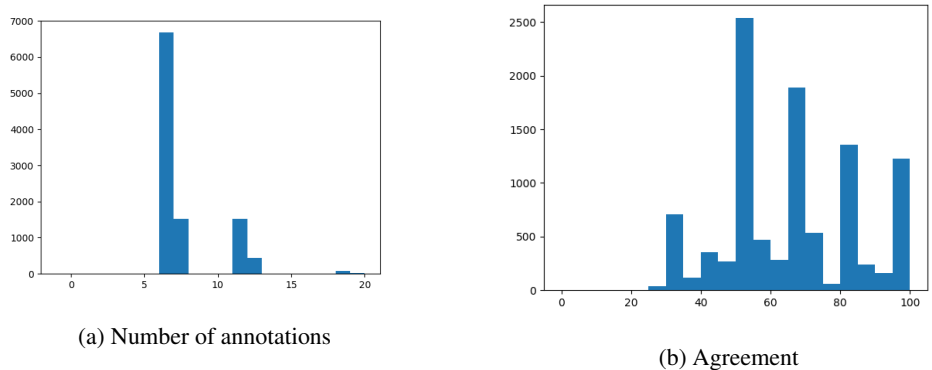


Figure 13: Histograms for the Pig Dataset

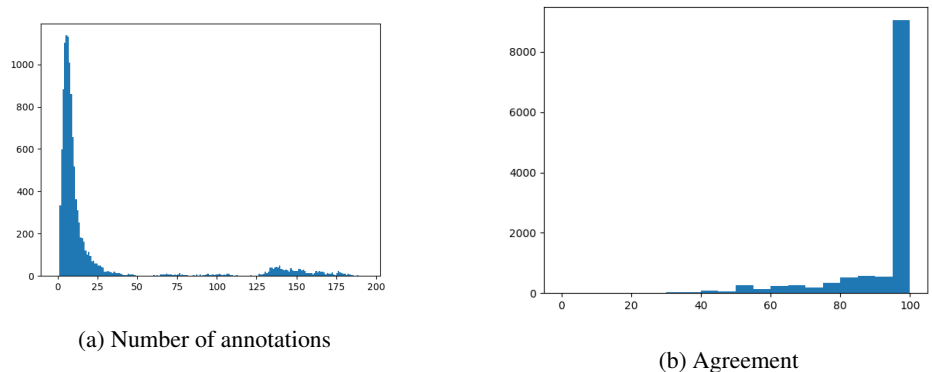


Figure 14: Histograms for the Plankton Dataset

The mentioned citizen scientist used the platform PlanktonID⁵. The total number of annotations and the agreement with the majority vote per image can be seen as a histogram in Figure 14.

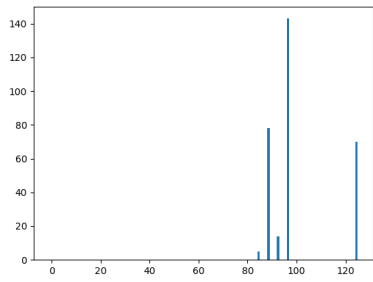
A.7.2 QualityMRI

The QualityMRI dataset consists of human magnetic resonance images (MRI) with a varying quality and multiple subjective quality ratings gathered in tests with radiologists. It was introduced and evaluated in [51, 69]. We received as raw data 70 images with around 31 annotations and 240 images with around 24 annotations. The annotations had a score from 1 to 5. We simplified these labels into a continuous score between 0 and 1. We converted the given annotations into 4 new annotations for this continuous score. For example, we interpreted an original annotation of 1 as 4 annotations of 0 and an original annotation of 2 as 3 annotations 0 and one annotation 1. The total number of annotations and the agreement with the majority vote per image can be seen as histogram in Figure 15.

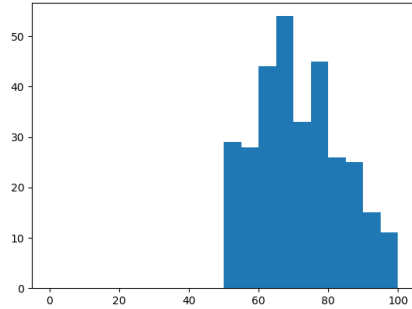
A.7.3 Synthetic

This dataset consists of images that contain one blue, red, or green circle or ellipse on a black background. We used a hue value of 0 (red), 120 (green) or 240 (blue) and the main axis ratio of 1 (circle) and 2 (ellipse). The combination of all colors and ratios leads to six distinct classes. We generated 1200 images (200 per class) of all classes per fold. The position and scale were determined randomly. Additionally, we generated 1800 images with a random hue and main axis ratio. Based on the random hue and ratio, we determined the class distribution of the six main classes. For example, an image with the hue 60 and an axis ratio of 1.3 would have marginal probabilities of 50% red, 50%

⁵<https://planktonid.geomar.de>

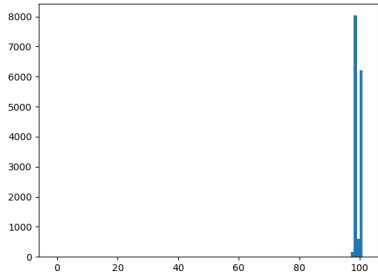


(a) Number of annotations

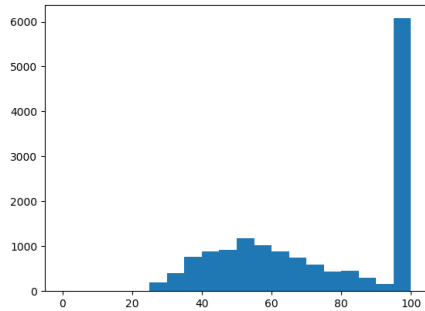


(b) Agreement

Figure 15: Histograms for the QualityMRI Dataset



(a) Number of annotations



(b) Agreement

Figure 16: Histograms for the Synthetic Dataset

green, 30% circle, and 70% ellipse. When we assume an independent combination, we arrive at the following ground truth distribution: red circle 0.15, red ellipse 0.35, blue circle 0.15, blue ellipse 0.35, green circle 0.0, green ellipse 0.0. We generated 100 annotations based on these probability distributions for each image.

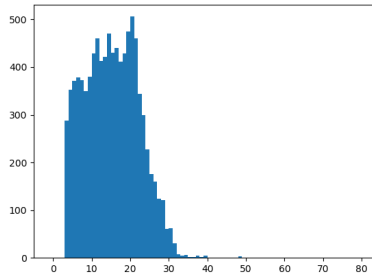
The total number of annotations and the agreement with the majority vote per image can be seen as a histogram in Figure 16.

A.7.4 Treeversity#1 and Treeversity#6

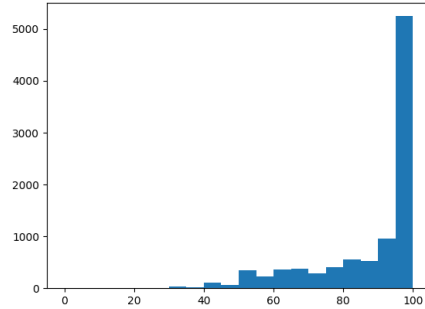
Both datasets are based on a publicly available crowdsourced dataset of plant images from the Arnold Arboretum of Harvard University⁶. The original task was to tag plant images with up to 21 original classes. The original crowd source page can be found at <https://www.zooniverse.org/projects/friedmaw/treeversity/about/research>. We removed the original photographer and location at the bottom of each image to prevent any information leakage. We used all tags from the original research and interpreted them as annotations. We simplified the original 22 tags to 6 classes as shown below.

```
'FLWR': 'flower',
'FLOWERINFLORESCENCE': 'flower',
'LEAFNEEDLE': 'leaf',
'LEAF': 'leaf', 'LF': 'leaf',
'BARK': 'bark', 'BRK': 'bark',
'BUDBREAK': 'bud',
```

⁶<https://arboretum.harvard.edu/research/data-resources/>



(a) Number of annotations



(b) Agreement

Figure 17: Histograms for the TreeVersity#1 Dataset

```

'BUD': 'bud', 'BD': 'bud',
'FRUIT': 'fruit',
'FRUITSEED': 'fruit', 'FRTSD': 'fruit',
'WHOLEPLANT': 'whole_plant', 'WHLPLNT': 'whole_plant',
'TRUNK': 'bark', 'TRNK': 'bark',
'AUTUMNLEAFCOLOR': 'leaf', 'TMNLFCLR': 'leaf',
'CONE': 'fruit', 'CN': 'fruit',
'LEAFLESS': None, 'LFLSS': None',
'PLNTHLTHSS': None, 'PLANTHEALTHISSUE': None,
'BRNCH': 'bark', 'BRANCH': 'bark',
'NSCTSPDRMT': None, 'INSECTSPIDERMITE': None,
'PRICKLESPINETHORN': None, 'PRCKLSPNTHRN': None
'LCHNMSSFNGS': None, 'LICHENMOSSFUNGUS': None
'POORIMAGEQUALITYNOFEATURES': None
'ROOT': 'bark'

```

We used a simplification due to overlapping classes because of the original tagging and small classes (e.g. health issues with 8 tags). We counted multiple tags which we simplified to the same annotation class only once per image and user and used only images with at least three different annotations. We saw that most people gave only one original tag per image (approx. 54%) and the majority did not give more than three (approx. 98%). Due to the fact that tags are not the same as class annotations, we investigate two subsets. In Treeversity#1, we restrict the annotations based on original tags where exactly one tag was given. In Treeversity#6, we do not use this restriction. The total number of annotations and the agreement with the majority vote per image can be seen as a histogram in Figure 17 and Figure 18.

A.7.5 Turkey

The turkey dataset with images of turkeys and their injuries [73, 74]. We use three classes head injury, plumage injury, or no injury. All injuries from the neck upwards to the eyes were counted as head injuries and the rest as plumage injuries. We used the original cross-analysis results between domain experts of the original papers. In addition, we collected additional annotations with a similar protocol as for the MiceBone dataset. The main difference is that reference images were not given but the distinction were discussed with all annotators and the domain expert multiple times. The total number of annotations and the agreement with the majority vote per image can be seen as a histogram in Figure 19.

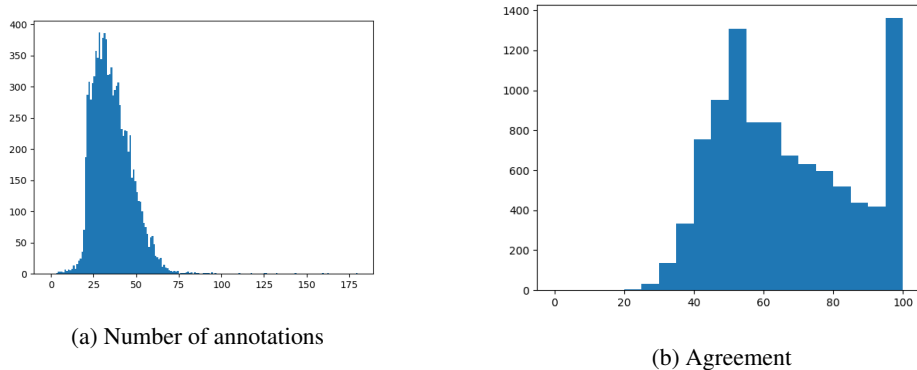


Figure 18: Histograms for the TreeVersity#6 Dataset

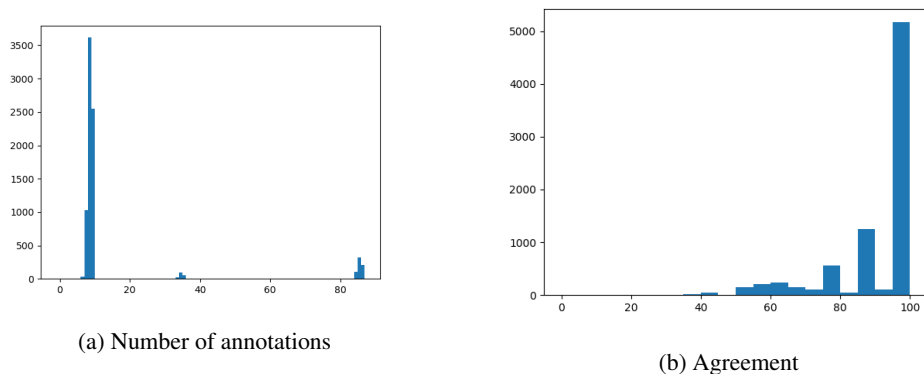


Figure 19: Histograms for the Turkey Dataset

A.8 Full result tables

We give the full result tables including Median and Mean \pm SEM for all figures in the main paper. Additionally, we create an overview for ACC and KL for a budget of 10%, 100%, and 1000%.

Table 4: Full table to Figure 7a

Budget	10%		20%		50%		100%		300%		500%		1000%	
	Median	Mean \pm SEM	Median	Mean \pm SEM	Median	Mean \pm SEM	Median	Mean \pm SEM	Median	Mean \pm SEM	Median	Mean \pm SEM	Median	Mean \pm SEM
KL	0.80	0.91 \pm 0.03	0.67	0.83 \pm 0.03	0.53	0.64 \pm 0.02	0.48	0.60 \pm 0.02	0.46	0.55 \pm 0.04	0.42	0.54 \pm 0.03	0.45	0.56 \pm 0.03
ECE	0.12	0.15 \pm 0.00	0.10	0.13 \pm 0.00	0.08	0.11 \pm 0.00	0.09	0.11 \pm 0.00	0.08	0.09 \pm 0.01	0.07	0.09 \pm 0.00	0.07	0.09 \pm 0.01
ACC	0.55	0.56 \pm 0.01	0.58	0.60 \pm 0.01	0.65	0.66 \pm 0.01	0.69	0.68 \pm 0.01	0.70	0.70 \pm 0.01	0.71	0.71 \pm 0.01	0.72	0.71 \pm 0.01
$F1$	0.52	0.53 \pm 0.01	0.57	0.57 \pm 0.01	0.62	0.63 \pm 0.01	0.65	0.65 \pm 0.01	0.69	0.68 \pm 0.01	0.70	0.70 \pm 0.01	0.70	0.70 \pm 0.01
κ	0.39	0.39 \pm 0.01	0.47	0.45 \pm 0.01	0.56	0.53 \pm 0.01	0.66	0.65 \pm 0.01	0.68	0.69 \pm 0.01	0.69	0.70 \pm 0.01	0.70	0.71 \pm 0.01

Table 5: Full table to Figure 7b

Budget	100%		300%		500%		1000%	
	Median	Mean \pm SEM	Median	Mean \pm SEM	Median	Mean \pm SEM	Median	Mean \pm SEM
Results for <i>KL</i>								
Difficult datasets	0.00	0.00 \pm 0.02	-0.01	-0.03 \pm 0.06	-0.04	-0.04 \pm 0.04	-0.01	-0.06 \pm 0.04
Easy datasets	0.00	-0.00 \pm 0.01	-0.01	-0.06 \pm 0.03	-0.02	-0.08 \pm 0.03	-0.01	-0.02 \pm 0.02
Results for <i>ECE</i>								
Difficult datasets	0.00	0.00 \pm 0.00	-0.02	-0.02 \pm 0.01	-0.02	-0.02 \pm 0.01	-0.01	-0.02 \pm 0.01
Easy datasets	0.00	0.00 \pm 0.00	-0.00	-0.01 \pm 0.01	-0.00	-0.01 \pm 0.00	0.00	-0.00 \pm 0.00
Results for <i>ACC</i>								
Difficult datasets	0.00	-0.00 \pm 0.00	0.02	0.02 \pm 0.01	0.03	0.02 \pm 0.01	0.03	0.04 \pm 0.01
Easy datasets	0.00	0.00 \pm 0.00	0.01	0.01 \pm 0.01	0.01	0.02 \pm 0.00	0.01	0.01 \pm 0.00
Results for <i>F1</i>								
Difficult datasets	0.00	-0.00 \pm 0.00	0.03	0.02 \pm 0.01	0.04	0.04 \pm 0.01	0.05	0.05 \pm 0.01
Easy datasets	0.00	-0.00 \pm 0.00	0.01	0.02 \pm 0.01	0.02	0.03 \pm 0.01	0.01	0.02 \pm 0.00
Results for κ								
Difficult datasets	0.00	-0.00 \pm 0.00	0.02	0.02 \pm 0.01	0.03	0.04 \pm 0.01	0.04	0.06 \pm 0.01
Easy datasets	0.00	-0.00 \pm 0.00	0.02	0.03 \pm 0.01	0.03	0.04 \pm 0.01	0.02	0.04 \pm 0.01

Table 6: Full table to Figure 7c

Budget	100%		300%		500%		1000%	
	Median	Mean \pm SEM	Median	Mean \pm SEM	Median	Mean \pm SEM	Median	Mean \pm SEM
Results for <i>KL</i>								
Using soft labels	0.00	-0.00 \pm 0.02	-0.11	-0.22 \pm 0.05	-0.13	-0.25 \pm 0.04	-0.16	-0.23 \pm 0.04
Using hard labels	0.00	0.00 \pm 0.01	0.01	0.06 \pm 0.05	0.01	0.06 \pm 0.03	0.02	0.07 \pm 0.02
Results for <i>ECE</i>								
Using soft labels	-0.00	-0.00 \pm 0.00	-0.02	-0.04 \pm 0.01	-0.03	-0.04 \pm 0.01	-0.03	-0.04 \pm 0.01
Using hard labels	0.00	0.00 \pm 0.00	-0.00	-0.00 \pm 0.00	-0.00	-0.00 \pm 0.00	0.00	-0.00 \pm 0.00
Results for <i>ACC</i>								
Using soft labels	0.00	0.00 \pm 0.01	0.02	0.03 \pm 0.01	0.02	0.03 \pm 0.01	0.03	0.03 \pm 0.01
Using hard labels	0.00	0.00 \pm 0.00	0.01	0.00 \pm 0.00	0.01	0.02 \pm 0.00	0.01	0.02 \pm 0.00
Results for <i>F1</i>								
Using soft labels	0.00	0.00 \pm 0.01	0.02	0.04 \pm 0.01	0.04	0.04 \pm 0.01	0.03	0.04 \pm 0.01
Using hard labels	0.00	-0.00 \pm 0.00	0.01	0.01 \pm 0.01	0.02	0.03 \pm 0.00	0.02	0.03 \pm 0.01
Results for κ								
Using soft labels	0.00	0.00 \pm 0.01	0.01	0.03 \pm 0.01	0.03	0.04 \pm 0.01	0.01	0.04 \pm 0.01
Using hard labels	0.00	-0.00 \pm 0.00	0.02	0.02 \pm 0.01	0.03	0.04 \pm 0.01	0.04	0.06 \pm 0.01

Table 7: Full table to Figure 5a

Budget	10%		20%		50%		100%		300%		500%		1000%	
	Median	Mean \pm SEM	Median	Mean \pm SEM	Median	Mean \pm SEM	Median	Mean \pm SEM	Median	Mean \pm SEM	Median	Mean \pm SEM	Median	Mean \pm SEM
<i>KL</i>	0.80	0.91 \pm 0.03	0.67	0.83 \pm 0.03	0.53	0.64 \pm 0.02	0.48	0.60 \pm 0.02	0.46	0.55 \pm 0.04	0.42	0.54 \pm 0.03	0.45	0.56 \pm 0.03
<i>KL</i>	1.48	1.70 \pm 0.05	1.21	1.52 \pm 0.05	0.89	1.21 \pm 0.04	0.74	1.08 \pm 0.04	0.72	1.02 \pm 0.06	0.73	0.96 \pm 0.06	0.65	0.95 \pm 0.07
<i>ACC</i>	0.55	0.56 \pm 0.01	0.58	0.60 \pm 0.01	0.65	0.66 \pm 0.01	0.69	0.68 \pm 0.01	0.70	0.70 \pm 0.01	0.71	0.71 \pm 0.01	0.72	0.71 \pm 0.01
<i>ACC</i>	0.54	0.54 \pm 0.01	0.57	0.58 \pm 0.01	0.65	0.63 \pm 0.01	0.67	0.66 \pm 0.01	0.70	0.69 \pm 0.01	0.71	0.70 \pm 0.01	0.72	0.71 \pm 0.01
<i>ECE</i>	0.12	0.15 \pm 0.00	0.10	0.13 \pm 0.00	0.08	0.11 \pm 0.00	0.09	0.11 \pm 0.00	0.08	0.09 \pm 0.01	0.07	0.09 \pm 0.00	0.07	0.09 \pm 0.01
<i>ECE</i>	0.22	0.23 \pm 0.01	0.19	0.21 \pm 0.01	0.15	0.17 \pm 0.01	0.12	0.15 \pm 0.00	0.09	0.13 \pm 0.01	0.08	0.12 \pm 0.01	0.09	0.13 \pm 0.01

Table 8: Full table to Figure 5b

Budget	10-0.10		05-0.20		02-0.50		01-1.00	
	Median	Mean \pm SEM	Median	Mean \pm SEM	Median	Mean \pm SEM	Median	Mean \pm SEM
Results for <i>KL</i>								
Pseudo v2 hard	0.84	0.95 \pm 0.12	0.77	0.98 \pm 0.15	0.61	0.67 \pm 0.05	0.44	0.51 \pm 0.05
Pseudo v2 soft	0.45	0.56 \pm 0.07	0.40	0.47 \pm 0.05	0.55	0.52 \pm 0.05	0.43	0.52 \pm 0.05
Results for <i>ACC</i>								
Pseudo v2 hard	0.65	0.63 \pm 0.03	0.64	0.64 \pm 0.03	0.71	0.67 \pm 0.03	0.75	0.71 \pm 0.03
Pseudo v2 soft	0.67	0.64 \pm 0.03	0.66	0.68 \pm 0.03	0.72	0.69 \pm 0.02	0.72	0.71 \pm 0.03
Results for <i>ECE</i>								
Pseudo v2 hard	0.12	0.13 \pm 0.02	0.13	0.14 \pm 0.02	0.10	0.11 \pm 0.02	0.08	0.10 \pm 0.01
Pseudo v2 soft	0.07	0.09 \pm 0.01	0.04	0.07 \pm 0.01	0.07	0.09 \pm 0.01	0.10	0.10 \pm 0.01

Table 9: Full table to Figure 5c

Budget	10%		20%		50%		100%		300%		500%		1000%	
	Median	Mean \pm SEM	Median	Mean \pm SEM	Median	Mean \pm SEM	Median	Mean \pm SEM	Median	Mean \pm SEM	Median	Mean \pm SEM	Median	Mean \pm SEM
Results for <i>KL</i>														
Baseline	0.83	1.39 \pm 0.25	0.63	0.98 \pm 0.17	0.52	0.70 \pm 0.08	0.52	0.69 \pm 0.09	0.34	0.37 \pm 0.04	0.37	0.39 \pm 0.04	0.29	0.33 \pm 0.04
Pseudo v2 soft	0.77	0.99 \pm 0.20	0.72	0.90 \pm 0.13	0.61	0.64 \pm 0.06	0.43	0.52 \pm 0.05	0.37	0.39 \pm 0.04	0.34	0.36 \pm 0.03	0.30	0.33 \pm 0.04
DivideMix	0.59	0.60 \pm 0.05	0.53	0.55 \pm 0.04	0.45	0.51 \pm 0.04	0.44	0.52 \pm 0.04	0.47	0.56 \pm 0.06	0.41	0.54 \pm 0.06	0.45	0.64 \pm 0.08
ELR+	0.78	0.80 \pm 0.07	0.57	0.59 \pm 0.06	0.45	0.51 \pm 0.07	0.47	0.52 \pm 0.08	0.48	0.55 \pm 0.09	0.44	0.70 \pm 0.15	0.50	0.57 \pm 0.06
Results for <i>ACC</i>														
Baseline	0.52	0.57 \pm 0.04	0.60	0.63 \pm 0.03	0.65	0.68 \pm 0.03	0.71	0.71 \pm 0.03	0.72	0.74 \pm 0.03	0.75	0.74 \pm 0.03	0.75	0.74 \pm 0.03
Pseudo v2 soft	0.61	0.60 \pm 0.02	0.63	0.63 \pm 0.03	0.69	0.68 \pm 0.03	0.72	0.71 \pm 0.03	0.73	0.74 \pm 0.02	0.77	0.74 \pm 0.03	0.78	0.75 \pm 0.03
DivideMix	0.62	0.62 \pm 0.03	0.68	0.66 \pm 0.03	0.72	0.72 \pm 0.03	0.73	0.73 \pm 0.03	0.74	0.74 \pm 0.03	0.76	0.75 \pm 0.03	0.75	0.74 \pm 0.03
ELR+	0.53	0.53 \pm 0.04	0.59	0.60 \pm 0.04	0.66	0.65 \pm 0.04	0.72	0.68 \pm 0.04	0.73	0.67 \pm 0.04	0.72	0.68 \pm 0.04	0.73	0.69 \pm 0.04
Results for <i>ECE</i>														
Baseline	0.16	0.19 \pm 0.03	0.14	0.17 \pm 0.02	0.12	0.14 \pm 0.02	0.13	0.13 \pm 0.01	0.04	0.07 \pm 0.01	0.05	0.07 \pm 0.01	0.03	0.07 \pm 0.01
Pseudo v2 soft	0.11	0.14 \pm 0.02	0.11	0.14 \pm 0.02	0.11	0.11 \pm 0.01	0.10	0.10 \pm 0.01	0.06	0.08 \pm 0.01	0.06	0.08 \pm 0.01	0.05	0.08 \pm 0.01
DivideMix	0.12	0.12 \pm 0.01	0.09	0.11 \pm 0.01	0.08	0.10 \pm 0.01	0.06	0.09 \pm 0.01	0.06	0.09 \pm 0.01	0.05	0.09 \pm 0.02	0.05	0.09 \pm 0.02
ELR+	0.09	0.15 \pm 0.02	0.07	0.10 \pm 0.02	0.06	0.09 \pm 0.01	0.05	0.09 \pm 0.02	0.05	0.09 \pm 0.02	0.05	0.09 \pm 0.02	0.05	0.09 \pm 0.02

Table 10: Improvements in KL across methods

Budget	10%		100%		1000%	
	Median	Mean \pm SEM	Median	Mean \pm SEM	Median	Mean \pm SEM
Baseline	-0.00	-0.00 \pm 0.07	0.00	-0.00 \pm 0.03	0.00	0.00 \pm 0.01
ELR+	-0.16	-0.59 \pm 0.22	-0.13	-0.17 \pm 0.06	0.15	0.24 \pm 0.06
Het	-0.06	-0.02 \pm 0.08	-0.01	0.01 \pm 0.02	0.22	0.30 \pm 0.05
SGNP	-0.26	-0.59 \pm 0.27	0.00	-0.15 \pm 0.08	0.20	0.26 \pm 0.04
DivideMix	-0.21	-0.78 \pm 0.25	-0.03	-0.17 \pm 0.08	0.16	0.31 \pm 0.07
Fixmatch	-0.22	-0.43 \pm 0.14	-0.05	-0.17 \pm 0.05	N/A	
Fixmatch + DC3	-0.29	-0.48 \pm 0.17	-0.06	-0.13 \pm 0.04	N/A	
Mean	-0.14	-0.59 \pm 0.22	-0.12	-0.22 \pm 0.08	N/A	
Mean+DC3	-0.20	-0.51 \pm 0.17	-0.08	-0.15 \pm 0.07	N/A	
π	-0.33	-0.63 \pm 0.19	-0.06	-0.17 \pm 0.05	N/A	
π +DC3	-0.32	-0.62 \pm 0.20	-0.10	-0.22 \pm 0.06	N/A	
Pseudo v1	-0.25	-0.47 \pm 0.19	-0.07	-0.17 \pm 0.04	N/A	
Pseudo v1 + DC3	-0.24	-0.56 \pm 0.22	-0.07	0.05 \pm 0.23	N/A	
Pseudo v2 hard	-0.30	-0.39 \pm 0.16	-0.03	-0.19 \pm 0.08	0.19	0.28 \pm 0.04
Pseudo v2 soft	-0.28	-0.40 \pm 0.19	-0.04	-0.17 \pm 0.06	0.01	0.00 \pm 0.02
Pseudo v2 not	0.12	-0.11 \pm 0.34	0.10	0.22 \pm 0.19	0.28	0.46 \pm 0.13
BYOL	-0.20	-0.47 \pm 0.21	-0.08	0.02 \pm 0.09	N/A	
MOCOv2	-0.29	-0.63 \pm 0.22	-0.08	-0.13 \pm 0.10	N/A	
SimCLR	-0.07	-0.40 \pm 0.22	0.01	0.04 \pm 0.06	N/A	
SWAV	-0.05	-0.43 \pm 0.22	0.19	0.17 \pm 0.08	N/A	

Table 11: Improvements in ACC across methods

Budget	10%		100%		1000%	
	Median	Mean \pm SEM	Median	Mean \pm SEM	Median	Mean \pm SEM
Baseline	0.00	0.00 \pm 0.01	0.00	0.00 \pm 0.01	-0.00	-0.00 \pm 0.01
ELR+	-0.02	-0.03 \pm 0.01	0.01	-0.03 \pm 0.03	-0.01	-0.05 \pm 0.02
Het	-0.06	-0.10 \pm 0.02	-0.00	-0.00 \pm 0.01	-0.00	-0.01 \pm 0.01
SGNP	-0.03	-0.05 \pm 0.02	-0.01	-0.01 \pm 0.01	-0.01	-0.01 \pm 0.01
DivideMix	0.05	0.05 \pm 0.02	0.03	0.02 \pm 0.02	0.00	-0.00 \pm 0.01
Fixmatch	0.05	0.05 \pm 0.01	0.01	0.01 \pm 0.01	N/A	
Fixmatch + DC3	0.03	0.02 \pm 0.01	-0.00	-0.00 \pm 0.01	N/A	
Mean	0.02	0.03 \pm 0.02	0.02	-0.01 \pm 0.02	N/A	
Mean+DC3	0.05	0.03 \pm 0.02	0.00	0.00 \pm 0.01	N/A	
π	0.05	0.04 \pm 0.02	0.02	0.01 \pm 0.01	N/A	
π +DC3	0.04	0.03 \pm 0.02	0.02	0.02 \pm 0.01	N/A	
Pseudo v1	0.07	0.03 \pm 0.02	0.01	0.03 \pm 0.01	N/A	
Pseudo v1 + DC3	0.03	0.02 \pm 0.02	0.02	0.03 \pm 0.01	N/A	
Pseudo v2 hard	0.05	0.04 \pm 0.03	0.01	0.00 \pm 0.01	-0.03	-0.02 \pm 0.02
Pseudo v2 soft	0.01	0.04 \pm 0.03	-0.00	-0.00 \pm 0.01	-0.00	0.01 \pm 0.01
Pseudo v2 not	-0.18	-0.18 \pm 0.04	-0.07	-0.14 \pm 0.03	-0.12	-0.17 \pm 0.03
BYOL	-0.05	-0.06 \pm 0.04	-0.11	-0.14 \pm 0.03	N/A	
MOCOv2	-0.04	-0.05 \pm 0.02	-0.10	-0.12 \pm 0.02	N/A	
SimCLR	0.01	0.01 \pm 0.01	-0.04	-0.04 \pm 0.01	N/A	
SWAV	-0.04	-0.06 \pm 0.02	-0.12	-0.13 \pm 0.02	N/A	

Table 12: Details 10% Budget KL

Dataset	Benthic	CIFAR10H	MiceBone	Pig	Plankton	QualityMRI	Synthetic	Treeversity#1	Treeversity#6	Turkey
Baseline	1.17 ± 0.04	0.41 ± 0.02	0.55 ± 0.06	0.75 ± 0.05	0.34 ± 0.02	1.73 ± 0.48	0.08 ± 0.01	0.49 ± 0.04	1.02 ± 0.03	0.40 ± 0.08
ELR+	0.70 ± 0.01	0.29 ± 0.02	0.29 ± 0.01	0.62 ± 0.09	0.24 ± 0.03	1.44 ± 0.83	0.18 ± 0.02	0.46 ± 0.01	0.47 ± 0.05	0.52 ± 0.05
Het	1.16 ± 0.15	0.39 ± 0.01	0.62 ± 0.18	0.70 ± 0.10	0.34 ± 0.03	N/A	0.10 ± 0.01	0.46 ± 0.01	0.99 ± 0.02	0.52 ± 0.07
SGNP	1.11 ± 0.05	0.38 ± 0.01	0.56 ± 0.14	0.77 ± 0.07	0.33 ± 0.02	0.25 ± 0.14	0.10 ± 0.00	0.46 ± 0.01	1.07 ± 0.05	0.42 ± 0.08
DivideMix	0.87 ± 0.07	0.36 ± 0.02	0.38 ± 0.05	0.95 ± 0.04	0.34 ± 0.01	0.46 ± 0.26	0.33 ± 0.00	0.47 ± 0.01	0.62 ± 0.05	0.43 ± 0.08
Fixmatch	0.88 ± 0.24	0.37 ± 0.02	0.41 ± 0.01	0.72 ± 0.05	0.27 ± 0.02	0.99 ± 0.30	0.11 ± 0.02	0.48 ± 0.06	0.51 ± 0.01	0.48 ± 0.05
Fixmatch + DC3	0.82 ± 0.02	0.34 ± 0.03	0.54 ± 0.12	0.71 ± 0.04	0.27 ± 0.02	1.41 ± 0.15	0.18 ± 0.15	0.44 ± 0.01	0.46 ± 0.01	0.47 ± 0.03
Mean	0.80 ± 0.06	0.28 ± 0.02	0.38 ± 0.02	0.64 ± 0.03	0.32 ± 0.01	0.35 ± 0.11	0.09 ± 0.01	0.61 ± 0.01	0.52 ± 0.03	0.75 ± 0.07
Mean+DC3	0.73 ± 0.02	0.28 ± 0.04	0.37 ± 0.00	0.71 ± 0.11	0.30 ± 0.02	1.42 ± 0.93	0.11 ± 0.02	0.51 ± 0.01	0.48 ± 0.02	0.55 ± 0.10
π	0.71 ± 0.03	0.33 ± 0.02	0.38 ± 0.00	0.83 ± 0.18	0.30 ± 0.02	0.98 ± 0.04	0.08 ± 0.01	0.52 ± 0.01	0.51 ± 0.03	0.55 ± 0.01
π +DC3	0.72 ± 0.06	0.30 ± 0.02	0.39 ± 0.04	0.67 ± 0.06	0.29 ± 0.01	0.88 ± 0.34	0.08 ± 0.00	0.48 ± 0.01	0.49 ± 0.00	0.44 ± 0.08
Pseudo v1	1.10 ± 0.13	0.35 ± 0.02	0.33 ± 0.01	0.71 ± 0.07	0.32 ± 0.02	1.25 ± 0.35	0.05 ± 0.00	0.42 ± 0.01	0.42 ± 0.01	0.33 ± 0.03
Pseudo v1 + DC3	1.10 ± 0.12	0.33 ± 0.03	0.34 ± 0.02	2.87 ± 3.09	0.31 ± 0.01	1.22 ± 0.51	0.06 ± 0.00	0.41 ± 0.01	0.43 ± 0.00	0.40 ± 0.04
Pseudo v2 hard	0.97 ± 0.10	0.43 ± 0.02	0.45 ± 0.10	0.67 ± 0.04	0.31 ± 0.03	0.29 ± 0.05	0.10 ± 0.01	0.46 ± 0.03	0.99 ± 0.09	0.39 ± 0.05
Pseudo v2 soft	1.00 ± 0.08	0.41 ± 0.02	0.40 ± 0.08	0.70 ± 0.06	0.32 ± 0.06	0.62 ± 0.16	0.10 ± 0.01	0.46 ± 0.01	0.83 ± 0.13	0.37 ± 0.08
Pseudo v2 not	1.05 ± 0.02	1.12 ± 0.04	0.46 ± 0.10	0.79 ± 0.09	2.70 ± 0.89	0.12 ± 0.02	1.00 ± 0.57	0.68 ± 0.17	0.67 ± 0.11	0.57 ± 0.06
BYOL	0.74 ± 0.03	1.61 ± 0.22	0.46 ± 0.02	0.64 ± 0.01	0.51 ± 0.05	1.07 ± 0.18	0.36 ± 0.01	0.82 ± 0.09	0.58 ± 0.03	0.34 ± 0.04
MOCOv2	0.91 ± 0.05	0.98 ± 0.02	0.37 ± 0.04	0.56 ± 0.01	0.52 ± 0.01	0.29 ± 0.11	0.13 ± 0.01	0.80 ± 0.03	0.61 ± 0.01	0.42 ± 0.08
SimCLR	1.19 ± 0.10	0.36 ± 0.02	0.48 ± 0.05	0.75 ± 0.09	0.29 ± 0.02	1.83 ± 1.01	0.38 ± 0.03	0.68 ± 0.00	0.94 ± 0.04	0.43 ± 0.06
SWAV	1.56 ± 0.16	0.70 ± 0.01	0.56 ± 0.09	1.33 ± 0.98	0.38 ± 0.01	1.90 ± 0.31	0.36 ± 0.03	0.71 ± 0.02	0.61 ± 0.03	0.51 ± 0.04

Table 13: Details 10% Budget Acc

Dataset	Benthic	CIFAR10H	MiceBone	Pig	Plankton	QualityMRI	Synthetic	Treeversity#1	Treeversity#6	Turkey
Baseline	0.64 ± 0.01	0.91 ± 0.00	0.62 ± 0.09	0.36 ± 0.04	0.90 ± 0.01	0.67 ± 0.04	0.88 ± 0.00	0.80 ± 0.02	0.57 ± 0.05	0.76 ± 0.03
ELR+	0.69 ± 0.01	0.89 ± 0.01	0.56 ± 0.05	0.39 ± 0.01	0.92 ± 0.01	0.50 ± 0.00	0.92 ± 0.01	0.80 ± 0.00	0.75 ± 0.02	0.36 ± 0.02
Het	0.63 ± 0.01	0.90 ± 0.01	0.64 ± 0.01	0.36 ± 0.01	0.90 ± 0.01	N/A	0.84 ± 0.02	0.80 ± 0.01	0.60 ± 0.01	0.72 ± 0.01
SGNP	0.64 ± 0.00	0.90 ± 0.01	0.61 ± 0.03	0.33 ± 0.07	0.91 ± 0.01	0.63 ± 0.11	0.84 ± 0.03	0.80 ± 0.01	0.56 ± 0.03	0.75 ± 0.05
DivideMix	0.69 ± 0.04	0.90 ± 0.01	0.66 ± 0.02	0.43 ± 0.02	0.92 ± 0.01	0.52 ± 0.02	0.93 ± 0.00	0.82 ± 0.01	0.77 ± 0.02	0.68 ± 0.02
Fixmatch	0.69 ± 0.04	0.91 ± 0.01	0.72 ± 0.02	0.29 ± 0.05	0.92 ± 0.01	0.72 ± 0.06	0.83 ± 0.03	0.78 ± 0.03	0.64 ± 0.02	0.69 ± 0.06
Fixmatch + DC3	0.69 ± 0.01	0.90 ± 0.00	0.59 ± 0.08	0.33 ± 0.03	0.92 ± 0.01	0.63 ± 0.07	0.81 ± 0.13	0.79 ± 0.01	0.67 ± 0.01	0.76 ± 0.03
Mean	0.69 ± 0.01	0.90 ± 0.01	0.64 ± 0.03	0.39 ± 0.02	0.91 ± 0.01	0.64 ± 0.06	0.90 ± 0.01	0.71 ± 0.01	0.66 ± 0.01	0.52 ± 0.01
Mean+DC3	0.71 ± 0.01	0.90 ± 0.02	0.66 ± 0.00	0.35 ± 0.03	0.91 ± 0.01	0.62 ± 0.07	0.89 ± 0.01	0.75 ± 0.00	0.66 ± 0.01	0.66 ± 0.06
π	0.71 ± 0.02	0.90 ± 0.00	0.65 ± 0.01	0.34 ± 0.01	0.91 ± 0.01	0.71 ± 0.01	0.92 ± 0.01	0.75 ± 0.01	0.66 ± 0.00	0.63 ± 0.02
π +DC3	0.70 ± 0.02	0.90 ± 0.01	0.64 ± 0.05	0.37 ± 0.04	0.92 ± 0.00	0.68 ± 0.06	0.91 ± 0.01	0.77 ± 0.00	0.66 ± 0.00	0.69 ± 0.03
Pseudo v1	0.65 ± 0.05	0.91 ± 0.00	0.71 ± 0.02	0.34 ± 0.08	0.91 ± 0.01	0.68 ± 0.05	0.92 ± 0.01	0.80 ± 0.01	0.69 ± 0.01	0.80 ± 0.04
Pseudo v1 + DC3	0.64 ± 0.04	0.90 ± 0.02	0.73 ± 0.01	0.30 ± 0.04	0.91 ± 0.01	0.75 ± 0.03	0.90 ± 0.02	0.82 ± 0.01	0.69 ± 0.00	0.79 ± 0.04
Pseudo v2 hard	0.66 ± 0.02	0.84 ± 0.01	0.64 ± 0.05	0.35 ± 0.01	0.89 ± 0.02	0.73 ± 0.09	0.87 ± 0.01	0.80 ± 0.01	0.60 ± 0.03	0.78 ± 0.04
Pseudo v2 soft	0.65 ± 0.02	0.85 ± 0.01	0.68 ± 0.01	0.31 ± 0.04	0.88 ± 0.04	0.74 ± 0.06	0.87 ± 0.01	0.79 ± 0.01	0.58 ± 0.04	0.71 ± 0.05
Pseudo v2 not	0.58 ± 0.01	0.59 ± 0.04	0.64 ± 0.04	0.33 ± 0.05	0.39 ± 0.14	0.60 ± 0.06	0.62 ± 0.10	0.69 ± 0.07	0.53 ± 0.10	0.68 ± 0.05
BYOL	0.64 ± 0.01	0.38 ± 0.06	0.54 ± 0.03	0.34 ± 0.02	0.80 ± 0.02	0.50 ± 0.02	0.68 ± 0.00	0.59 ± 0.03	0.59 ± 0.02	0.62 ± 0.04
MOCOv2	0.58 ± 0.01	0.64 ± 0.01	0.52 ± 0.03	0.35 ± 0.01	0.79 ± 0.01	0.56 ± 0.02	0.89 ± 0.02	0.61 ± 0.01	0.58 ± 0.01	0.40 ± 0.05
SimCLR	0.58 ± 0.03	0.87 ± 0.01	0.65 ± 0.05	0.35 ± 0.07	0.88 ± 0.01	0.63 ± 0.11	0.79 ± 0.00	0.69 ± 0.01	0.54 ± 0.00	0.66 ± 0.05
SWAV	0.24 ± 0.02	0.74 ± 0.01	0.53 ± 0.04	0.35 ± 0.04	0.86 ± 0.01	0.60 ± 0.08	0.66 ± 0.03	0.65 ± 0.01	0.60 ± 0.03	0.56 ± 0.10

Table 14: Details 100% Budget Kl

Dataset	Benthic	CIFAR10H	MiceBone	Pig	Plankton	QualityMRI	Synthetic	Treeversity#1	Treeversity#6	Turkey
Baseline	1.17 ± 0.04	0.41 ± 0.02	0.55 ± 0.06	0.75 ± 0.05	0.34 ± 0.02	1.73 ± 0.48	0.08 ± 0.01	0.49 ± 0.04	1.02 ± 0.03	0.40 ± 0.08
ELR+	0.70 ± 0.01	0.29 ± 0.02	0.29 ± 0.01	0.62 ± 0.09	0.24 ± 0.03	1.44 ± 0.83	0.18 ± 0.02	0.46 ± 0.01	0.47 ± 0.05	0.52 ± 0.05
Het	1.16 ± 0.15	0.39 ± 0.01	0.62 ± 0.18	0.70 ± 0.10	0.34 ± 0.03	N/A	0.10 ± 0.01	0.46 ± 0.01	0.99 ± 0.02	0.52 ± 0.07
SGNP	1.11 ± 0.05	0.38 ± 0.01	0.56 ± 0.14	0.77 ± 0.07	0.33 ± 0.02	0.25 ± 0.14	0.10 ± 0.00	0.46 ± 0.01	1.07 ± 0.05	0.42 ± 0.08
DivideMix	0.87 ± 0.07	0.36 ± 0.02	0.38 ± 0.05	0.95 ± 0.04	0.34 ± 0.01	0.46 ± 0.26	0.33 ± 0.00	0.47 ± 0.01	0.62 ± 0.05	0.43 ± 0.08
Fixmatch	0.88 ± 0.24	0.37 ± 0.02	0.41 ± 0.01	0.72 ± 0.05	0.27 ± 0.02	0.99 ± 0.30	0.11 ± 0.02	0.48 ± 0.06	0.51 ± 0.01	0.48 ± 0.05
Fixmatch + DC3	0.82 ± 0.02	0.34 ± 0.03	0.54 ± 0.12	0.71 ± 0.04	0.27 ± 0.02	1.41 ± 0.15	0.18 ± 0.15	0.44 ± 0.01	0.46 ± 0.01	0.47 ± 0.03
Mean	0.80 ± 0.06	0.28 ± 0.02	0.38 ± 0.02	0.64 ± 0.03	0.32 ± 0.01	0.35 ± 0.11	0.09 ± 0.01	0.61 ± 0.01	0.52 ± 0.03	0.75 ± 0.07
Mean+DC3	0.73 ± 0.02	0.28 ± 0.04	0.37 ± 0.00	0.71 ± 0.11	0.30 ± 0.02	1.42 ± 0.93	0.11 ± 0.02	0.51 ± 0.01	0.48 ± 0.02	0.55 ± 0.10
π	0.71 ± 0.03	0.33 ± 0.02	0.38 ± 0.00	0.83 ± 0.18	0.30 ± 0.02	0.98 ± 0.04	0.08 ± 0.01	0.52 ± 0.01	0.51 ± 0.03	0.55 ± 0.01
π +DC3	0.72 ± 0.06	0.30 ± 0.02	0.39 ± 0.04	0.67 ± 0.06	0.29 ± 0.01	0.88 ± 0.34	0.08 ± 0.00	0.48 ± 0.01	0.49 ± 0.00	0.44 ± 0.08
Pseudo v1	1.10 ± 0.13	0.35 ± 0.02	0.33 ± 0.01	0.71 ± 0.07	0.32 ± 0.02	1.25 ± 0.35	0.05 ± 0.00	0.42 ± 0.01	0.42 ± 0.01	0.33 ± 0.03
Pseudo v1 + DC3	1.10 ± 0.12	0.33 ± 0.03	0.34 ± 0.02	2.87 ± 3.09	0.31 ± 0.01	1.22 ± 0.51	0.06 ± 0.00	0.41 ± 0.01	0.43 ± 0.00	0.40 ± 0.04
Pseudo v2 hard	0.97 ± 0.10	0.43 ± 0.02	0.45 ± 0.10	0.67 ± 0.04	0.31 ± 0.03	0.29 ± 0.05	0.10 ± 0.01	0.46 ± 0.03	0.99 ± 0.09	0.39 ± 0.05
Pseudo v2 soft	1.00 ± 0.08	0.41 ± 0.02	0.40 ± 0.08	0.70 ± 0.06	0.32 ± 0.06	0.62 ± 0.16	0.10 ± 0.01	0.46 ± 0.01	0.83 ± 0.13	0.37 ± 0.08
Pseudo v2 not	1.05 ± 0.02	1.12 ± 0.04	0.46 ± 0.10	0.79 ± 0.09	2.70 ± 0.89	0.12 ± 0.02	1.00 ± 0.57	0.68 ± 0.17	0.67 ± 0.11	0.57 ± 0.06
BYOL	0.74 ± 0.03	1.61 ± 0.22	0.46 ± 0.02	0.64 ± 0.01	0.51 ± 0.05	1.07 ± 0.18	0.36 ± 0.01	0.82 ± 0.09	0.58 ± 0.03	0.34 ± 0.04
MOCOv2	0.91 ± 0.05	0.98 ± 0.02	0.37 ± 0.04	0.56 ± 0.01	0.52 ± 0.01	0.29 ± 0.11	0.13 ± 0.01	0.80 ± 0.03	0.61 ± 0.01	0.42 ± 0.08
SimCLR	1.19 ± 0.10	0.36 ± 0.02	0.48 ± 0.05	0.75 ± 0.09	0.29 ± 0.02	1.83 ± 1.01	0.38 ± 0.03	0.68 ± 0.00	0.94 ± 0.04	0.43 ± 0.06
SWAV	1.56 ± 0.16	0.70 ± 0.01	0.56 ± 0.09	1.33 ± 0.98	0.38 ± 0.01	1.90 ± 0.31	0.36 ± 0.03	0.71 ± 0.02	0.61 ± 0.03	0.51 ± 0.04

Table 15: Details 100% Budget Acc

Dataset	Benthic	CIFAR10H	MiceBone	Pig	Plankton	QualityMRI	Synthetic	Treversity#1	Treversity#6	Turkey
Baseline	0.64 ± 0.01	0.91 ± 0.00	0.62 ± 0.09	0.36 ± 0.04	0.90 ± 0.01	0.67 ± 0.04	0.88 ± 0.00	0.80 ± 0.02	0.57 ± 0.05	0.76 ± 0.03
ELR+	0.69 ± 0.01	0.89 ± 0.01	0.56 ± 0.05	0.39 ± 0.01	0.92 ± 0.01	0.50 ± 0.00	0.92 ± 0.01	0.80 ± 0.00	0.75 ± 0.02	0.36 ± 0.02
Het	0.63 ± 0.01	0.90 ± 0.01	0.64 ± 0.01	0.36 ± 0.01	0.90 ± 0.01	N/A	0.84 ± 0.02	0.80 ± 0.01	0.60 ± 0.01	0.72 ± 0.01
SGNP	0.64 ± 0.00	0.90 ± 0.01	0.61 ± 0.03	0.33 ± 0.07	0.91 ± 0.01	0.63 ± 0.11	0.84 ± 0.03	0.80 ± 0.01	0.56 ± 0.03	0.75 ± 0.05
DivideMix	0.69 ± 0.04	0.90 ± 0.01	0.66 ± 0.02	0.43 ± 0.02	0.92 ± 0.01	0.52 ± 0.02	0.93 ± 0.00	0.82 ± 0.01	0.77 ± 0.02	0.68 ± 0.02
Fixmatch	0.69 ± 0.04	0.91 ± 0.01	0.72 ± 0.02	0.29 ± 0.05	0.92 ± 0.01	0.72 ± 0.06	0.83 ± 0.03	0.78 ± 0.03	0.64 ± 0.02	0.69 ± 0.06
Fixmatch + DC3	0.69 ± 0.01	0.90 ± 0.00	0.59 ± 0.08	0.33 ± 0.03	0.92 ± 0.01	0.63 ± 0.07	0.81 ± 0.13	0.79 ± 0.01	0.67 ± 0.01	0.76 ± 0.03
Mean	0.69 ± 0.01	0.90 ± 0.01	0.64 ± 0.03	0.39 ± 0.02	0.91 ± 0.01	0.64 ± 0.06	0.90 ± 0.01	0.71 ± 0.01	0.66 ± 0.01	0.52 ± 0.01
Mean+DC3	0.71 ± 0.01	0.90 ± 0.02	0.66 ± 0.00	0.35 ± 0.03	0.91 ± 0.01	0.62 ± 0.07	0.89 ± 0.01	0.75 ± 0.00	0.66 ± 0.01	0.66 ± 0.06
π	0.71 ± 0.02	0.90 ± 0.00	0.65 ± 0.01	0.34 ± 0.01	0.91 ± 0.01	0.71 ± 0.01	0.92 ± 0.01	0.75 ± 0.01	0.66 ± 0.00	0.63 ± 0.02
π +DC3	0.70 ± 0.02	0.90 ± 0.01	0.64 ± 0.05	0.37 ± 0.04	0.92 ± 0.00	0.68 ± 0.06	0.91 ± 0.01	0.77 ± 0.00	0.66 ± 0.00	0.69 ± 0.03
Pseudo v1	0.65 ± 0.05	0.91 ± 0.00	0.71 ± 0.02	0.34 ± 0.08	0.91 ± 0.01	0.68 ± 0.05	0.92 ± 0.01	0.80 ± 0.01	0.69 ± 0.01	0.80 ± 0.04
Pseudo v1 + DC3	0.64 ± 0.04	0.90 ± 0.02	0.73 ± 0.01	0.30 ± 0.04	0.91 ± 0.01	0.75 ± 0.03	0.90 ± 0.02	0.82 ± 0.01	0.69 ± 0.00	0.79 ± 0.04
Pseudo v2 hard	0.66 ± 0.02	0.84 ± 0.01	0.64 ± 0.05	0.35 ± 0.01	0.89 ± 0.02	0.73 ± 0.09	0.87 ± 0.01	0.80 ± 0.01	0.60 ± 0.03	0.78 ± 0.04
Pseudo v2 soft	0.65 ± 0.02	0.85 ± 0.01	0.68 ± 0.01	0.31 ± 0.04	0.88 ± 0.04	0.74 ± 0.06	0.87 ± 0.01	0.79 ± 0.01	0.58 ± 0.04	0.71 ± 0.05
Pseudo v2 not	0.58 ± 0.01	0.59 ± 0.04	0.64 ± 0.04	0.33 ± 0.05	0.39 ± 0.14	0.60 ± 0.06	0.62 ± 0.10	0.69 ± 0.07	0.53 ± 0.10	0.68 ± 0.05
BYOL	0.64 ± 0.01	0.38 ± 0.06	0.54 ± 0.03	0.34 ± 0.02	0.80 ± 0.02	0.50 ± 0.02	0.68 ± 0.00	0.59 ± 0.03	0.59 ± 0.02	0.62 ± 0.04
MOCov2	0.58 ± 0.01	0.64 ± 0.01	0.52 ± 0.03	0.35 ± 0.01	0.79 ± 0.01	0.56 ± 0.02	0.89 ± 0.02	0.61 ± 0.01	0.58 ± 0.01	0.40 ± 0.05
SimCLR	0.58 ± 0.03	0.87 ± 0.01	0.65 ± 0.05	0.35 ± 0.07	0.88 ± 0.01	0.63 ± 0.11	0.79 ± 0.00	0.69 ± 0.01	0.54 ± 0.00	0.66 ± 0.05
SWAV	0.24 ± 0.02	0.74 ± 0.01	0.53 ± 0.04	0.35 ± 0.04	0.86 ± 0.01	0.60 ± 0.08	0.66 ± 0.03	0.65 ± 0.01	0.60 ± 0.03	0.56 ± 0.10

Table 16: Details 1000% Budget K1

Dataset	Benthic	CIFAR10H	MiceBone	Pig	Plankton	QualityMRI	Synthetic	Treversity#1	Treversity#6	Turkey
Baseline	0.75 ± 0.03	0.26 ± 0.02	0.23 ± 0.02	0.54 ± 0.04	0.20 ± 0.02	0.31 ± 0.14	0.04 ± 0.00	0.36 ± 0.02	0.33 ± 0.01	0.24 ± 0.06
ELR+	0.75 ± 0.05	0.28 ± 0.02	0.34 ± 0.04	0.73 ± 0.02	0.27 ± 0.03	1.26 ± 0.56	0.49 ± 0.06	0.45 ± 0.01	0.64 ± 0.10	0.50 ± 0.13
Het	1.19 ± 0.05	0.38 ± 0.02	0.47 ± 0.03	0.87 ± 0.33	0.36 ± 0.04	N/A	0.26 ± 0.03	0.48 ± 0.03	1.25 ± 0.07	0.39 ± 0.03
SGNP	1.15 ± 0.04	0.36 ± 0.02	0.48 ± 0.13	1.02 ± 0.26	0.35 ± 0.04	0.25 ± 0.18	0.21 ± 0.03	0.49 ± 0.01	1.06 ± 0.04	0.47 ± 0.10
DivideMix	0.83 ± 0.05	0.37 ± 0.03	0.35 ± 0.05	1.04 ± 0.25	0.34 ± 0.01	1.34 ± 0.84	0.43 ± 0.04	0.46 ± 0.01	0.77 ± 0.03	0.41 ± 0.07
Pseudo v2 hard	0.95 ± 0.06	0.42 ± 0.01	0.45 ± 0.09	0.67 ± 0.02	0.43 ± 0.17	1.02 ± 0.27	0.20 ± 0.09	0.48 ± 0.04	1.00 ± 0.05	0.42 ± 0.10
Pseudo v2 soft	0.70 ± 0.02	0.43 ± 0.02	0.22 ± 0.02	0.61 ± 0.07	0.25 ± 0.01	1.12 ± 0.04	0.06 ± 0.01	0.37 ± 0.02	0.37 ± 0.02	0.21 ± 0.02
Pseudo v2 not	1.04 ± 0.13	1.04 ± 0.03	0.31 ± 0.05	0.57 ± 0.01	2.42 ± 0.98	0.16 ± 0.03	0.72 ± 0.32	0.66 ± 0.07	0.60 ± 0.09	0.35 ± 0.04

Table 17: Details 1000% Budget Acc

Dataset	Benthic	CIFAR10H	MiceBone	Pig	Plankton	QualityMRI	Synthetic	Treversity#1	Treversity#6	Turkey
Baseline	0.68 ± 0.01	0.91 ± 0.01	0.69 ± 0.07	0.42 ± 0.04	0.92 ± 0.01	0.56 ± 0.01	0.91 ± 0.01	0.82 ± 0.01	0.76 ± 0.01	0.75 ± 0.07
ELR+	0.68 ± 0.02	0.90 ± 0.01	0.64 ± 0.05	0.38 ± 0.00	0.92 ± 0.01	0.50 ± 0.00	0.93 ± 0.02	0.81 ± 0.01	0.79 ± 0.01	0.38 ± 0.04
Het	0.66 ± 0.02	0.91 ± 0.01	0.68 ± 0.02	0.39 ± 0.04	0.91 ± 0.01	N/A	0.91 ± 0.01	0.82 ± 0.01	0.68 ± 0.02	0.79 ± 0.05
SGNP	0.66 ± 0.01	0.91 ± 0.01	0.68 ± 0.02	0.36 ± 0.04	0.90 ± 0.02	0.68 ± 0.08	0.92 ± 0.01	0.81 ± 0.01	0.70 ± 0.01	0.74 ± 0.06
DivideMix	0.72 ± 0.01	0.90 ± 0.01	0.68 ± 0.04	0.40 ± 0.02	0.92 ± 0.01	0.57 ± 0.08	0.94 ± 0.00	0.82 ± 0.01	0.78 ± 0.01	0.69 ± 0.01
Pseudo v2 hard	0.67 ± 0.01	0.85 ± 0.01	0.68 ± 0.07	0.34 ± 0.06	0.85 ± 0.08	0.73 ± 0.08	0.87 ± 0.04	0.80 ± 0.01	0.66 ± 0.05	0.74 ± 0.05
Pseudo v2 soft	0.68 ± 0.01	0.84 ± 0.01	0.73 ± 0.03	0.39 ± 0.08	0.90 ± 0.01	0.70 ± 0.05	0.91 ± 0.01	0.81 ± 0.01	0.76 ± 0.01	0.79 ± 0.07
Pseudo v2 not	0.57 ± 0.05	0.62 ± 0.02	0.64 ± 0.08	0.40 ± 0.04	0.35 ± 0.13	0.56 ± 0.05	0.67 ± 0.09	0.68 ± 0.05	0.57 ± 0.09	0.67 ± 0.01

A.9 Raw Data

In the following, we provide the raw data aggregated across the three slices as mean \pm standard deviation (STD). The content is best viewed digitally. Some results are missing (N/A) due to hardware restrictions, degenerated training, or not applicable methods (e.g., the method Het does not work with only two classes as in QualityMRI).

Method	m	n	F1	ACC	KL	ECE	\hat{F}_1	\hat{ACC}	\hat{KL}	\hat{ECE}	κ	b	\hat{b}
BYOL	01	01	0.6060 ± 0.0060	0.6131 ± 0.0126	0.4437 ± 0.0154	0.0353 ± 0.0063	0.5715 ± 0.0230	0.5758 ± 0.0215	0.8207 ± 0.1118	0.1385 ± 0.0243	0.5073 ± 0.0134	0.1000 ± 0.0000	0.1000 ± 0.0000
BYOL	01	02	0.6389 ± 0.0025	0.6452 ± 0.0224	0.3869 ± 0.0056	0.0391 ± 0.0176	0.5965 ± 0.0097	0.6010 ± 0.0074	0.6531 ± 0.0359	0.1052 ± 0.0061	0.6234 ± 0.0096	0.2000 ± 0.0000	0.2000 ± 0.0000
BYOL	01	05	0.6513 ± 0.0161	0.6552 ± 0.0140	0.3823 ± 0.0123	0.0487 ± 0.0076	0.6037 ± 0.0086	0.6099 ± 0.0063	0.6672 ± 0.1158	0.0996 ± 0.0289	0.5928 ± 0.0237	0.5000 ± 0.0000	0.5000 ± 0.0000
BYOL	01	10	0.6733 ± 0.0013	0.6773 ± 0.0024	0.3603 ± 0.0055	0.0581 ± 0.0139	0.6272 ± 0.0159	0.6322 ± 0.0180	0.6658 ± 0.0338	0.0959 ± 0.0133	0.6179 ± 0.0204	1.0000 ± 0.0000	1.0000 ± 0.0000
DivideMix	01	01	0.8276 ± 0.0155	0.8717 ± 0.0152	0.2862 ± 0.0507	0.0537 ± 0.0257	0.8845 ± 0.0065	0.8840 ± 0.0063	0.1202 ± 0.0674	0.0154 ± 0.0039	0.8363 ± 0.0206	0.1000 ± 0.0000	0.1000 ± 0.0000
DivideMix	01	02	0.8811 ± 0.0060	0.8813 ± 0.0064	0.2531 ± 0.0238	0.0441 ± 0.0062	0.9030 ± 0.0080	0.9031 ± 0.0084	0.1263 ± 0.0209	0.0135 ± 0.0021	0.8557 ± 0.0050	0.2000 ± 0.0000	0.2000 ± 0.0000
DivideMix	01	05	0.8888 ± 0.0066	0.8873 ± 0.0064	0.2837 ± 0.0202	0.0367 ± 0.0042	0.9105 ± 0.0047	0.9110 ± 0.0049	0.1980 ± 0.0496	0.0086 ± 0.0009	0.8665 ± 0.0029	0.5000 ± 0.0000	0.5000 ± 0.0000
DivideMix	01	10	0.9277 ± 0.0034	0.9279 ± 0.0034	0.3344 ± 0.0040	0.0371 ± 0.0101	0.9358 ± 0.0015	0.9361 ± 0.0013	0.3708 ± 0.0175	0.0024 ± 0.0014	0.9240 ± 0.0021	1.0000 ± 0.0000	1.0000 ± 0.0000
DivideMix	02	05	0.8030 ± 0.0197	0.8370 ± 0.0220	0.1327 ± 0.0682	0.1001 ± 0.0833	0.8458 ± 0.0178	0.8460 ± 0.0180	1.5025 ± 0.1002	0.1306 ± 0.0199	0.8677 ± 0.0053	1.0000 ± 0.0000	1.0000 ± 0.0000
DivideMix	03	10	0.9034 ± 0.0092	0.9043 ± 0.0094	0.4777 ± 0.0600	0.0165 ± 0.0035	0.9198 ± 0.0044	0.9205 ± 0.0042	0.5923 ± 0.1182	0.0008 ± 0.0005	0.9226 ± 0.0118	3.0000 ± 0.0000	3.0000 ± 0.0000
DivideMix	05	02	0.8960 ± 0.0064	0.8960 ± 0.0063	0.7122 ± 0.0076	0.0337 ± 0.0055	0.9113 ± 0.0015	0.9115 ± 0.0016	1.3934 ± 0.1405	0.0662 ± 0.0047	0.8728 ± 0.0076	1.0000 ± 0.0000	1.0000 ± 0.0000
DivideMix	10	10	0.9202 ± 0.0117	0.9207 ± 0.0114	0.4244 ± 0.0676	0.0206 ± 0.0078	0.9338 ± 0.0041	0.9342 ± 0.0041	1.9600 ± 0.1079	0.0013 ± 0.0013	0.9306 ± 0.0086	5.0000 ± 0.0000	5.0000 ± 0.0000
DivideMix	10	10	0.8949 ± 0.0118	0.8954 ± 0.0117	0.7347 ± 0.0667	0.0309 ± 0.0060	0.9081 ± 0.0050	0.9084 ± 0.0049	1.5903 ± 0.1605	0.0691 ± 0.0079	0.9040 ± 0.0052	1.0000 ± 0.0000	1.0000 ± 0.0000
DivideMix	10	10	0.9372 ± 0.0027	0.9374 ± 0.0026	0.4341 ± 0.0390	0.0268 ± 0.0051	0.9459 ± 0.0011	0.9462 ± 0.0012	0.4922 ± 0.0943	0.0019 ± 0.0016	0.9400 ± 0.0046	10.0000 ± 0.0000	10.0000 ± 0.0000
ELR+	01	01	0.8408 ± 0.0032	0.8488 ± 0.0033	0.1667 ± 0.0061	0.0795 ± 0.0203	0.8580 ± 0.0037	0.8575 ± 0.0034	0.2255 ± 0.0251	0.0391 ± 0.0169	0.8050 ± 0.0211	0.1000 ± 0.0000	0.1000 ± 0.0000
ELR+	01	02	0.8814 ± 0.0078	0.8806 ± 0.0080	0.1565 ± 0.0050	0.0699 ± 0.0027	0.8921 ± 0.0049	0.8915 ± 0.0055	0.2465 ± 0.0208	0.0281 ± 0.0028	0.8487 ± 0.0069	0.2000 ± 0.0000	0.2000 ± 0.0000
ELR+	01	05	0.8987 ± 0.0134	0.8989 ± 0.0132	0.1349 ± 0.0244	0.0943 ± 0.0226	0.9167 ± 0.0052	0.9170 ± 0.0050	0.2295 ± 0.0240	0.0473 ± 0.0101	0.8865 ± 0.0052	0.5000 ± 0.0000	0.5000 ± 0.0000
ELR+	01	10	0.9154 ± 0.0085	0.9154 ± 0.0090	0.1765 ± 0.0163	0.0744 ± 0.0152	0.9388 ± 0.0029	0.9386 ± 0.0031	0.2507 ± 0.0189	0.0499 ± 0.0089	0.9267 ± 0.0064	1.0000 ± 0.0000	1.0000 ± 0.0000
ELR+	02	05	0.7916 ± 0.0068	0.7930 ± 0.0058	0.4627 ± 0.0462	0.0734 ± 0.0140	0.8056 ± 0.0032	0.8078 ± 0.0028	0.4995 ± 0.0478	0.0965 ± 0.0127	0.8946 ± 0.0081	1.0000 ± 0.0000	1.0000 ± 0.0000
ELR+	03	10	0.8728 ± 0.0226	0.8736 ± 0.0212	0.2131 ± 0.1045	0.0800 ± 0.0444	0.8906 ± 0.0133	0.8950 ± 0.0136	0.2579 ± 0.1567	0.0726 ± 0.0333	0.8746 ± 0.0147	3.0000 ± 0.0000	3.0000 ± 0.0000
ELR+	05	02	0.8694 ± 0.0169	0.8682 ± 0.0185	0.2462 ± 0.0250	0.0400 ± 0.0223	0.8890 ± 0.0157	0.8882 ± 0.0169	0.3311 ± 0.0630	0.0161 ± 0.0097	0.8447 ± 0.0164	1.0000 ± 0.0000	1.0000 ± 0.0000
ELR+	05	10	0.8843 ± 0.0201	0.8836 ± 0.0225	0.2501 ± 0.1216	0.0520 ± 0.0289	0.8990 ± 0.0185	0.8991 ± 0.0187	0.3134 ± 0.1390	0.0401 ± 0.0319	0.8855 ± 0.0129	5.0000 ± 0.0000	5.0000 ± 0.0000
ELR+	10	10	0.8805 ± 0.0064	0.8800 ± 0.0056	0.2151 ± 0.0147	0.0551 ± 0.0117	0.8942 ± 0.0027	0.8939 ± 0.0029	0.3346 ± 0.0398	0.0240 ± 0.0142	0.8613 ± 0.0032	1.0000 ± 0.0000	1.0000 ± 0.0000
ELR+	10	10	0.9259 ± 0.0179	0.9260 ± 0.0180	0.4924 ± 0.0621	0.0280 ± 0.0115	0.9431 ± 0.0074	0.9432 ± 0.0075	0.6926 ± 0.0560	0.0142 ± 0.0055	0.9440 ± 0.0038	10.0000 ± 0.0000	10.0000 ± 0.0000
Fixmatch	01	01	0.8061 ± 0.0090	0.8062 ± 0.0094	0.3590 ± 0.0653	0.0388 ± 0.0086	0.8011 ± 0.0130	0.8011 ± 0.0131	1.3545 ± 0.3515	0.1461 ± 0.0254	0.6715 ± 0.0110	0.1000 ± 0.0000	0.1000 ± 0.0000
Fixmatch	01	02	0.8385 ± 0.0098	0.8397 ± 0.0109	0.1284 ± 0.0143	0.0840 ± 0.0215	0.8220 ± 0.0073	0.8224 ± 0.0072	0.2008 ± 0.0364	0.0237 ± 0.0104	0.7203 ± 0.0114	0.2000 ± 0.0000	0.2000 ± 0.0000
Fixmatch	01	05	0.8987 ± 0.0134	0.8989 ± 0.0132	0.1349 ± 0.0244	0.0943 ± 0.0226	0.9167 ± 0.0052	0.9170 ± 0.0050	0.2295 ± 0.0240	0.0473 ± 0.0101	0.8865 ± 0.0052	0.5000 ± 0.0000	0.5000 ± 0.0000
Fixmatch	01	10	0.9154 ± 0.0085	0.9154 ± 0.0090	0.1765 ± 0.0163	0.0744 ± 0.0152	0.9388 ± 0.0029	0.9386 ± 0.0031	0.2507 ± 0.0189	0.0499 ± 0.0089	0.9267 ± 0.0064	1.0000 ± 0.0000	1.0000 ± 0.0000
Fixmatch	02	05	0.7916 ± 0.0068	0.7930 ± 0.0058	0.4627 ± 0.0462	0.0734 ± 0.0140	0.8056 ± 0.0032	0.8078 ± 0.0028	0.4995 ± 0.0478	0.0965 ± 0.0127	0.8946 ± 0.0081	1.0000 ± 0.0000	1.0000 ± 0.0000
Fixmatch	03	10	0.8728 ± 0.0226	0.8736 ± 0.0212	0.2131 ± 0.1045	0.0800 ± 0.0444	0.8906 ± 0.0133	0.8950 ± 0.0136	0.2579 ± 0.1567	0.0726 ± 0.0333	0.8746 ± 0.0147	3.0000 ± 0.0000	3.0000 ± 0.0000
Fixmatch	05	02	0.8694 ± 0.0169	0.8682 ± 0.0185	0.2462 ± 0.0250	0.0400 ± 0.0223	0.8890 ± 0.0157	0.8882 ± 0.0169	0.3311 ± 0.0630	0.0161 ± 0.0097	0.8447 ± 0.0164	1.0000 ± 0.0000	1.0000 ± 0.0000
Fixmatch	05	10	0.8843 ± 0.0201	0.8836 ± 0.0225	0.2501 ± 0.1216	0.0520 ± 0.0289	0.8990 ± 0.0185	0.8991 ± 0.0187	0.3134 ± 0.1390	0.0401 ± 0.0319	0.8855 ± 0.0129	5.0000 ± 0.0000	5.0000 ± 0.0000
Fixmatch	10	10	0.8805 ± 0.0064	0.8800 ± 0.0056	0.2151 ± 0.0147	0.0551 ± 0.0117	0.8942 ± 0.0027	0.8939 ± 0.0029	0.3346 ± 0.0398	0.0240 ± 0.0142	0.8613 ± 0.0032	1.0000 ± 0.0000	1.0000 ± 0.0000
Fixmatch	10	10	0.9259 ± 0.0179	0.9260 ± 0.0180	0.4924 ± 0.0621	0.0280 ± 0.0115	0.9431 ± 0.0074	0.9432 ± 0.0075	0.6926 ± 0.0560	0.0142 ± 0.0055	0.9440 ± 0.0038	10.0000 ± 0.0000	10.0000 ± 0.0000
Fixmatch + S2C2	01	01	0.8061 ± 0.0090	0.8062 ± 0.0094	0.3590 ± 0.0653	0.0388 ± 0.0086	0.8011 ± 0.0130	0.8011 ± 0.0131	1.3545 ± 0.3515	0.1461 ± 0.0254	0.6715 ± 0.0110	0.1000 ± 0.0000	0.1000 ± 0.0000
Fixmatch + S2C2	01	02	0.8385 ± 0.0098	0.8397 ± 0.0109	0.1284 ± 0.0143	0.0840 ± 0.0215	0.8220 ± 0.0073	0.8224 ± 0.0072	0.2008 ± 0.0364	0.0237 ± 0.0104	0.7203 ± 0.0114	0.2000 ± 0.0000	0.2000 ± 0.0000
Fixmatch + S2C2	01	05	0.8987 ± 0.0134	0.8989 ± 0.0132	0.1349 ± 0.0244	0.0943 ± 0.0226	0.9167 ± 0.0052	0.9170 ± 0.0050	0.2295 ± 0.0240	0.0473 ± 0.0101	0.8865 ± 0.0052	0.5000 ± 0.0000	0.5000 ± 0.0000
Fixmatch + S2C2	01	10	0.9154 ± 0.0085	0.9154 ± 0.0090	0.1765 ± 0.0163	0.0744 ± 0.0152	0.9388 ± 0.0029	0.9386 ± 0.0031	0.2507 ± 0.0189	0.0499 ± 0.0089	0.9267 ± 0.0064	1.0000 ± 0.0000	1.0000 ± 0.0000
Fixmatch + S2C2	02	05	0.7916 ± 0.0068	0.7930 ± 0.0058	0.4627 ± 0.0462	0.0734 ± 0.0140	0.8056 ± 0.0032	0.8078 ± 0.0028	0.4995 ± 0.0478	0.0965 ± 0.0127	0.8946 ± 0.0081	1.0000 ± 0.0000	1.0000 ± 0.0000
Fixmatch + S2C2	03	10	0.8728 ± 0.0226	0.8736 ± 0.0212	0.2131 ± 0.1045	0.0800 ± 0.0444	0.8906 ± 0.0133	0.8950 ± 0.0136	0.2579 ± 0.1567	0.0726 ± 0.0333	0.8746 ± 0.0147	3.0000 ± 0.0000	3.0000 ± 0.0000
Fixmatch + S2C2	05	02	0.8694 ± 0.0169	0.8682 ± 0.0185	0.2462 ± 0.0250	0.0400 ± 0.0223	0.8890 ± 0.0157	0.8882 ± 0.0169	0.3311 ± 0.0630	0.0161 ± 0.0097	0.8447 ± 0.0164	1.0000 ± 0.0000	1.0000 ± 0.0000
Fixmatch + S2C2	05	10	0.8843 ± 0.0201	0.8836 ± 0.0225	0.2501 ± 0.1216	0.0520 ± 0.0289	0.8990 ± 0.0185	0.8991 ± 0.0187	0.3134 ± 0.1390	0.0401 ± 0.0319	0.8855 ± 0.0129	5.0000 ± 0.0000	5.0000 ± 0.0000
Fixmatch + S2C2	10	10	0.8805 ± 0.0064	0.8800 ± 0.0056	0.2151 ± 0.0147	0.0551 ± 0.0117	0.8942 ± 0.0027	0.8939 ± 0.0029	0.3346 ± 0.0398	0.0240 ± 0.0142	0.8613 ± 0.0032	1.0000 ± 0.0000	1.0000 ± 0.0000
Fixmatch + S2C2	10	10	0.9259 ± 0.0179	0.9260 ± 0.0180	0.4924 ± 0.0621	0.0280 ± 0.0115	0.9431 ± 0.0074	0.9432 ± 0.0075	0.6926 ± 0.0560	0.0142 ± 0.0055	0.9440 ± 0.0038	10.0000 ± 0.0000	10.0000 ± 0.0000
Fixmatch + S2C2	10	10	0.8805 ± 0.0064	0.8800 ± 0.0056	0.2151 ± 0.0147	0.0551 ± 0.0117	0.8942 ± 0.0027	0.8939 ± 0.0029	0.3346 ± 0.0398	0.0240 ± 0.0142	0.8613 ± 0.0032	1.0000 ± 0.0000	1.0000 ± 0.0000
Fixmatch + S2C2	10	10	0.9259 ± 0.0179	0.9260 ± 0.0180	0.4924 ± 0.0621	0.0280 ± 0.0115	0.9431 ± 0.0074	0.9432 ± 0.0075	0.6926 ± 0.0560	0.0142 ± 0.0055	0.9440 ± 0.0038	10.0000 ± 0.0000	10.0000 ± 0.0000
Fixmatch + S2C2	10	10	0.8805 ± 0.0064	0.8800 ± 0.0056	0.2151 ± 0.0147	0.0551 ± 0.0117	0.8942 ± 0.0027	0.8939 ± 0.0029	0.3346 ± 0.0398	0.0240 ± 0.0142	0.8613 ± 0.0032	1.0000 ± 0.0000	1.0000 ± 0.0000
Fixmatch + S2C2	10	10	0.9259 ± 0.0179	0.9260 ± 0.0180	0.4924 ± 0.0621	0.0280 ± 0.0115	0.9431 ± 0.0074	0.9432 ± 0.0075	0.6926 ± 0.0560	0.0142 ± 0.0055	0.9440 ± 0.0038	10.0000 ± 0.0000	10.0000 ± 0.0000
Fixmatch + S2C2	10	10	0.8805 ± 0.0064	0.8800 ± 0.0056	0.2151 ± 0.0147	0.0551 ± 0.0117	0.8942 ± 0.0027	0.8939 ± 0.0029	0.3346 ± 0.0398	0.0240 ± 0.0142	0.8613 ± 0.0032	1.0000 ± 0.0000	1.0000 ± 0.0000
Fixmatch + S2C2	10	10	0.9259 ± 0.0179	0.9260 ± 0.0180	0.4924 ± 0.0621	0.0280 ± 0.0115	0.9431 ± 0.0074	0.9432 ± 0.0075	0.6926 ± 0.0560	0.0142 ± 0.0055	0.9440 ± 0.0038	10.0000 ± 0.0000	10.0000 ± 0.0000
Fixmatch + S2C2	10	10	0.8805 ± 0.0064	0.8800 ± 0.0056	0.2151 ± 0.0147	0.0551 ± 0.0117	0.8942 ± 0.0027	0.8939 ± 0.0029	0.3346 ± 0.0398	0.0240 ± 0.0142	0.8613 ± 0.0032	1.0000 ± 0.0000	1.0000 ± 0.0000
Fixmatch + S2C2	10	10	0.9259 ± 0.0179	0.9260 ± 0.0180	0.4924 ± 0.0621	0.0280 ± 0.0115							

Method	<i>m</i>	<i>n</i>	<i>F1</i>	<i>ACC</i>	<i>KL</i>	<i>ECE</i>	<i>F1</i>	<i>ACC</i>	<i>KL</i>	<i>ECE</i>	κ	<i>b</i>	\hat{b}
BYOL	01	0.10	0.5555 ± 0.0181	0.5709 ± 0.0138	0.9523 ± 0.0454	0.0847 ± 0.0097	0.5240 ± 0.0081	0.5305 ± 0.0103	1.4802 ± 0.0827	0.2180 ± 0.0111	0.4813 ± 0.0086	0.1000 ± 0.0000	0.1000 ± 0.0000
BYOL	01	0.20	0.6068 ± 0.0352	0.6183 ± 0.0355	0.7976 ± 0.0417	0.0432 ± 0.0161	0.5536 ± 0.0244	0.5579 ± 0.0241	1.2286 ± 0.0252	0.1867 ± 0.0023	0.5127 ± 0.0282	0.1000 ± 0.0000	0.1999 ± 0.0000
BYOL	01	0.50	0.6216 ± 0.0191	0.6265 ± 0.0166	0.7486 ± 0.0496	0.0315 ± 0.0054	0.5745 ± 0.0157	0.5782 ± 0.0154	1.1168 ± 0.0447	0.1584 ± 0.0131	0.5707 ± 0.0158	0.5000 ± 0.0000	0.5000 ± 0.0000
BYOL	01	1.00	0.5882 ± 0.0451	0.5921 ± 0.0356	0.8180 ± 0.0909	0.0370 ± 0.0151	0.5250 ± 0.0191	0.5323 ± 0.0298	1.2806 ± 0.1846	0.1909 ± 0.0282	0.5197 ± 0.0412	1.0000 ± 0.0000	1.0000 ± 0.0000
DivideMix	01	0.10	0.7430 ± 0.0077	0.7431 ± 0.0057	0.5952 ± 0.0267	0.0844 ± 0.0073	0.7399 ± 0.0080	0.7543 ± 0.0061	0.1689 ± 0.0172	0.0758 ± 0.0009	0.7555 ± 0.0067	0.1000 ± 0.0000	0.1000 ± 0.0000
DivideMix	01	0.20	0.7611 ± 0.0098	0.7684 ± 0.0114	0.5341 ± 0.0050	0.0603 ± 0.0022	0.7701 ± 0.0139	0.7850 ± 0.0131	0.1616 ± 0.0025	0.0590 ± 0.0067	0.8087 ± 0.0094	0.1999 ± 0.0000	0.1999 ± 0.0000
DivideMix	01	0.50	0.7950 ± 0.0091	0.8005 ± 0.0102	0.4693 ± 0.0084	0.0370 ± 0.0051	0.8195 ± 0.0093	0.8321 ± 0.0087	0.1364 ± 0.0177	0.0554 ± 0.0053	0.8444 ± 0.0018	0.5000 ± 0.0000	0.5000 ± 0.0000
DivideMix	01	1.00	0.8134 ± 0.0069	0.8200 ± 0.0067	0.4725 ± 0.0110	0.0150 ± 0.0024	0.8407 ± 0.0148	0.8540 ± 0.0133	0.1811 ± 0.0169	0.0222 ± 0.0019	0.8977 ± 0.0119	1.0000 ± 0.0000	1.0000 ± 0.0000
DivideMix	02	0.50	0.8006 ± 0.0163	0.8020 ± 0.0175	0.5968 ± 0.0328	0.0834 ± 0.0092	0.8270 ± 0.0100	0.8338 ± 0.0092	0.7362 ± 0.0147	0.1032 ± 0.0042	0.8525 ± 0.0070	0.9999 ± 0.0001	0.9999 ± 0.0001
DivideMix	05	1.00	0.8205 ± 0.0092	0.8274 ± 0.0085	0.4596 ± 0.0121	0.0199 ± 0.0076	0.8476 ± 0.0140	0.8590 ± 0.0136	0.1327 ± 0.0123	0.0268 ± 0.0033	0.8970 ± 0.0115	3.0000 ± 0.0000	3.0000 ± 0.0000
DivideMix	05	0.20	0.7713 ± 0.0088	0.7741 ± 0.0082	0.6322 ± 0.0181	0.0813 ± 0.0060	0.7740 ± 0.0135	0.7879 ± 0.0132	0.0752 ± 0.0110	0.1194 ± 0.0041	0.8310 ± 0.0028	0.9999 ± 0.0001	0.9999 ± 0.0001
DivideMix	05	1.00	0.8216 ± 0.0103	0.8264 ± 0.0108	0.4597 ± 0.0078	0.0204 ± 0.0096	0.8473 ± 0.0109	0.8576 ± 0.0125	0.1462 ± 0.0169	0.0241 ± 0.0039	0.9000 ± 0.0105	5.0000 ± 0.0000	5.0000 ± 0.0000
DivideMix	10	0.10	0.7331 ± 0.0113	0.7376 ± 0.0134	0.6941 ± 0.0296	0.0791 ± 0.0106	0.7347 ± 0.0047	0.7463 ± 0.0083	0.8033 ± 0.0216	0.1194 ± 0.0044	0.7685 ± 0.0147	0.9999 ± 0.0001	0.9999 ± 0.0001
DivideMix	10	0.20	0.7480 ± 0.0094	0.7519 ± 0.0127	0.5964 ± 0.0068	0.0231 ± 0.0035	0.6662 ± 0.0070	0.6852 ± 0.0096	0.6471 ± 0.0169	0.1162 ± 0.0104	0.6425 ± 0.0074	0.9999 ± 0.0001	0.9999 ± 0.0001
DivideMix	10	0.50	0.7825 ± 0.0102	0.7862 ± 0.0123	0.7052 ± 0.0469	0.0488 ± 0.0132	0.6279 ± 0.0259	0.6264 ± 0.0185	0.6812 ± 0.0483	0.0383 ± 0.0183	0.7224 ± 0.0314	0.1000 ± 0.0000	0.1000 ± 0.0000
DivideMix	10	1.00	0.8243 ± 0.0027	0.8142 ± 0.0061	0.4496 ± 0.0148	0.0536 ± 0.0070	0.8532 ± 0.0092	0.8529 ± 0.0111	0.4313 ± 0.0115	0.0552 ± 0.0023	0.9024 ± 0.0109	10.0000 ± 0.0000	10.0000 ± 0.0000
DivideMix	10	0.10	0.6241 ± 0.0219	0.6262 ± 0.0123	0.7052 ± 0.0469	0.0488 ± 0.0132	0.6279 ± 0.0259	0.6264 ± 0.0185	0.6812 ± 0.0483	0.0383 ± 0.0183	0.7224 ± 0.0314	0.1000 ± 0.0000	0.1000 ± 0.0000
DivideMix	10	0.20	0.7488 ± 0.0089	0.7342 ± 0.0055	0.5241 ± 0.0145	0.0279 ± 0.0106	0.6723 ± 0.0122	0.6732 ± 0.0088	0.5012 ± 0.0124	0.0253 ± 0.0028	0.8113 ± 0.0073	0.1999 ± 0.0000	0.1999 ± 0.0000
DivideMix	10	0.50	0.7914 ± 0.0222	0.7743 ± 0.0244	0.4670 ± 0.0362	0.0325 ± 0.0121	0.8137 ± 0.0223	0.8049 ± 0.0263	0.4345 ± 0.0320	0.0321 ± 0.0154	0.8554 ± 0.0102	0.5000 ± 0.0000	0.5000 ± 0.0000
DivideMix	10	1.00	0.8104 ± 0.0064	0.7989 ± 0.0044	0.4643 ± 0.0089	0.0492 ± 0.0050	0.8386 ± 0.0118	0.8342 ± 0.0098	0.4239 ± 0.0089	0.0521 ± 0.0068	0.8884 ± 0.0103	1.0000 ± 0.0000	1.0000 ± 0.0000
DivideMix	10	0.50	0.7922 ± 0.0085	0.7886 ± 0.0084	0.4769 ± 0.0203	0.0344 ± 0.0141	0.8053 ± 0.0151	0.7963 ± 0.0165	0.4776 ± 0.0250	0.0535 ± 0.0179	0.8498 ± 0.0004	0.9999 ± 0.0001	0.9999 ± 0.0001
DivideMix	10	1.00	0.8232 ± 0.0144	0.8152 ± 0.0125	0.4432 ± 0.0147	0.0465 ± 0.0088	0.8459 ± 0.0102	0.8455 ± 0.0095	0.4280 ± 0.0222	0.0524 ± 0.0056	0.8964 ± 0.0121	3.0000 ± 0.0000	3.0000 ± 0.0000
DivideMix	10	0.50	0.7540 ± 0.0067	0.7407 ± 0.0062	0.5252 ± 0.0087	0.0151 ± 0.0016	0.7695 ± 0.0068	0.7594 ± 0.0037	0.4670 ± 0.0123	0.0257 ± 0.0065	0.8296 ± 0.0063	0.9999 ± 0.0001	0.9999 ± 0.0001
DivideMix	10	1.00	0.8194 ± 0.0044	0.8093 ± 0.0052	0.4751 ± 0.0069	0.0495 ± 0.0028	0.8465 ± 0.0088	0.8445 ± 0.0106	0.4281 ± 0.0093	0.0566 ± 0.0042	0.9003 ± 0.0115	5.0000 ± 0.0000	5.0000 ± 0.0000
DivideMix	10	0.10	0.6162 ± 0.0579	0.6098 ± 0.0538	0.7153 ± 0.0718	0.0701 ± 0.0343	0.6372 ± 0.0283	0.6233 ± 0.0283	0.6852 ± 0.0484	0.0570 ± 0.0322	0.7447 ± 0.0273	0.9999 ± 0.0001	0.9999 ± 0.0001
DivideMix	10	0.20	0.7483 ± 0.0027	0.7442 ± 0.0061	0.4496 ± 0.0148	0.0536 ± 0.0070	0.8532 ± 0.0092	0.8529 ± 0.0111	0.4313 ± 0.0115	0.0552 ± 0.0023	0.9024 ± 0.0109	10.0000 ± 0.0000	10.0000 ± 0.0000
DivideMix	10	0.50	0.7893 ± 0.0091	0.7971 ± 0.0091	0.4858 ± 0.0207	0.0427 ± 0.0185	0.6467 ± 0.0205	0.6478 ± 0.0080	0.3727 ± 0.0068	0.1417 ± 0.0057	0.6379 ± 0.0064	0.9999 ± 0.0001	0.9999 ± 0.0001
DivideMix	10	1.00	0.8194 ± 0.0044	0.8093 ± 0.0052	0.4751 ± 0.0069	0.0495 ± 0.0028	0.8465 ± 0.0088	0.8445 ± 0.0106	0.4281 ± 0.0093	0.0566 ± 0.0042	0.9003 ± 0.0115	5.0000 ± 0.0000	5.0000 ± 0.0000
DivideMix	10	0.10	0.6162 ± 0.0579	0.6098 ± 0.0538	0.7153 ± 0.0718	0.0701 ± 0.0343	0.6372 ± 0.0283	0.6233 ± 0.0283	0.6852 ± 0.0484	0.0570 ± 0.0322	0.7447 ± 0.0273	0.9999 ± 0.0001	0.9999 ± 0.0001
DivideMix	10	0.20	0.7483 ± 0.0027	0.7442 ± 0.0061	0.4496 ± 0.0148	0.0536 ± 0.0070	0.8532 ± 0.0092	0.8529 ± 0.0111	0.4313 ± 0.0115	0.0552 ± 0.0023	0.9024 ± 0.0109	10.0000 ± 0.0000	10.0000 ± 0.0000
DivideMix	10	0.50	0.7893 ± 0.0091	0.7971 ± 0.0091	0.4858 ± 0.0207	0.0427 ± 0.0185	0.6467 ± 0.0205	0.6478 ± 0.0080	0.3727 ± 0.0068	0.1417 ± 0.0057	0.6379 ± 0.0064	0.9999 ± 0.0001	0.9999 ± 0.0001
DivideMix	10	1.00	0.8194 ± 0.0044	0.8093 ± 0.0052	0.4751 ± 0.0069	0.0495 ± 0.0028	0.8465 ± 0.0088	0.8445 ± 0.0106	0.4281 ± 0.0093	0.0566 ± 0.0042	0.9003 ± 0.0115	5.0000 ± 0.0000	5.0000 ± 0.0000
DivideMix	10	0.10	0.6162 ± 0.0579	0.6098 ± 0.0538	0.7153 ± 0.0718	0.0701 ± 0.0343	0.6372 ± 0.0283	0.6233 ± 0.0283	0.6852 ± 0.0484	0.0570 ± 0.0322	0.7447 ± 0.0273	0.9999 ± 0.0001	0.9999 ± 0.0001
DivideMix	10	0.20	0.7483 ± 0.0027	0.7442 ± 0.0061	0.4496 ± 0.0148	0.0536 ± 0.0070	0.8532 ± 0.0092	0.8529 ± 0.0111	0.4313 ± 0.0115	0.0552 ± 0.0023	0.9024 ± 0.0109	10.0000 ± 0.0000	10.0000 ± 0.0000
DivideMix	10	0.50	0.7893 ± 0.0091	0.7971 ± 0.0091	0.4858 ± 0.0207	0.0427 ± 0.0185	0.6467 ± 0.0205	0.6478 ± 0.0080	0.3727 ± 0.0068	0.1417 ± 0.0057	0.6379 ± 0.0064	0.9999 ± 0.0001	0.9999 ± 0.0001
DivideMix	10	1.00	0.8194 ± 0.0044	0.8093 ± 0.0052	0.4751 ± 0.0069	0.0495 ± 0.0028	0.8465 ± 0.0088	0.8445 ± 0.0106	0.4281 ± 0.0093	0.0566 ± 0.0042	0.9003 ± 0.0115	5.0000 ± 0.0000	5.0000 ± 0.0000
DivideMix	10	0.10	0.6162 ± 0.0579	0.6098 ± 0.0538	0.7153 ± 0.0718	0.0701 ± 0.0343	0.6372 ± 0.0283	0.6233 ± 0.0283	0.6852 ± 0.0484	0.0570 ± 0.0322	0.7447 ± 0.0273	0.9999 ± 0.0001	0.9999 ± 0.0001
DivideMix	10	0.20	0.7483 ± 0.0027	0.7442 ± 0.0061	0.4496 ± 0.0148	0.0536 ± 0.0070	0.8532 ± 0.0092	0.8529 ± 0.0111	0.4313 ± 0.0115	0.0552 ± 0.0023	0.9024 ± 0.0109	10.0000 ± 0.0000	10.0000 ± 0.0000
DivideMix	10	0.50	0.7893 ± 0.0091	0.7971 ± 0.0091	0.4858 ± 0.0207	0.0427 ± 0.0185	0.6467 ± 0.0205	0.6478 ± 0.0080	0.3727 ± 0.0068	0.1417 ± 0.0057	0.6379 ± 0.0064	0.9999 ± 0.0001	0.9999 ± 0.0001
DivideMix	10	1.00	0.8194 ± 0.0044	0.8093 ± 0.0052	0.4751 ± 0.0069	0.0495 ± 0.0028	0.8465 ± 0.0088	0.8445 ± 0.0106	0.4281 ± 0.0093	0.0566 ± 0.0042	0.9003 ± 0.0115	5.0000 ± 0.0000	5.0000 ± 0.0000
DivideMix	10	0.10	0.6162 ± 0.0579	0.6098 ± 0.0538	0.7153 ± 0.0718	0.0701 ± 0.0343	0.6372 ± 0.0283	0.6233 ± 0.0283	0.6852 ± 0.0484	0.0570 ± 0.0322	0.7447 ± 0.0273	0.9999 ± 0.0001	0.9999 ± 0.0001
DivideMix	10	0.20	0.7483 ± 0.0027	0.7442 ± 0.0061	0.4496 ± 0.0148	0.0536 ± 0.0070	0.8532 ± 0.0092	0.8529 ± 0.0111	0.4313 ± 0.0115	0.0552 ± 0.0023	0.9024 ± 0.0109	10.0000 ± 0.0000	10.0000 ± 0.0000
DivideMix	10	0.50	0.7893 ± 0.0091	0.7971 ± 0.0091	0.4858 ± 0.0207	0.0427 ± 0.0185	0.6467 ± 0.0205	0.6478 ± 0.0080	0.3727 ± 0.0068	0.1417 ± 0.0057	0.6379 ± 0.0064	0.9999 ± 0.0001	0.9999 ± 0.0001
DivideMix	10	1.00	0.8194 ± 0.0044	0.8093 ± 0.0052	0.4751 ± 0.0069	0.0495 ± 0.0028	0.8465 ± 0.0088	0.8445 ± 0.0106	0.4281 ± 0.0093	0.0566 ± 0.0042	0.9003 ± 0.0115	5.0000 ± 0.0000	5.0000 ± 0.0000
DivideMix	10	0.10	0.6162 ± 0.0579	0.6098 ± 0.0538	0.7153 ± 0.0718	0.0701 ± 0.0343	0.6372 ± 0.0283	0.6233 ± 0.0283	0.6852 ± 0.0484	0.0570 ± 0.0322	0.7447 ± 0.0273	0.9999 ± 0.0001	0.9999 ± 0.0001
DivideMix	10	0.20	0.7483 ± 0.0027	0.7442 ± 0.0061	0.4496 ± 0.0148	0.0536 ± 0.0070	0.8532 ± 0.0092	0.8529 ± 0.0111	0.4313 ± 0.0115	0.0552 ± 0.0023	0.9024 ± 0.0109	10.0000 ± 0.0000	10.0000 ± 0.0000
DivideMix	10	0.50	0.7893 ± 0.0091	0.7971 ± 0.0091	0.4858 ± 0.0207	0.0427 ± 0.0185	0.6467 ± 0.0205	0.6478 ± 0.0080	0.3727 ± 0.0068	0.1417 ± 0.0057	0.6379 ± 0.0064	0.9999 ± 0.0001	0.9999 ± 0.0001
DivideMix	10	1.00	0.8194 ± 0.0044	0.8093 ± 0.0052	0.4751 ± 0.0069	0.0495 ± 0.0028	0.8465 ± 0.0088	0.8445 ± 0.0106	0.4281 ± 0.0093	0.0566 ± 0.0042	0.9003 ± 0.0115	5.0000 ± 0.0000	5.0000 ± 0.0000
DivideMix	10	0.10	0.6162 ± 0.0579	0.6098 ± 0.0538	0.7153 ± 0.0718	0.0701 ± 0.0343	0.6372 ± 0.0283	0.6233 ± 0.0283	0.6852 ± 0.0484	0.0570 ± 0.0322	0.7447 ± 0.0273	0.9999 ± 0.0001	0.9999 ± 0.0001
DivideMix	10	0.20	0.7483 ± 0.0027	0.7442 ± 0.0061	0.4496 ± 0.0148	0.0536 ± 0.0070	0.8532 ± 0.0092	0.8529 ± 0.0111	0.4313 ± 0.0115	0.0552 ± 0.0023	0.9024 ± 0.0109	10.0000 ± 0.0000	10.0000 ± 0.0000
DivideMix	10	0.50	0.7893 ± 0.0091	0.7971 ± 0.0091	0.4858 ± 0.0207	0.0427 ± 0.0185	0.6467 ± 0.0205	0.6478 ± 0.0080	0.3727 ± 0.0068	0.1417 ± 0.0057	0.6379 ± 0.0064	0.9999 ± 0.0001	0.9999 ± 0.0001
DivideMix	10	1.00	0.										

Method	m	n	F1	ACC	KL	ECE	F1	ACC	KL	ECE	κ	b	\hat{b}
BYOL	01	01	0.6020 ± 0.0913	0.6356 ± 0.0857	0.3303 ± 0.0194	0.0556 ± 0.0200	0.5386 ± 0.0936	0.5193 ± 0.0830	0.5542 ± 0.1467	0.0813 ± 0.0367	0.4975 ± 0.0426	0.0999 ± 0.0000	0.0999 ± 0.0000
BYOL	01	020	0.5243 ± 0.0526	0.5225 ± 0.0466	0.4098 ± 0.0937	0.0724 ± 0.0137	0.4959 ± 0.0388	0.4877 ± 0.0334	0.5160 ± 0.1512	0.0892 ± 0.0448	0.4644 ± 0.0588	0.1999 ± 0.0000	0.1999 ± 0.0000
BYOL	01	050	0.5913 ± 0.0084	0.6047 ± 0.0096	0.3375 ± 0.0387	0.0489 ± 0.0148	0.5597 ± 0.0370	0.5525 ± 0.0283	0.4688 ± 0.0942	0.0669 ± 0.0316	0.4690 ± 0.0436	0.5000 ± 0.0000	0.5000 ± 0.0000
BYOL	01	100	0.6256 ± 0.0191	0.6245 ± 0.0445	0.3360 ± 0.0400	0.0223 ± 0.0064	0.5632 ± 0.0169	0.5633 ± 0.0290	0.5796 ± 0.088	0.1033 ± 0.0258	0.4679 ± 0.0535	1.0000 ± 0.0000	1.0000 ± 0.0000
DivideMix	01	01	0.4193 ± 0.1057	0.4330 ± 0.0887	0.5163 ± 0.0954	0.1386 ± 0.0165	0.4275 ± 0.0843	0.4396 ± 0.0728	0.5090 ± 0.0396	0.0290 ± 0.0131	0.5994 ± 0.0708	0.0999 ± 0.0000	0.0999 ± 0.0000
DivideMix	01	020	0.4165 ± 0.0969	0.4409 ± 0.0999	0.5243 ± 0.0592	0.1416 ± 0.0441	0.5121 ± 0.0651	0.4964 ± 0.0592	0.0442 ± 0.0540	0.0292 ± 0.0114	0.4448 ± 0.0891	0.1999 ± 0.0000	0.1999 ± 0.0000
DivideMix	01	050	0.5975 ± 0.0345	0.6303 ± 0.0097	0.4612 ± 0.0725	0.1351 ± 0.0147	0.7368 ± 0.0412	0.7294 ± 0.0401	0.0112 ± 0.0070	0.0140 ± 0.0033	0.7088 ± 0.0286	0.5000 ± 0.0000	0.5000 ± 0.0000
DivideMix	01	100	0.6677 ± 0.0186	0.6761 ± 0.0157	0.4305 ± 0.0784	0.0967 ± 0.0091	0.7500 ± 0.0541	0.7377 ± 0.0607	0.0227 ± 0.0209	0.0142 ± 0.0100	0.7804 ± 0.0280	1.0000 ± 0.0000	1.0000 ± 0.0000
DivideMix	02	050	0.6372 ± 0.0080	0.6900 ± 0.0180	0.5664 ± 0.0282	0.0771 ± 0.0032	0.7725 ± 0.0400	0.7843 ± 0.0411	0.4439 ± 0.0311	0.0540 ± 0.0033	0.7325 ± 0.0240	0.9999 ± 0.0001	0.9999 ± 0.0001
DivideMix	03	100	0.6493 ± 0.0183	0.6810 ± 0.0406	0.4618 ± 0.0434	0.0949 ± 0.0279	0.7455 ± 0.0627	0.7351 ± 0.0611	0.0276 ± 0.0239	0.0253 ± 0.0233	0.7890 ± 0.0337	3.0000 ± 0.0000	3.0000 ± 0.0000
DivideMix	05	020	0.4435 ± 0.1158	0.4784 ± 0.1492	0.6101 ± 0.1139	0.0926 ± 0.0363	0.4601 ± 0.1189	0.4681 ± 0.0896	0.5746 ± 0.0787	0.1176 ± 0.0322	0.3808 ± 0.1734	0.9995 ± 0.0001	0.9995 ± 0.0001
DivideMix	10	010	0.7122 ± 0.0726	0.7522 ± 0.0780	0.3906 ± 0.0639	0.1088 ± 0.0307	0.7981 ± 0.0294	0.7887 ± 0.0362	0.0051 ± 0.0076	0.0091 ± 0.0021	0.8143 ± 0.0311	5.0000 ± 0.0000	5.0000 ± 0.0000
DivideMix	10	010	0.4345 ± 0.1356	0.4387 ± 0.1193	0.5823 ± 0.1728	0.1056 ± 0.0592	0.4382 ± 0.1054	0.4450 ± 0.0925	0.6176 ± 0.1453	0.0290 ± 0.0585	0.5316 ± 0.1519	0.9987 ± 0.0000	0.9987 ± 0.0000
DivideMix	10	010	0.6769 ± 0.0170	0.6893 ± 0.0139	0.4130 ± 0.0727	0.1247 ± 0.0112	0.7377 ± 0.0666	0.7470 ± 0.0461	0.0430 ± 0.0882	0.0124 ± 0.0046	0.7867 ± 0.0448	10.0000 ± 0.0000	10.0000 ± 0.0000
DivideMix	10	010	0.2859 ± 0.1010	0.3333 ± 0.0000	0.9133 ± 0.3174	0.1895 ± 0.0501	0.2867 ± 0.1012	0.3337 ± 0.0005	0.9757 ± 0.3281	0.1869 ± 0.0539	0.1243 ± 0.1758	0.1999 ± 0.0000	0.1999 ± 0.0000
DivideMix	10	010	0.5982 ± 0.0080	0.5959 ± 0.0542	0.7384 ± 0.0280	0.1918 ± 0.0483	0.2966 ± 0.0129	0.3386 ± 0.0039	0.6760 ± 0.3371	0.1892 ± 0.0512	0.2361 ± 0.2668	0.5000 ± 0.0000	0.5000 ± 0.0000
DivideMix	10	010	0.3308 ± 0.0309	0.3585 ± 0.0202	0.5209 ± 0.0499	0.1540 ± 0.0436	0.3330 ± 0.0193	0.3387 ± 0.0094	0.5232 ± 0.0747	0.1555 ± 0.0463	0.3456 ± 0.2415	1.0000 ± 0.0000	1.0000 ± 0.0000
DivideMix	10	010	0.5911 ± 0.1006	0.3827 ± 0.0637	0.4782 ± 0.1333	0.1328 ± 0.0261	0.3664 ± 0.0881	0.3811 ± 0.0498	0.4589 ± 0.1239	0.1319 ± 0.0552	0.2413 ± 0.1909	0.9999 ± 0.0001	0.9999 ± 0.0001
DivideMix	10	010	0.3192 ± 0.0351	0.3512 ± 0.0136	0.5074 ± 0.0842	0.1597 ± 0.0354	0.3374 ± 0.0258	0.3397 ± 0.0084	0.5162 ± 0.0834	0.1616 ± 0.0311	0.3404 ± 0.2313	3.0000 ± 0.0000	3.0000 ± 0.0000
DivideMix	10	010	0.2859 ± 0.0010	0.3333 ± 0.0000	1.2334 ± 0.3168	0.2291 ± 0.0520	0.2859 ± 0.0110	0.3333 ± 0.0000	1.1978 ± 0.2641	0.2427 ± 0.0510	N/A	0.9995 ± 0.0001	0.9995 ± 0.0001
DivideMix	10	010	0.4268 ± 0.0327	0.4228 ± 0.0312	0.4256 ± 0.0074	0.1048 ± 0.0096	0.4127 ± 0.0328	0.4085 ± 0.0266	0.4363 ± 0.0297	0.1155 ± 0.0082	0.4803 ± 0.1149	5.0000 ± 0.0000	5.0000 ± 0.0000
DivideMix	10	010	0.2859 ± 0.1010	0.3333 ± 0.0000	1.4371 ± 0.3876	0.2424 ± 0.0517	0.2859 ± 0.1010	0.3333 ± 0.0000	1.4060 ± 0.2592	0.2440 ± 0.0509	N/A	0.9987 ± 0.0000	0.9987 ± 0.0000
DivideMix	10	010	0.5994 ± 0.0508	0.3844 ± 0.0372	0.5046 ± 0.1315	0.1486 ± 0.0528	0.4031 ± 0.0324	0.3999 ± 0.0254	0.4825 ± 0.0877	0.1340 ± 0.0488	0.4844 ± 0.1782	10.0000 ± 0.0000	10.0000 ± 0.0000
DivideMix	10	010	0.4857 ± 0.0511	0.5010 ± 0.0421	0.5788 ± 0.0729	0.0953 ± 0.0389	0.4858 ± 0.0310	0.4395 ± 0.0333	1.3318 ± 0.2710	0.1898 ± 0.0289	0.3142 ± 0.0797	0.9999 ± 0.0000	0.9999 ± 0.0000
DivideMix	10	010	0.5401 ± 0.0282	0.5705 ± 0.0024	0.5430 ± 0.0616	0.0860 ± 0.0368	0.6139 ± 0.0770	0.6061 ± 0.0856	0.9724 ± 0.0960	0.1283 ± 0.0205	0.4422 ± 0.0205	0.1999 ± 0.0000	0.1999 ± 0.0000
DivideMix	10	010	0.5933 ± 0.0603	0.6778 ± 0.0175	0.4676 ± 0.0739	0.0770 ± 0.0337	0.6137 ± 0.0666	0.6632 ± 0.0142	0.5336 ± 0.0312	0.5070 ± 0.0091	0.4721 ± 0.0145	0.5000 ± 0.0000	0.5000 ± 0.0000
DivideMix	10	010	0.6041 ± 0.0334	0.6946 ± 0.0578	0.4805 ± 0.0535	0.1241 ± 0.0424	0.5994 ± 0.0816	0.6461 ± 0.1089	0.4815 ± 0.0783	0.0430 ± 0.0205	0.5343 ± 0.0383	1.0000 ± 0.0000	1.0000 ± 0.0000
DivideMix	10	010	0.5450 ± 0.0290	0.5362 ± 0.0834	0.5128 ± 0.0620	0.0620 ± 0.0264	N/A	N/A	N/A	N/A	0.3171 ± 0.0570	0.0999 ± 0.0000	0.0999 ± 0.0000
DivideMix	10	010	0.5747 ± 0.0179	0.5825 ± 0.0305	0.4570 ± 0.0681	0.0569 ± 0.0279	0.1014 ± 0.0100	0.3333 ± 0.0000	0.8544 ± 0.0000	0.3206 ± 0.0000	0.1567 ± 0.2217	0.1999 ± 0.0000	0.1999 ± 0.0000
DivideMix	10	010	0.6701 ± 0.0112	0.6701 ± 0.0112	0.6701 ± 0.0112	0.6701 ± 0.0112	0.6701 ± 0.0112	0.6701 ± 0.0112	0.6701 ± 0.0112	0.6701 ± 0.0112	0.6701 ± 0.0112	0.6701 ± 0.0112	0.6701 ± 0.0112
DivideMix	10	010	0.6415 ± 0.0461	0.7558 ± 0.0295	0.4666 ± 0.0303	0.0601 ± 0.0295	0.6705 ± 0.0000	0.6908 ± 0.0000	0.5520 ± 0.0000	0.0499 ± 0.0000	0.5842 ± 0.0554	1.0000 ± 0.0000	1.0000 ± 0.0000
DivideMix	10	010	0.3988 ± 0.0660	0.3993 ± 0.0458	0.6575 ± 0.1837	0.1217 ± 0.0454	0.3854 ± 0.3039	0.3823 ± 0.0228	2.1511 ± 0.3574	0.2286 ± 0.0391	0.1843 ± 0.0354	0.0999 ± 0.0000	0.0999 ± 0.0000
DivideMix	10	010	0.5982 ± 0.0080	0.5959 ± 0.0542	0.7384 ± 0.0280	0.1918 ± 0.0483	0.2966 ± 0.0129	0.3386 ± 0.0039	0.6760 ± 0.3371	0.1892 ± 0.0512	0.2361 ± 0.2668	0.5000 ± 0.0000	0.5000 ± 0.0000
DivideMix	10	010	0.5911 ± 0.1006	0.3827 ± 0.0637	0.4782 ± 0.1333	0.1328 ± 0.0261	0.3664 ± 0.0881	0.3811 ± 0.0498	0.4589 ± 0.1239	0.1319 ± 0.0552	0.2413 ± 0.1909	0.9999 ± 0.0001	0.9999 ± 0.0001
DivideMix	10	010	0.3192 ± 0.0351	0.3512 ± 0.0136	0.5074 ± 0.0842	0.1597 ± 0.0354	0.3374 ± 0.0258	0.3397 ± 0.0084	0.5162 ± 0.0834	0.1616 ± 0.0311	0.3404 ± 0.2313	3.0000 ± 0.0000	3.0000 ± 0.0000
DivideMix	10	010	0.2859 ± 0.0010	0.3333 ± 0.0000	1.2334 ± 0.3168	0.2291 ± 0.0520	0.2859 ± 0.0110	0.3333 ± 0.0000	1.1978 ± 0.2641	0.2427 ± 0.0510	N/A	0.9995 ± 0.0001	0.9995 ± 0.0001
DivideMix	10	010	0.4268 ± 0.0327	0.4228 ± 0.0312	0.4256 ± 0.0074	0.1048 ± 0.0096	0.4127 ± 0.0328	0.4085 ± 0.0266	0.4363 ± 0.0297	0.1155 ± 0.0082	0.4803 ± 0.1149	5.0000 ± 0.0000	5.0000 ± 0.0000
DivideMix	10	010	0.2859 ± 0.1010	0.3333 ± 0.0000	1.4371 ± 0.3876	0.2424 ± 0.0517	0.2859 ± 0.1010	0.3333 ± 0.0000	1.4060 ± 0.2592	0.2440 ± 0.0509	N/A	0.9987 ± 0.0000	0.9987 ± 0.0000
DivideMix	10	010	0.5994 ± 0.0508	0.3844 ± 0.0372	0.5046 ± 0.1315	0.1486 ± 0.0528	0.4031 ± 0.0324	0.3999 ± 0.0254	0.4825 ± 0.0877	0.1340 ± 0.0488	0.4844 ± 0.1782	10.0000 ± 0.0000	10.0000 ± 0.0000
DivideMix	10	010	0.4857 ± 0.0511	0.5010 ± 0.0421	0.5788 ± 0.0729	0.0953 ± 0.0389	0.4858 ± 0.0310	0.4395 ± 0.0333	1.3318 ± 0.2710	0.1898 ± 0.0289	0.3142 ± 0.0797	0.9999 ± 0.0000	0.9999 ± 0.0000
DivideMix	10	010	0.5401 ± 0.0282	0.5705 ± 0.0024	0.5430 ± 0.0616	0.0860 ± 0.0368	0.6139 ± 0.0770	0.6061 ± 0.0856	0.9724 ± 0.0960	0.1283 ± 0.0205	0.4422 ± 0.0205	0.1999 ± 0.0000	0.1999 ± 0.0000
DivideMix	10	010	0.5933 ± 0.0603	0.6778 ± 0.0175	0.4676 ± 0.0739	0.0770 ± 0.0337	0.6137 ± 0.0666	0.6632 ± 0.0142	0.5336 ± 0.0312	0.5070 ± 0.0091	0.4721 ± 0.0145	0.5000 ± 0.0000	0.5000 ± 0.0000
DivideMix	10	010	0.6041 ± 0.0334	0.6946 ± 0.0578	0.4805 ± 0.0535	0.1241 ± 0.0424	0.5994 ± 0.0816	0.6461 ± 0.1089	0.4815 ± 0.0783	0.0430 ± 0.0205	0.5343 ± 0.0383	1.0000 ± 0.0000	1.0000 ± 0.0000
DivideMix	10	010	0.5450 ± 0.0290	0.5362 ± 0.0834	0.5128 ± 0.0620	0.0620 ± 0.0264	N/A	N/A	N/A	N/A	0.3171 ± 0.0570	0.0999 ± 0.0000	0.0999 ± 0.0000
DivideMix	10	010	0.5747 ± 0.0179	0.5825 ± 0.0305	0.4570 ± 0.0681	0.0569 ± 0.0279	0.1014 ± 0.0100	0.3333 ± 0.0000	0.8544 ± 0.0000	0.3206 ± 0.0000	0.1567 ± 0.2217	0.1999 ± 0.0000	0.1999 ± 0.0000
DivideMix	10	010	0.6701 ± 0.0112	0.6701 ± 0.0112	0.6701 ± 0.0112	0.6701 ± 0.0112	0.6701 ± 0.0112	0.6701 ± 0.0112	0.6701 ± 0.0112	0.6701 ± 0.0112	0.6701 ± 0.0112	0.6701 ± 0.0112	0.6701 ± 0.0112
DivideMix	10	010	0.6415 ± 0.0461	0.7558 ± 0.0295	0.4666 ± 0.0303	0.0601 ± 0.0295	0.6705 ± 0.0000	0.6908 ± 0.0000	0.5520 ± 0.0000	0.0499 ± 0.0000	0.5842 ± 0.0554	1.0000 ± 0.0000	1.0000 ± 0.0000
DivideMix	10	010	0.3988 ± 0.0660	0.3993 ± 0.0458	0.6575 ± 0.1837	0.1217 ± 0.0454	0.3854 ± 0.3039	0.3823 ± 0.0228	2.1511 ± 0.3574	0.2286 ± 0.0391	0.1843 ± 0.0354	0.0999 ± 0.0000	0.0999 ± 0.0000
DivideMix	10	010	0.5982 ± 0.0080	0.5959 ± 0.0542	0.7384 ± 0.0280	0.1918 ± 0.0483	0.2966 ± 0.0129	0.3386 ± 0.0039	0.6760 ± 0.3371	0.1892 ± 0.0512	0.2361 ± 0.2668	0.5000 ± 0.0000	0.5000 ± 0.0000
DivideMix	10	010	0.5911 ± 0.1006	0.3827 ± 0.0637	0.4782 ± 0.1333	0.1328 ± 0.0261	0.3664 ± 0.0881	0.3811 ± 0.0498	0.4589 ± 0.1239	0.1319 ± 0.0552	0.2413 ± 0.1909	0.9999 ± 0.0001	0.9999 ± 0.0001
DivideMix	10	010	0.3192 ± 0.0351	0.3512 ± 0.0136	0.5074 ± 0.0842	0.1597 ± 0.0354	0.3374 ± 0.0258	0.3397 ± 0.0084	0.5162 ± 0.0834	0.1616 ± 0.0311	0.3404 ± 0.2313	3.0000 ± 0.0000	3.0000 ± 0.0000
DivideMix	10	010	0.2859 ± 0.0010	0.3333 ± 0.0000	1.2334 ± 0.3168	0.2291 ± 0.0520	0.2859 ± 0.0110	0.3333 ± 0.0000	1.1978 ± 0.2641	0.2427 ± 0.0510	N/A	0.9995 ± 0.0001	0.9995 ± 0.0001
DivideMix	10	010	0.4268 ± 0.0327	0.4228 ± 0.0312	0.425								